

NORTHWESTERN UNIVERSITY

Residential Crack Response to Vibrations from Underground Mining

A Thesis

Submitted to the Graduate School In Partial Fulfillment of the Requirements

For the Degree

MASTER OF SCIENCE

Field of Civil Engineering

By

Mike J. Waldron

EVANSTON, IL

June 2006

Acknowledgements

The completion of this thesis has been made possible from the support of several individuals in which I would like to acknowledge. First and foremost, I would like to thank my advisor, Dr. Charles H. Dowding, for granting me the educational opportunity to further develop his Autonomous Crack Monitoring system. Professor Dowding provided expertise, guidance, motivation, and challenges throughout all stages of my research. A thanks is extended to Steven D. Scherer whom, by suggesting I consider pursuing graduate studies at Northwestern University, altered the course of my career path from structural to geotechnical engineering.

The financial support from the Infrastructure Technology Institute (ITI) at Northwestern University through grants from the U.S. Department of Transportation has been greatly appreciated. I would like to express my utmost gratitude particularly to Dan Marron, Dave Kosnik, and Matt Kotowsky who designed and installed the digital data acquisition and communication system in both test houses. Without the dedicated support of the aforementioned three, the projects contained within this thesis could not have been possible.

I would like to extend appreciation to Professor Richard J. Finno who has been an integral part of my further learning of and increased interest in geotechnical engineering. Again, thanks to Professor Dowding who shared his vast knowledge of specialty topics throughout coursework. I would like to recognize Gordon Revey of Revey Associates for providing requested information in timely fashion to my numerous phone calls and emails.

Thanks to all the geotechnical students who offered advice, support, motivation, and laughs throughout my 18 months of study. I would like to specially recognize Brandon H.

Hughes and Luke B. Erickson for the unforgettable times we have shared in and outside of the Technological Building. Thank you to all who participated in Intramural Sports.

Last, but not least, I thank my family, especially mom, dad, and grandma who were always supportive and available for advice throughout life's decisions. I appreciate the old friendships sustained and new ones formed in the past 18 months which allowed me to enjoy life to the fullest outside the confines of graduate school.

Abstract

This thesis summarizes two further developments of the Autonomous Crack Monitoring (ACM) system, which facilitates simultaneous measurement of crack response to environmental changes and various dynamic events. The first component was measurement of crack responses in three different materials and locations in a residential structure subjected to ground vibrations produced by an underground mine in Frankfort, Kentucky. These crack responses to blast vibrations were compared to responses to environmental changes as well as occupant activities. The second component was the design and qualification of a mounting system to measure for the first time crack response perpendicular to the wall (or surface) which contains the crack. These out-of-plane crack responses were compared to traditional in-plane responses of a ceiling crack in a house adjacent to a surface quarry in Milwaukee, Wisconsin.

Measurements in Kentucky indicate crack response is heavily dependant on material and location within the structure. The results also show that environmentally induced crack displacements can be 12 to 120 times greater than the largest blast induced crack displacements. The out-of-plane crack responses to ground motions are similar to in-plane responses to ground motions; however, they are less than in-plane responses to environmental changes for this ceiling crack.

Table of Contents

| | |
|---|------------|
| Acknowledgements | <i>i</i> |
| Abstract | <i>iii</i> |
| Table of Contents | <i>iv</i> |
| List of Figures | <i>vi</i> |
| List of Tables | <i>xi</i> |
| Chapter 1. Introduction | 1 |
| Chapter 2. Crack Response to Underground Mining; Frankfort, Kentucky | 4 |
| Introduction | 4 |
| Site Description | 4 |
| Installation of Sensors | 8 |
| Long-term Crack Behavior | 14 |
| - <i>Environmental Correlations to Crack Displacement</i> | |
| - <i>Long-term Response Compared to Blast-induced ground motions</i> | |
| Dynamic Crack Behavior | 32 |
| - <i>Underground vs. Surface Quarries</i> | |
| - <i>Attic Response</i> | |
| Occupant Activity | 48 |
| Detection of Unusual Behavior | 53 |
| - <i>Noise Considerations</i> | |
| - <i>Wind Effects</i> | |
| Summary | 69 |
| Chapter 3. Out-of-Plane Crack Behavior | 71 |
| Design and Construction | 72 |
| Laboratory Qualification | 77 |
| - <i>Dynamic Qualification</i> | |
| - <i>Long-term Qualification</i> | |

Table of Contents (con't.)

| | |
|--------------------------------|------------|
| Field Qualification | 86 |
| - <i>Long-term Response</i> | |
| - <i>Dynamic Response</i> | |
| - <i>Occupant Activity</i> | |
| Wind Effects | 96 |
| - <i>Unexplained Responses</i> | |
| Chapter 4. Conclusion | 104 |
| References | |

List of Figures

| | |
|---|----|
| Figure 2.1 Front View of the instrumented house..... | 4 |
| Figure 2.2 Plan view of the extent of the underground mine in relation to the nearby subdivision..... | 5 |
| Figure 2.3 Cross-section profile of Frankfort, KY site showing the location of residence in relation to blasting..... | 6 |
| Figure 2.4 Plan view showing location of sensors; a) bedroom crack in drywall, indoor environment sensors b) indoor basement crack in CMU blocks, outdoor crack in exterior brick, ground motion sensors, and outdoor environment sensors..... | 9 |
| Figure 2.5 Photographs showing location and detail of each of the three monitored cracks..... | 10 |
| Figure 2.6 Definition of crack displacement..... | 11 |
| Figure 2.7 Installation photos of environmental sensors a) outdoor b) indoor..... | 12 |
| Figure 2.8 Installation photos of eDAQ data collection system..... | 13 |
| Figure 2.9 Crack response to temperature over a two-day period..... | 15 |
| Figure 2.10 Exterior crack response compared with temperature and humidity..... | 16 |
| Figure 2.11 Long-term response of all three cracks during monitoring period..... | 17 |
| Figure 2.12 Bedroom crack displacement compared to both interior and exterior environmental conditions a) bedroom crack displacement compared to indoor environment conditions b) bedroom crack displacement compared to exterior environmental conditions..... | 19 |
| Figure 2.13 Interior crack displacements compared to both indoor and outdoor temperature changes..... | 21 |
| Figure 2.14 Basement and bedroom crack displacement compared to indoor environment conditions..... | 23 |
| Figure 2.15 Exterior crack displacements compared to outdoor environmental conditions..... | 24 |
| Figure 2.16 Comparison of null sensor displacements to measured crack displacements for the exterior and bedroom cracks..... | 25 |

List of Figures (con't.)

| | |
|--|----|
| Figure 2.17 Long-term response of all three cracks including to scale the largest corresponding dynamic response..... | 27 |
| Figure 2.18 Long-term exterior crack behavior compared to blast response..... | 29 |
| Figure 2.19 Long-term bedroom crack behavior compared to blast response..... | 30 |
| Figure 2.20 Long-term basement crack behavior compared to blast response..... | 31 |
| Figure 2.21 Ground motions and crack response to the March 7 th blast..... | 34 |
| Figure 2.22 Ground motions and crack response to the January 20 th blast..... | 35 |
| Figure 2.23 Ground motions and crack response to the March 16 th blast..... | 36 |
| Figure 2.24 Ground motions and crack response for the May 17 th blast..... | 37 |
| Figure 2.25 Correlations between measured crack displacement and computed displacements and peak ground velocities..... | 40 |
| Figure 2.26 Pseudo-velocity response spectra of the longitudinal excitation ground motions for the four example events..... | 41 |
| Figure 2.27 Relative displacement time histories of a 12 Hz structure with 5% damping to the March 7 th ground motions..... | 42 |
| Figure 2.28 Comparison of ground motions and crack response between Kentucky and Wisconsin test structures..... | 44 |
| Figure 2.29 Picture showing the placement of the velocity transducer near the attic rafters..... | 45 |
| Figure 2.30 Plot of blast vibrations and measured attic movements on the same date of March 22 nd | 47 |
| Figure 2.31 Induced occupant activity for bedroom crack..... | 50 |
| Figure 2.32 Induced occupant activity for exterior and basement cracks..... | 51 |
| Figure 2.33 Elevation view of the brick wall which contains the exterior crack..... | 52 |
| Figure 2.34 Comparison of hourly data and 50 Hz data for the exterior crack (March 4 th)..... | 54 |

List of Figures (con't.)

| | |
|---|----|
| Figure 2.35 Exterior crack behavior during a non-blast period compared to a blast event a) 24 hour crack behavior recorded during 50 Hz testing with 4 second time window expanded below b) exterior crack response to blast event (Feb. 8 th)..... | 55 |
| Figure 2.36 Basement crack response during recorded 50 Hz testing..... | 56 |
| Figure 2.37 Comparison of deliberate and presumed occupant activity bedroom crack response a) induced response during installation of equipment b) and c) presumed response recorded during 50 Hz data collection on respective dates..... | 58 |
| Figure 2.38 Comparison of basement and bedroom spikes seen during 50 Hz testing.... | 59 |
| Figure 2.39 Comparison of basement crack displacement for blast and non-blast responses a) 50 Hz data collected during a time period when no blasting occurred (March 9 th) b) basement crack response to blast (Feb. 8 th) | 60 |
| Figure 2.40 Comparison of bedroom crack displacement for blast and non-blast responses a) 50 Hz data collected during a time period when no blasting occurred (March 10 th) b) bedroom crack response to blast (March 7 th)..... | 61 |
| Figure 2.41 Comparison of exterior crack displacement for blast and non-blast responses a) 50 Hz data collected during a time period when no blasting occurred (March 7 th) b) exterior crack response to blast (March 7 th)..... | 62 |
| Figure 2.42 Respective crack behavior from blast event compared to crack displacement measured each hour..... | 64 |
| Figure 2.43 Comparison of noise levels for different ACM systems. Shielded CAT5 cables were employed in Kentucky while Petrina utilized instrumentation cable..... | 66 |
| Figure 2.44 Exterior crack displacement due to unknown event recorded during electrical noise spike and a blast event (February 16 th , 2005)..... | 67 |
| Figure 2.45 Possible ways to define crack displacement..... | 69 |
| Figure 3.1 Three possible directions of crack response..... | 71 |
| Figure 3.2 Mounting bracket design to measure out-of-plane crack response..... | 73 |
| Figure 3.3 Photographs showing the system used to test the out-of-plane crack measuring system a) overall view showing the testing of the LAVA block b) side view showing the testing of the LAVA block..... | 75 |

List of Figures (con't.)

| | |
|---|----|
| Figure 3.4 Drawing showing the dimensions of the out-of-plane displacement testing apparatus a) elevation view b) plan view..... | 77 |
| Figure 3.5 Dynamic testing of the out-of-plane displacement measuring system..... | 79 |
| Figure 3.6 Comparison of measured and computed crack displacements for the out-of-plane testing laboratory qualification..... | 81 |
| Figure 3.7 Hysteresis loops for out-of-plane (normal) system laboratory qualification tests a) two sensors mounted on glass block; null measures glass response only; crack measures difference between plastic, aluminum, and glass as shown in Figure 3.4 b) two sensors mounted on aluminum plate..... | 83 |
| Figure 3.8 Comparison of field null sensors and laboratory null sensors a) null sensors displacements for a six-day period b) temperature conditions affecting null sensors for the corresponding six-day period..... | 85 |
| Figure 3.9 Picture of the out-of-plane system installed on a ceiling crack near previously installed in-plane sensors..... | 86 |
| Figure 3.10 Ten day comparison of long-term in-plane and out-of-plane crack behavior a) crack and null behavior for both directions measured b) enlargement of null behavior only for both directions measured..... | 88 |
| Figure 3.11 Comparison of net displacement and actual measured crack displacement in the field application of the out-of-plane measuring system..... | 89 |
| Figure 3.12 Ground motions and associated crack displacements for December 15 th blast..... | 90 |
| Figure 3.13 Crack response to occupant activity a) both directions of crack response to a variety of activities b) first level floor plan indicating where the occupant activity tests were performed..... | 92 |
| Figure 3.14 Crack response comparison of induced occupant activity (opening and closing of a door) and a blast event (Dec. 28 th PPV = .07 ips) for both directions of displacement measured..... | 94 |
| Figure 3.15 Comparison of crack response to ceiling fan and blast event (Dec. 28 th PPV = .07 ips)..... | 95 |
| Figure 3.16 Comparison of 20 hours wind and air pressure data vs. crack displacement a) Milwaukee airport wind data b) air pressure data obtained at site c) in-plane crack displacement d) out-of-plane crack displacement..... | 98 |

List of Figures (con't.)

Figure 3.17 Crack behavior during varying degrees of windiness a) a period of low winds b) a period of moderate winds c) a period of high winds.....100

Figure 3.18 Crack behavior when no wind present.....101

Figure 3.19 Comparison of crack behavior to outdoor winds and a blasting event a) period of high wind b) January 26th 2006 blast event of PPV = 0.09 ips c) wind induced crack movement obtained on October 30th 2004.....102

List of Tables

| | |
|--|----|
| Table 2.1 Blast log of 10 largest blasts..... | 7 |
| Table 2.2 Environmental and vibration effects on crack displacement..... | 28 |
| Table 2.3 Ground motions, frequency, and crack displacement for all blast events in Kentucky..... | 33 |
| Table 2.4 Comparison of ground displacement to crack displacement ratios..... | 38 |
| Table 2.5 Summary of recorded attic vibrations compared to recorded blast vibrations for the period in which the attic velocity transducer was installed..... | 46 |
| Table 2.6 Measured crack displacements associated with dynamic events..... | 48 |
| Table 2.7 Summary of results from Figure 2.42..... | 65 |
| Table 2.8 Maximum crack displacements measured from various sources..... | 70 |

Chapter 1

Introduction

This thesis summarizes two further increments of the development of the autonomous crack monitoring (ACM) system: 1) measurement of crack response in three materials in a structure subjected to blast vibrations from an underground aggregate mine 2) design and development of a mounting system to measure normal, or out-of-plane, crack response. The three cracks were located in exterior brick, drywall near an interior doorframe, and joint mortar between concrete masonry units of a basement wall. The mounting system involved a non-responsive block to which both the crack and null sensors were mounted, which was qualified by installation on a ceiling crack in a home adjacent to an operating quarry.

Response of cracks in multiple materials was measured in a house in Kentucky near an underground aggregate mine. As with most ACM applications, a null sensor was placed adjacent to each crack sensor on uncracked material to obtain long-term material and sensors responses. The site was not instrumented with an air over pressure transducer to capture wind activity or potential pressure pulses associated with blasting.

The out-of-plane, or normal, response apparatus was field qualified by placement in the Milwaukee test house adjacent to a surface aggregate quarry. The mounting system was developed with the same Kaman eddy-current sensors as in Kentucky by securing them to a block, which allowed sensing of the crack displacement in the out-of-plane

direction. The system was first qualified in laboratory conditions and then mounted across a ceiling crack in the Milwaukee test house. The out-of-plane system was mounted along side of a traditional (in-plane) measuring system to compare the crack behavior in respective directions. Appropriately affixed and orientated null sensors for both directions were also placed near the responding crack. The ground vibrations were recorded with a standard tri-axial geophone velocity transducer.

The thesis is divided into four chapters including this introduction as Chapter 1. Chapter 2 compares the responses of multiple crack types and Chapter 3 describes the qualification of the normal, or out-of-plane, crack measuring system. Finally, Chapter 4 presents the conclusions and recommendations for each chapter. The main content of the thesis is contained within Chapters 2 and 3, which are further described below.

Chapter 2 presents the results and discussion of crack response to subsurface quarry blasting in Kentucky and is divided into six components: site description, installation of sensors, long-term crack behavior, dynamic crack behavior produced by blast induced ground motions, occupant activity, and unusual behavior.

The site description component of Chapter 2 summarizes the geometrical relationships of the subsurface quarry blast locations and the structure. Next is a description of the sensors used in the study, how and where they were installed within the structure, descriptions of each crack studied, and the manner in which the system was triggered to record dynamic effects as well as long-term or environmental effects. Description of the long-term crack behavior includes effects of environmental changes on each crack as well as the differences noted to occur between the crack responses. Dynamic crack response is divided into blast induced response, occupant induced

response, and unusual behavior. Comparisons are then made between excitation descriptors and crack response to occupant activity, wind, and blast vibrations as well as unusual events from unidentified excitation.

Chapter 3 presents the approach used to measure out-of-plane crack movements and discusses the results of installing such a system. This chapter is divided into four components: design and construction, laboratory qualification, field qualification, and wind effects.

The chapter begins with a discussion of the considerations for design and construction of this system, which required laboratory qualification prior to field installation. Laboratory qualification included tests for both dynamic and long-term response and a comparison between expected and measured performance. Field qualification was accomplished by installation across a ceiling crack in a structure adjacent to an operational surface aggregate quarry. During the qualification testing, it was possible to evaluate out-of-plane responses to both long-term environmental effects and dynamic excitation. Dynamic out-of-plane crack responses to blast induced ground motions and air over pressures were compared to those induced by occupant activity, wind, as well as the in-plane responses.

Chapter 2

Crack Response to Underground Mining; Frankfort, Kentucky

Introduction

Blasting from underground mining of aggregate raised concern for nearby homeowners and lead to the installation of an autonomous crack monitoring (ACM) system. The structure shown in Figure 2.1 was instrumented to monitor the response of three cracks in interior drywall, exterior brick, and basement concrete block as well as the ground motions. The ACM system was in place for approximately 4 ½ months from January to June 2005 while weekly blasting occurred.



Figure 2.1 Front view of the instrumented house

Site Description

Located just west of the Kentucky River, plan view Figure 2.2 shows the mining operations in relation to the surrounding residential structures. Green rectangular shapes represent nearby residential structures; structure 3 was instrumented; and other red-encircled

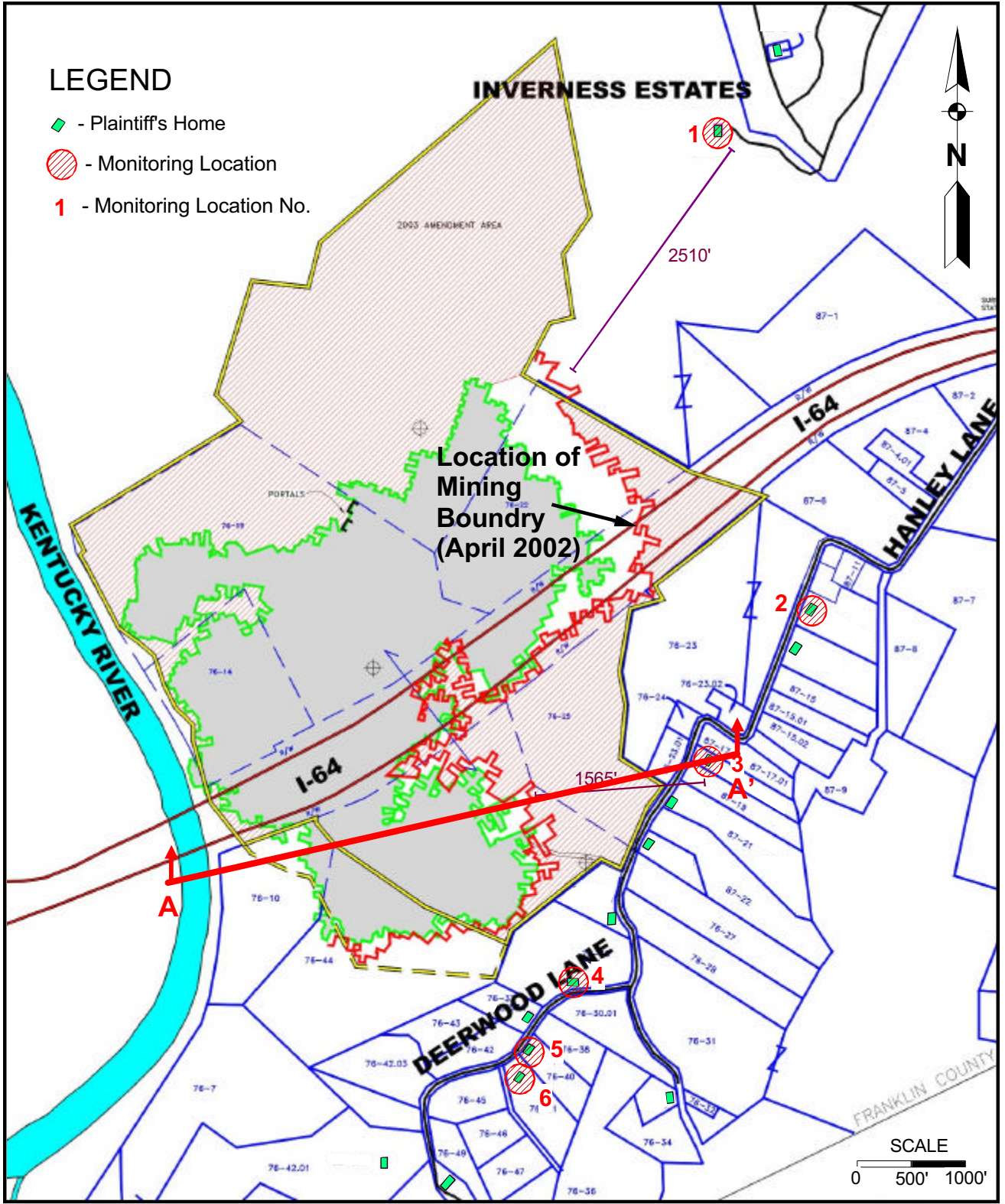


Figure 2.2 Plan view of the extent of the underground mine in relation to the nearby subdivision

structures denote other locations for monitoring ground motions for another study. The outer red boundary shown in Figure 2.2 represents the extents of mining through 2002 whereas the majority of blasting performed during this study (2005) was to expand the mine further east towards the structures.

The cross-section labeled in red as A-A' on Figure 2.2 is shown in Figure 2.3 in true scale to present the relevant profile of the ground surface, mine, and the structure in consideration. The mine entrance, near the Kentucky riverbed, slopes down to an elevation of 457' where it remains level for the extent of the mine. The structure and the geophones that monitored ground motions are located at an elevation of 842', approximately 385 ft above the mine elevation. Blasts during this study were denoted approximately 1,650 ft horizontally from the buried geophones.

The structure monitored for this study is a single story wooden-framed residential home. It is founded upon a partial basement constructed of concrete masonry block. The sloping ground to the southwest (right in Figure 2.1) allows a walk out exit at the end of the structure. The majority of the outside of the structure is covered by non-load bearing exterior brick.

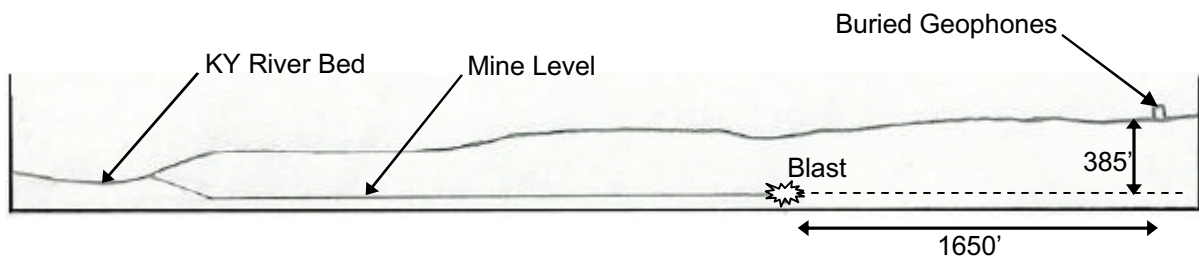


Figure 2.3 Cross-section profile of Frankfort, KY site showing location of residence in relation to blasting. Location of the cross-section is shown above in Figure 2.2

Blasting typically occurred twice a week for the 19 weeks the site was monitored. A total of 37 blast events were recorded. Except for one morning blast, all blasts were

performed consistently between 4:00pm and 4:30pm. The 10 largest blasts that produced the highest peak-particle-velocity (PPV) are tabulated in Table 2.1 to describe the blasting environment. The largest blast that produced a PPV of 0.168 inches per second (ips) is listed at the top of the Table 2.1, with subsequent blasts listed in decreasing PPV down to 0.088 ips.

Table 2.1 Blast log of 10 largest blasts

| Largest Blasts | Date | max.PPV (ips) | Direction | Blast Type | lbs / delay W | Distance (ft.) D | D / W ^{1/2} |
|----------------|----------|---------------|-----------|------------|---------------|------------------|----------------------|
| 1 | 03/07/05 | 0.168 | L | - | - | - | - |
| 2 | 01/20/05 | 0.154 | L | V | 50.5 | 1638 | 230 |
| 3 | 02/16/05 | 0.142 | L | V | 50.5 | 1626 | 229 |
| 4 | 02/02/05 | 0.138 | L | V | 50.5 | 1626 | 229 |
| 5 | 02/15/05 | 0.138 | L | V | 50.5 | 1626 | 229 |
| 6 | 01/25/05 | 0.135 | L | V | 50.5 | 1638 | 230 |
| 7 | 02/08/05 | 0.129 | L | V | 50.5 | 1626 | 229 |
| 8 | 01/26/05 | 0.120 | L | V | 50.5 | 1638 | 230 |
| 9 | 01/18/05 | 0.113 | L | V | 50.5 | 1656 | 233 |
| 10 | 03/03/05 | 0.088 | L | - | - | - | - |

The maximum PPV for each blast occurred in the longitudinal direction (denoted by L in column 4), which is perpendicular to the long axis of the structure. Blasts 2 through 9 were vertical (denoted by V in column 5) as opposed to horizontal, which describes the direction blast holes were drilled in order to place the explosives. Typically, 50 lbs/delay was employed in each hole, which results in a square root scaled distance of 230 ft/(lb^{1/2}). Scaled

distance is defined by Equation 2.1 where W is the explosive weight in lbs/delay and D is the distance in feet from the blast location to the buried geophones.

$$\text{Scaled Distance} = \frac{D}{W^{1/2}} \quad (2.1)$$

Installation of Sensors

As shown in Figure 2.4, the structure was instrumented with tri-axial geophones to record ground motion, 3 sets of sensors to measure changes in crack width, and both indoor and outdoor temperature and humidity sensors. Figure 2.4a shows the location of the bedroom displacement sensors and the indoor environment sensors on a plan view of the 1st level. Figure 2.4b shows the location of the basement and exterior displacement sensors, the outdoor environment sensors, and geophones on a plan view of the basement level.

The tri-axial geophones were buried in the backyard soil approximately 4 ft from the rear of the house to measure particle velocity in three mutually orthogonal directions longitudinal, transverse, and vertical. The longitudinal axis was placed perpendicular to the rear face of the structure (short axis). The transverse direction, in-turn, is then parallel to the rear face of the structure (long axis). The vertical direction is then orthogonal to both the longitudinal and transverse directions, and thus measures ground motions in the vertical direction.

The three cracks were instrumented with 2U series SMU 9000 Kaman sensors (Kaman, 2005), which are capable of measuring displacements as small as 4 μ in. All crack sensors were in place from January 14th of 2005 to June 2nd of 2005. Weekly blasting occurred throughout the 4 ½ months during which the sensors were in place.

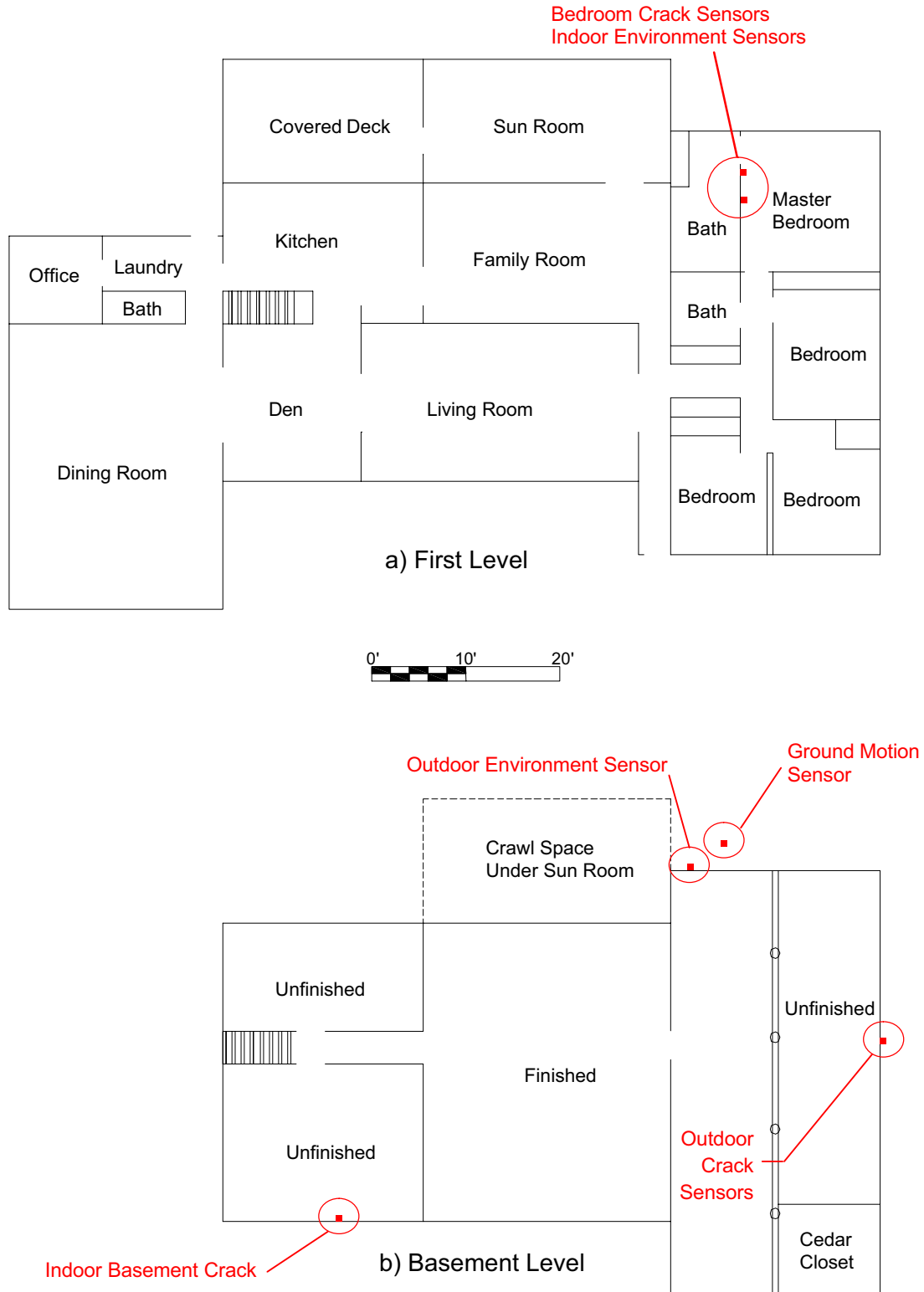


Figure 2.4 Plan view showing locations of sensors; a) bedroom crack in drywall, indoor environment sensors b) indoor basement crack in CMU blocks, outdoor crack in exterior brick, ground motion sensors, and outdoor environment sensors



a) Indoor Bedroom Crack



b) Indoor Basement Crack



c) Exterior Crack



Figure 2.5 Photographs showing the location and detail of each of the three monitored cracks

As shown in Figure 2.5, the instrumented cracks occur in three different locations and materials. Each crack is described with a close-up view as well as a wider orientation view. The bedroom crack is located in drywall at the upper corner of a doorframe that leads to the bathroom. It is approximately 10,000 micro-inches wide. The other interior crack, located in the basement is horizontal at the mid-wall in the mortar between two concrete masonry blocks that form the basement wall. It is approximately 40,000 micro-inches wide. The exterior crack occurs in the exterior brick on the Southwest face of the structure. It is approximately 90,000 micro-inches wide. Each crack sensor is accompanied by a null sensor, which is placed on uncracked material adjacent to the crack being monitored. The null sensor accounts for both material and sensor response to changes in temperature and humidity. The actual crack response itself is obtained by subtracting the null sensor response from the crack sensor response.

These sensors measure micro-inch changes in crack width. As shown in Figure 2.6, these changes are small compared to the crack width. They occur perpendicular to the crack

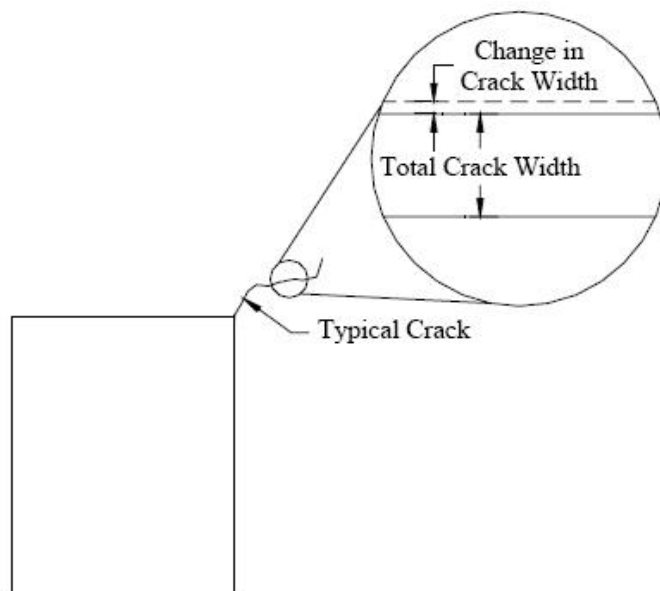


Figure 2.6 Definition of crack displacement (Seibert, 2000)

length and reflect the tendency of the crack to lengthen at its tip as described by Dowding and McKenna (2003). Since “changes in crack width” is a cumbersome description, henceforth this change will be described simply as “displacement”. By measuring crack displacement instead of crack width, it is possible to install the sensor without disturbing the crack itself during installation and monitoring. Further details of this concept are available in Dowding and Seibert (2000) and at

http://iti.birl.northwestern.edu/acm/vegas/crack_displacement.html.

Environment sensors, which measure both humidity and temperature, were installed both inside and outside the structure as shown in Figure 2.7. The interior environment sensor was located in the same bedroom as the bedroom crack sensor while the exterior environment sensor was placed on the rear wall of the house near the geophones.



a) Outdoor Sensors



b) Indoor Sensors

Figure 2.7 Installation photos of environmental sensors a) outdoor b) indoor

All instrumentation, including all three crack sensors and their corresponding null sensors, the geophones, and environment sensors were wired to an eDAQ data acquisition system shown in Figure 2.8. This data acquisition system facilitates recording of dynamic

(transient) and long-term (weather) response of all three cracks and is described further by McKenna (2002). Transient response of crack sensors and their nulls is acquired whenever the vibration level at the outside geophones exceeds a predetermined minimum excitation (or trigger) threshold of particle velocity (0.04 ips). Environmental or long-term response data were obtained once an hour, however, the eDAQ processed data at a rate of one sample per second. A “rolling” average was performed where each data point was actually an average of the 30 preceding readings and 30 subsequent readings. Therefore, each point represents an average value over a minute. Finally, one of these points was recorded every hour in order to obtain the long-term data. A total of 13 recording channels were wired into the eDAQ: 3 geophone directions, 3 crack sensors, 3 null sensors, 2 temperature sensors, and 2 humidity sensors. This equipment was designed and installed by Infrastructure Technology Institute instrument staff (Dan Marron, 2005).



a) Data monitoring secure enclosure houses eDAQ in corner of basement



b) Close-up picture of eDAQ and wiring

Figure 2.8 Installation photos of eDAQ data collection system

Long-Term Crack Behavior

Changes in long-term crack displacement are affected by the material in which the crack resides, the location of the crack relative to structural members, and most importantly the environmental conditions to which it is subjected. For example, a crack located in a humidity sensitive material such as drywall nailed to a wooden frame will respond more to changes in humidity than would a crack in brick. Furthermore, the location of a crack within a structure may become important when a crack is located near a structural member that responds greatly to environmental changes even if the material itself doesn't respond significantly to the environmental changes. Such an example would be a concrete basement founded in expansive soils.

Environmental Correlations to Crack Displacement

Typical long-term daily changes in the outside and bedroom crack displacement are compared to temperature in Figure 2.9 for two days. These long-term time histories are produced by data sampled once an hour. The outside crack displacement along with corresponding temperature conditions is portrayed by the thick black line. The bedroom crack displacement along with corresponding temperature conditions is portrayed by the thin red line.

As seen in Figure 2.9 the exterior crack displacement slightly exceeded the sensor's range of 20,000 micro-inches. During some 24-hour periods, the exterior crack displacement well exceeded 20,000 micro-inches. The bedroom crack often times displaced 2,500 to 3,000 micro-inches in a 24-hour period even though the indoor temperature maintained almost constant throughout most of the study.

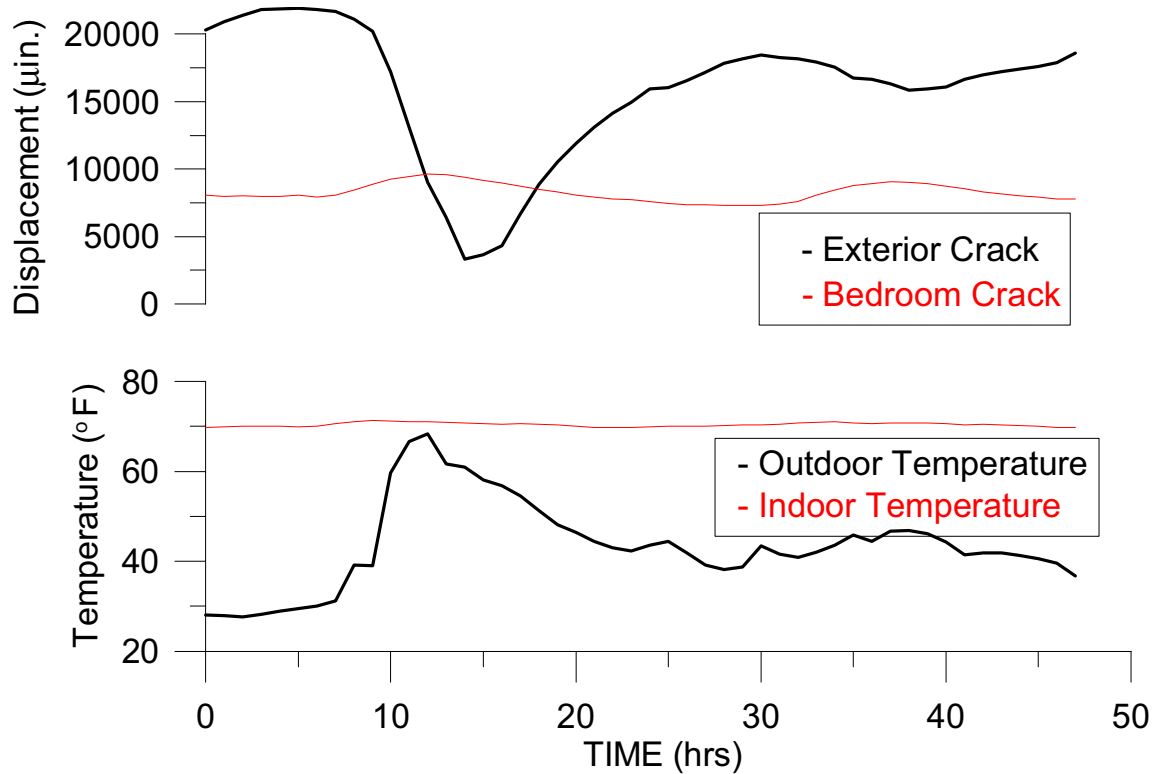


Figure 2.9 Crack responses to temperature over a two-day period

Response of the exterior crack for a two-week duration is shown along with associated environmental conditions in Figure 2.10. The exterior crack is highly sensitive to the temperature change as shown by the similarity in the changes in the temperature and crack displacement. As the temperature increases, it causes the bricks to expand, thus “closing” the crack. The exterior crack in the loose brick is less sensitive to the changes in humidity as illustrated by the failure of the crack displacement pattern to follow the dip in the humidity between the 12th and 18th of March. When analyzing long-term crack response, it is important to assess changes and trends noticeable on time scales larger than daily and weekly cycles to fully understand the effect of seasonal changes. It is also important to compare differences in crack response over long periods. Response of all three cracks is compared in Figure 2.11 throughout the monitoring period which extends through winter into late spring.

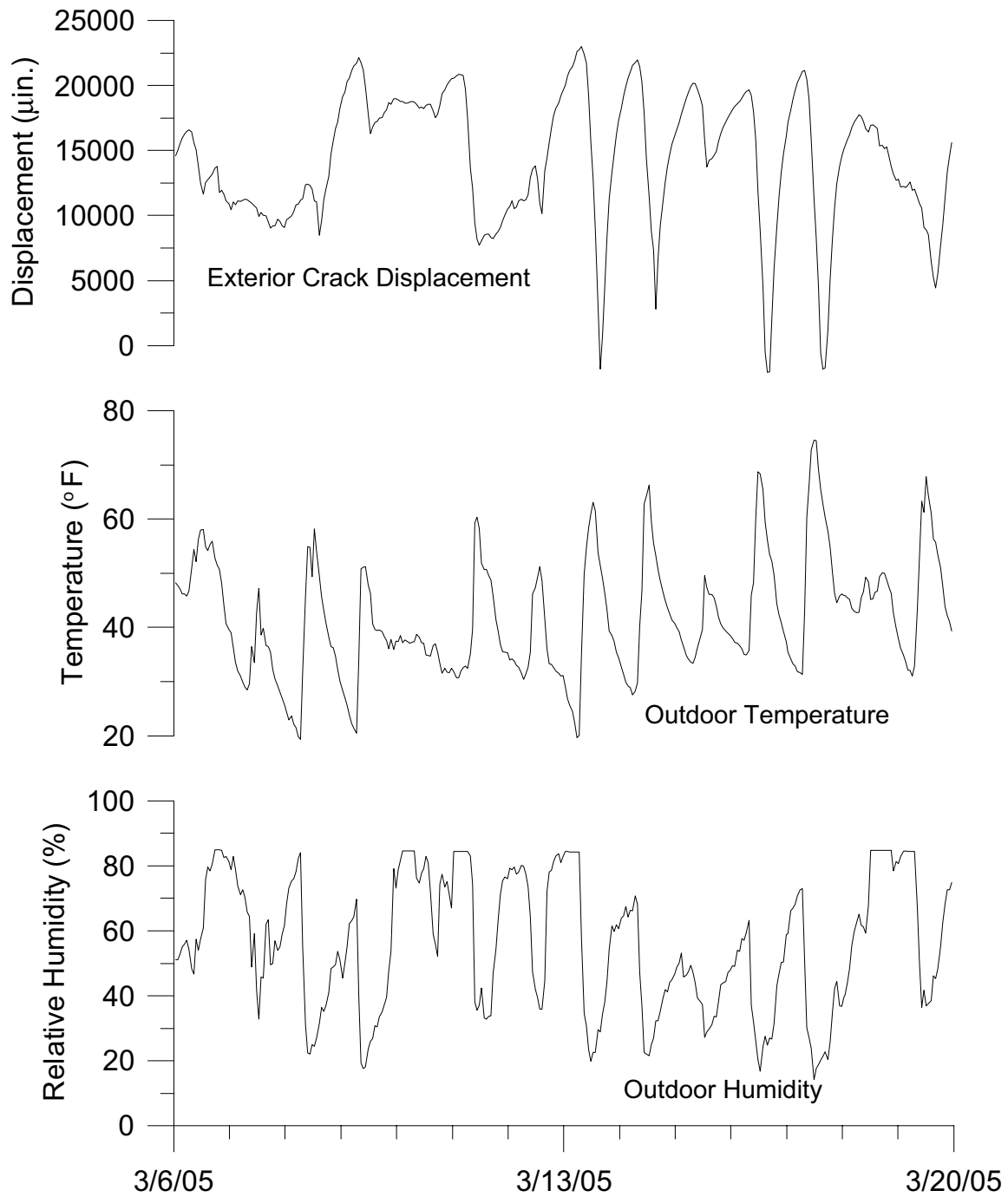


Figure 2.10 Exterior crack response compared with temperature and humidity

The exterior crack responds highly on a daily basis though it does not exhibit as noticeable seasonal affects. On the other hand, the bedroom and basement exhibit greater response to seasonal affects than to daily environmental changes. The basement crack seems to close

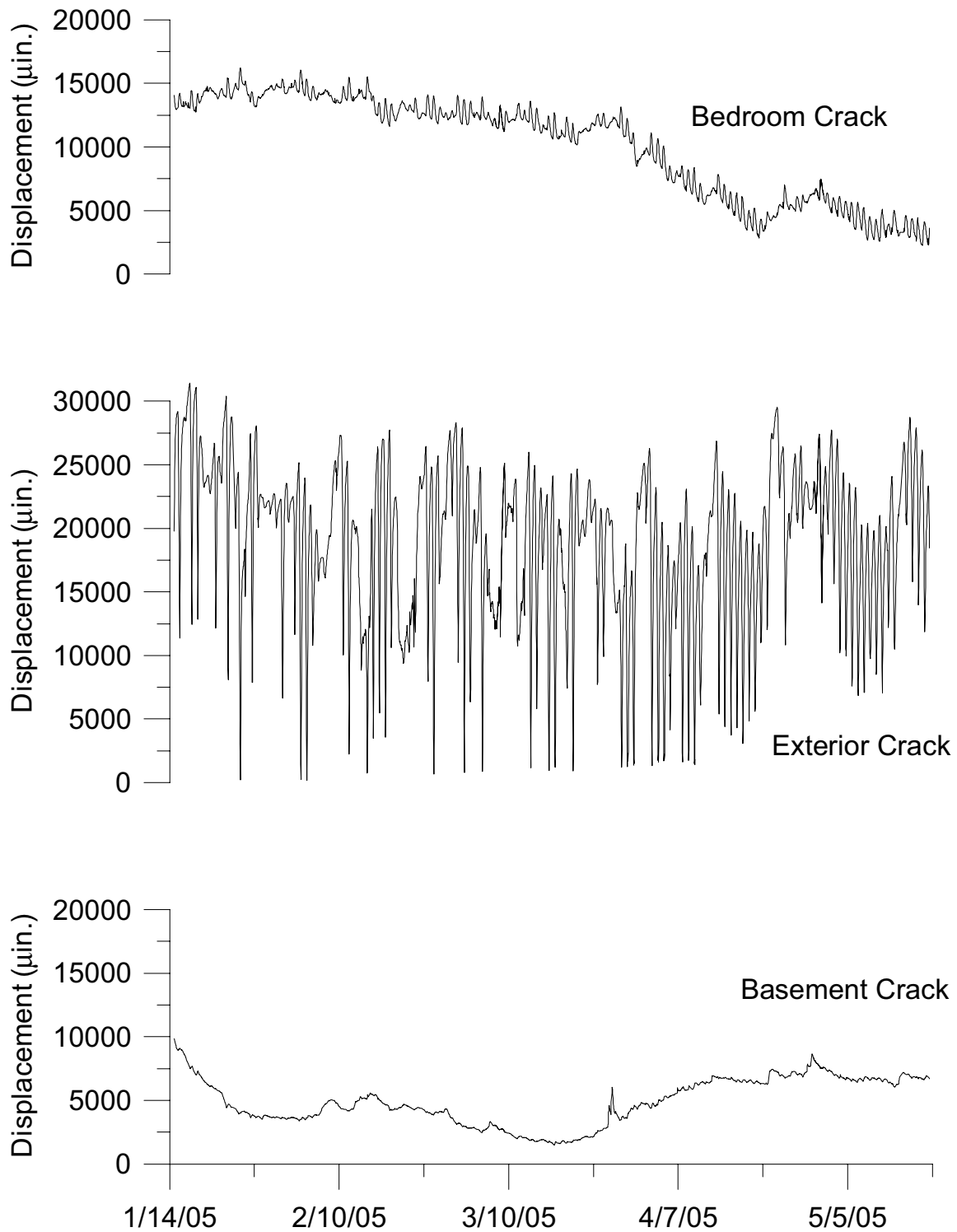


Figure 2.11 Long-term response of all three cracks during monitoring period during the transition from winter to summer and began to re-open as summer approaches. The bedroom crack's daily responses are easily noticed; however, the seasonal effects

produce larger changes in displacement than daily trends. The bedroom crack displacement gradually declines (crack closes) until April where a sharp decline occurs and continues for the remainder of the monitoring period.

To further address the sharp closing of the bedroom crack beginning in April, the bedroom crack displacement is compared to both indoor and outdoor environmental conditions in Figure 2.12. The downward trend can be explained by considering both the interior and exterior environment conditions. Part a (left) compares bedroom crack displacement to indoor temperature and humidity while part b (right) compares bedroom crack displacement to outdoor temperature and humidity. At approximately the same time, a general increase is seen in both the outdoor temperature and indoor humidity. These increases in environmental conditions seem to occur around the time the bedroom crack experiences an increase in its rate of closing. The outdoor temperature would not be suspected to affect the seasonal trends of the bedroom crack displacement because the bedroom temperature is controlled by the central heating of the structure during the cold months. However, it is believed that an increase in outdoor temperature directly increases the interior humidity for several reasons. The wooden rafters and studs in the house as well as the drywall itself will distort when subjected to large humidity changes, which would result in a closing of the bedroom crack.

Detailed comparison of the two indoor cracks and indoor and outdoor temperature reveals information about likely actions of the homeowner in response to weather. First, significant trends in the weather and crack response are illustrated in Figure 2.13 by the blue arrowed lines. The blue arrows in the outdoor temperature show general increases or decreases in temperature for an extended period of time (days to weeks). Also shown are

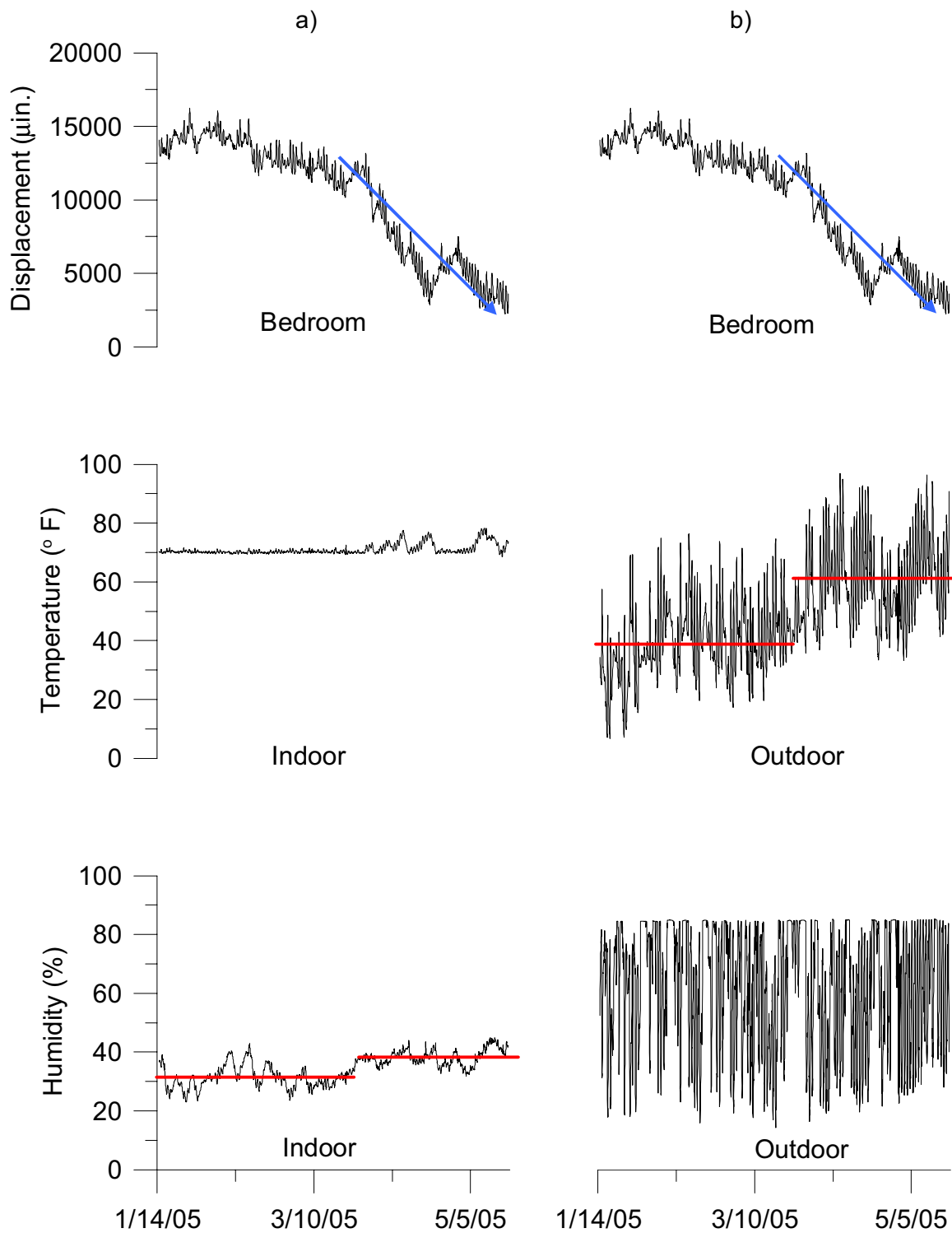


Figure 2.12 Bedroom crack displacement compared to both interior and exterior environmental conditions a) bedroom crack displacement compared to indoor environment conditions b) bedroom crack displacement compared to exterior environment conditions

corresponding, yet oppositely sloped, blue arrows in the bedroom crack behavior for the same time periods. As expressed earlier, an increase in outdoor temperature induces a closing behavior of the bedroom crack and vice-versa for a decrease in outdoor temperature. This is on the basis that outdoor temperature has a direct impact on the indoor humidity, which ultimately affects the bedroom crack behavior.

The vertical dashed lines in Figure 2.13 help illustrate the correlation between the outdoor and indoor temperature conditions while incorporating the actions of the resident. For a majority of the study, the interior temperature was maintained constant with controlled heating or air-conditioning. However, beginning in April there are periods when indoor temperature follows the outdoor trends (bounded by the dashed lines). The humps in indoor temperature are believed to be a result of the resident turning the heat off and opening windows to accommodate the rise in outdoor temperatures. Within the general humps observed in the indoor temperature, the daily cyclic changes become noticeable. It seems that even though the indoor temperature increases and decreases in daily cycles, the outdoor temperature governs the bedroom crack behavior due to its effect on the humidity. Complex analysis, such as discussed above, must be conducted to fully understand the nature of crack behavior in structures.

Long-term response of both interior cracks is compared to the indoor environment conditions in Figure 2.14. Response of the bedroom crack to changes in indoor and outdoor effects has already been discussed. Spikes in the interior humidity correlate to spikes in the basement crack shown by the corresponding vertical lines. The response implies that increases in indoor humidity increases crack opening of the basement crack. However, CMU blocks would not be expected to be sensitive to humidity because of their cementitious

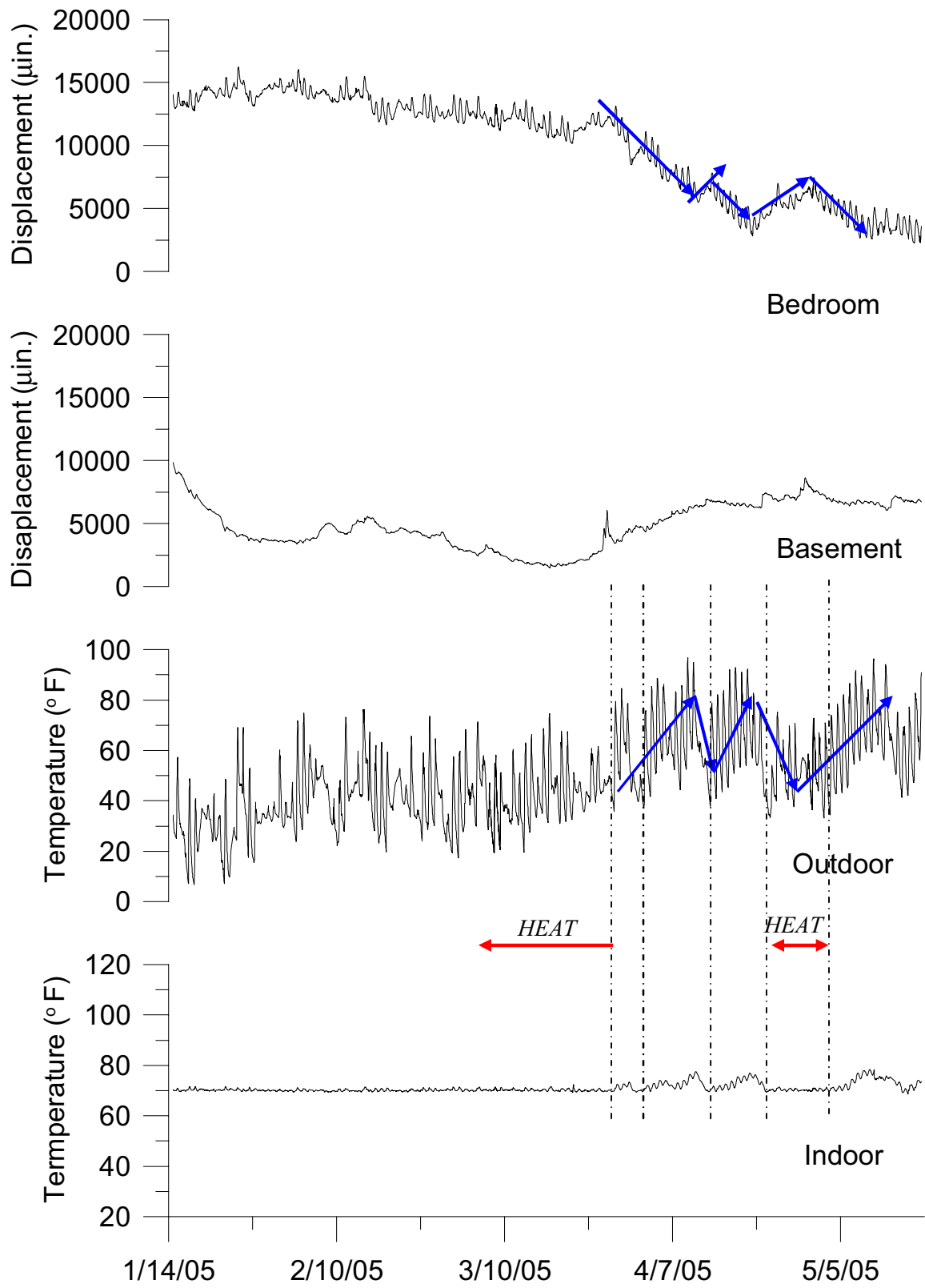


Figure 2.13 Interior crack displacements compared to both indoor and outdoor temperature changes

nature. Therefore, it is presumed the increase in indoor humidity causes swelling in the wooden frame of the structure in a fashion to further open the basement crack, through the attachment of the basement wall to the sill plate.

Long-term response of the exterior brick crack is compared to changes in outdoor temperature and humidity is shown in Figure 2.15 at the same crack scale as Figure 2.14. The daily exterior crack displacements in Figure 2.15 are far greater than either of the interior cracks. This large difference may result from the direct afternoon sunlight on the loose brick wall. It is evident the exterior crack responds more to changes in temperature than humidity. With such large changes in outdoor temperature, the exterior crack repeatedly opens and closes exceeding the 20 mil (20,000 micro-inch) range of the Kaman sensor. Responses outside the range of the sensor are not exactly known, though are believed to be reasonably accurate and still plotted to portray the extrapolated magnitudes. As previously discussed, increases in outdoor temperature cause the bricks to expand therefore inducing closing of the exterior crack. This phenomenon is illustrated in Figure 2.15 by the blue circles for daily spikes and the blue arrowed line for longer apparent trends.

The outdoor humidity in Figure 2.15 appears to have a maximum value of approximately 84%. It is strongly suspected that the humidity often times exceeded this value and that the cap of 84% relative outdoor humidity results from a sensor malfunction.

As mentioned earlier, every crack sensor is accompanied by a null sensor, which measures long-term changes in material and sensor response to changes in temperature. Thus, the actual movements of the crack can be determined by subtracting the null values from the measured crack displacements. However, often times the displacements measured by the null

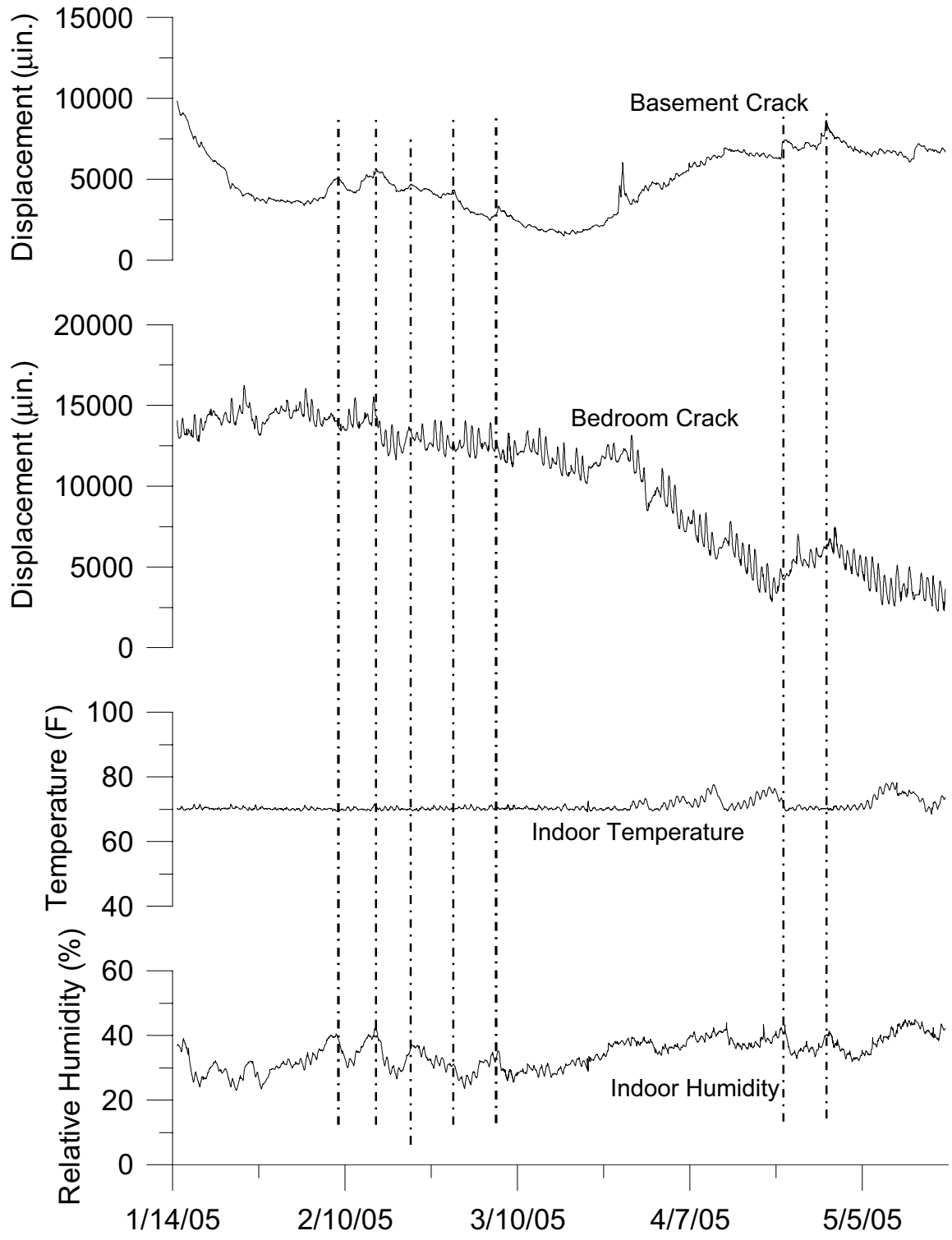


Figure 2.14 Basement and bedroom crack displacement compared to indoor environment conditions

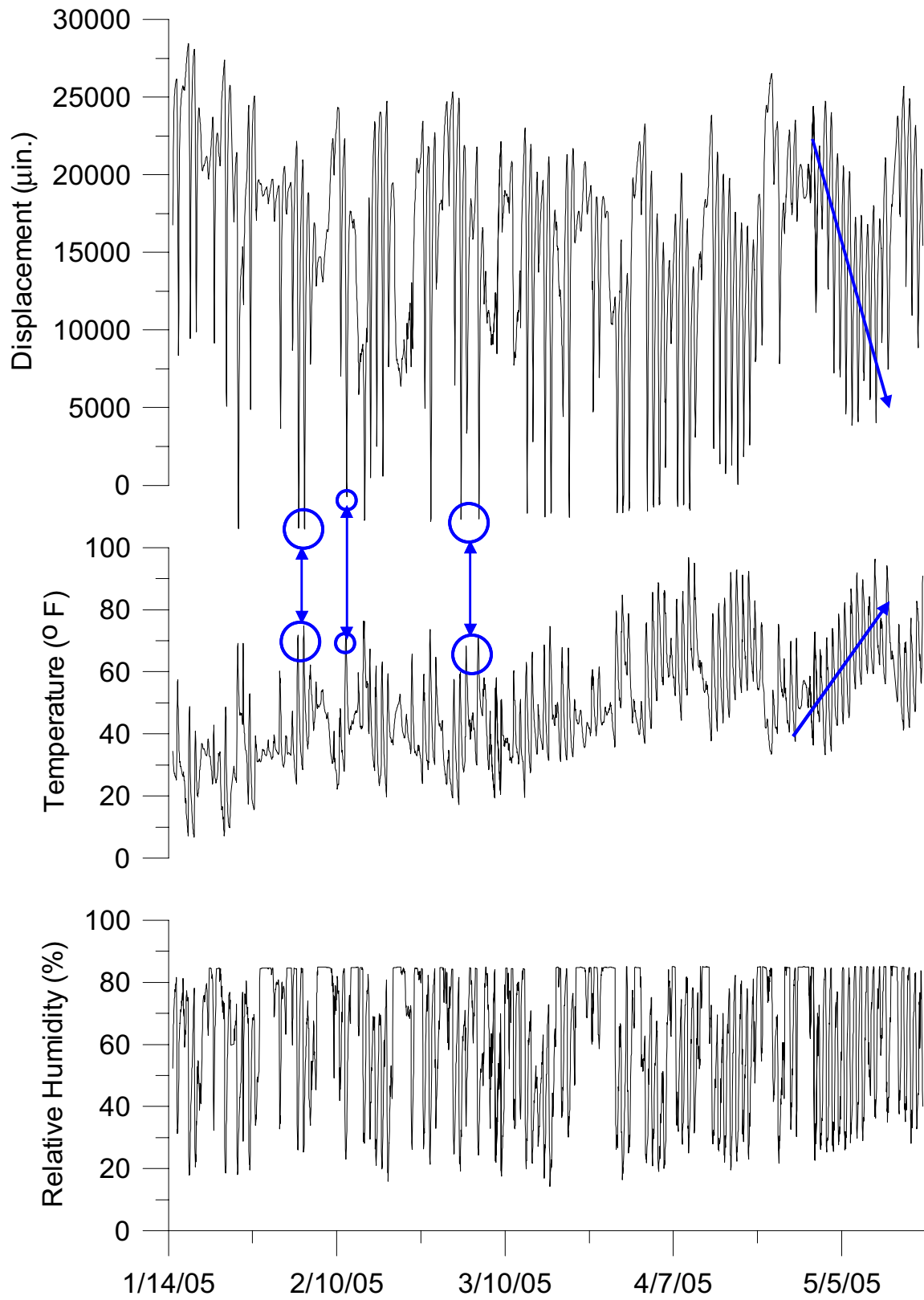


Figure 2.15 Exterior crack displacements compared to outdoor environmental conditions

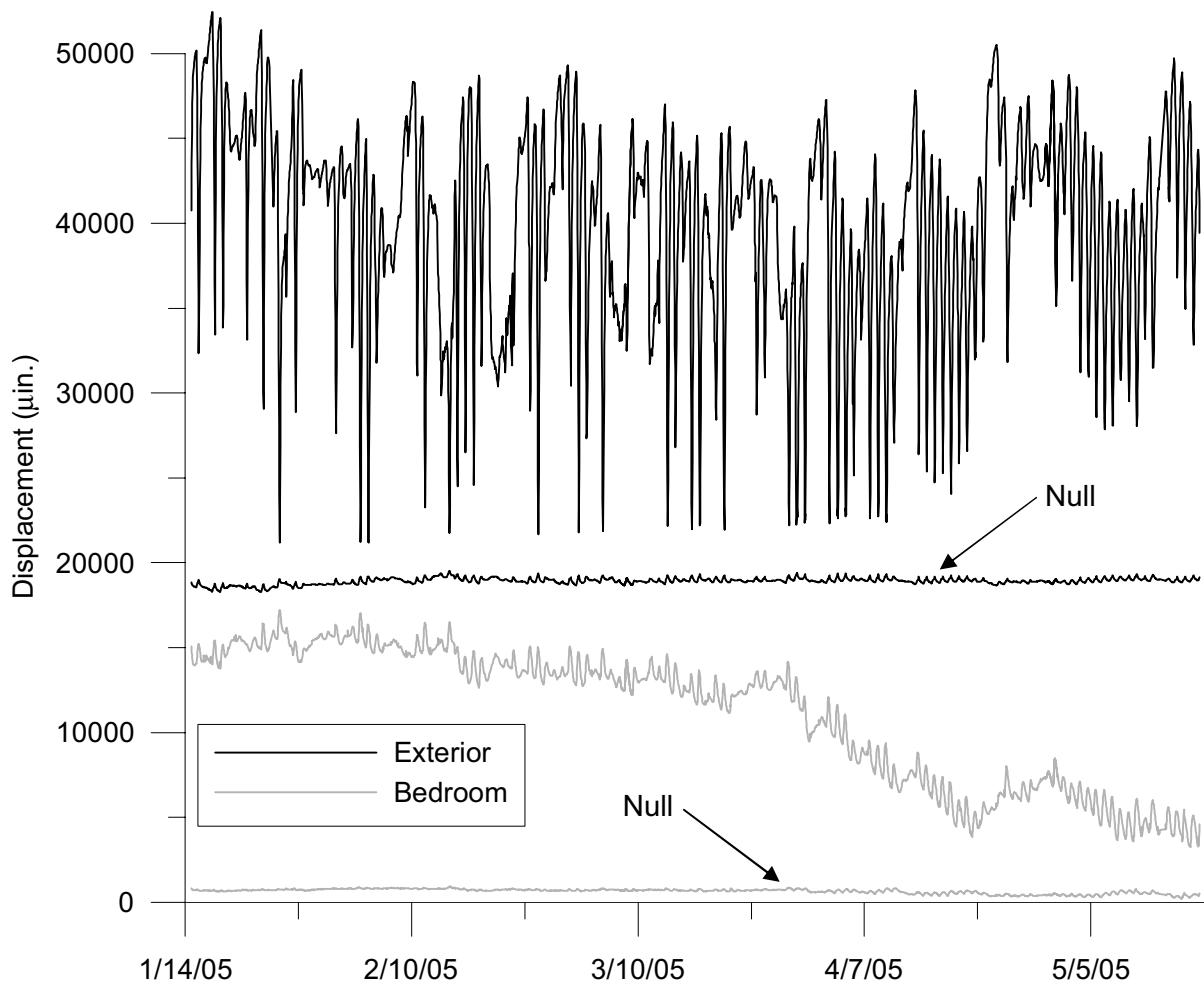


Figure 2.16 Comparison of null sensor displacements to measured crack displacements for the exterior and bedroom cracks

sensors are miniscule and insignificant relative to the large changes in crack displacement as shown in Figure 2.16. In these cases, the null sensor can be ignored and the measured crack displacements accurately represent the crack behavior. Further discussion on the applicability of null sensors can be found in Chapter 3.

Long-term Response Compared to Blast-induced Ground Vibrations

To assess the significance of blast-induced ground vibrations on cracks, it is important to compare the dynamic responses to the long-term environmental behavior. Figure 2.17 compares the behavior of all three cracks during the entire monitoring period. The actual long-term crack displacement recorded is shown in light gray, while 24-hour average values shown in black. These 24-hour “rolling” averages were calculated by averaging measurements from 11 hours prior to the point, the point itself at that time, and 12 hours after each hourly measurement. Therefore, each point is an average of 24 points, or 24 hours of actual crack displacement. The first and last 12 hours of each crack displacement are neglected in the 24-hour rolling average and not shown by the black lines. The 24-hour rolling averages factor out daily effects and represent crack displacement trends produced by changing weather fronts.

As seen in Figure 2.17, the bedroom and exterior cracks have noticeable daily effects, which differ from 24-hour average weather effects. The black line portrays a multi-day or weekly trend while the daily gray line cycles with respect to these long-term weather effects. However, the basement crack rarely responds to daily changes, as the hourly data do not deviate from the 24-hour average. This pattern implies the basement crack responds more or less to weather fronts only.

Also included in Figure 2.17 are the maximum crack displacements caused by blast vibrations for each crack shown in red. Each maximum displacement is shown to scale relative to long-term behavior and circled by a red-dashed line for clarity. The greatest basement dynamic crack response of 687 micro-inches peak-to-peak is a miniscule 9.0% of the peak-to-peak 24-hour average of the basement crack shown by the vertical bar in

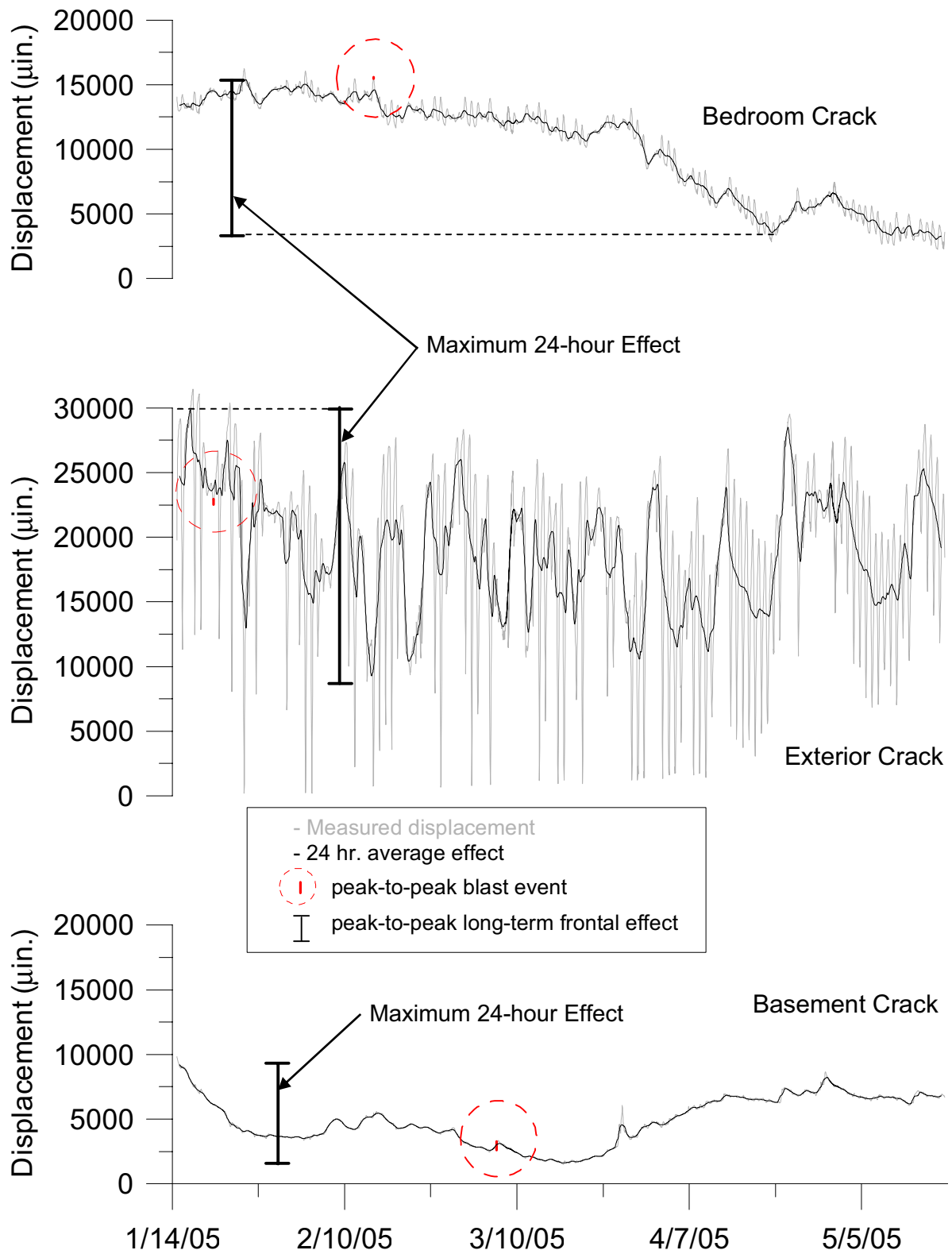


Figure 2.17 Long-term response of all three cracks including to scale the largest corresponding dynamic response

Figure 2.17. The maximum exterior crack dynamic response is only 2.2% of the peak-to-peak 24-hour average of the exterior crack while the bedroom is at 0.9%.

Table 2.2 summarizes the crack displacements due to long-term environmental effects and dynamic blast events. Included in the table are the peak-to-peak measured long-term values for all three cracks and the indoor and outdoor environment conditions as well as the maximum peak-to-peak changes seen in the 24-hour average response. Maximum and typical crack displacements due to blasting events are also included for comparison. The “typical” ground motion listed at 0.08 ips and all of the typical crack displacements in Table 2.2 were obtained by taking an average value from all 37 recorded blasts. The values listed for typical crack displacements may not necessarily correlate to a blast with a PPV of 0.08 ips.

Similarly, the maximum ground motion of 0.17 ips was produced by the March 7th blast; however, the maximum crack displacements listed are not necessarily due to that same blast. As seen in Table 2.2, the ratio of the largest change in long-term measured crack response to that of the maximum blast-induced crack response ranges from 12 for the basement crack to 120 for the bedroom crack, indicating the relative insensitivity of cracks to vibrations.

Table 2.2 Environmental and vibration effects on crack displacement

| | Temperature Change (degF) | | Humidity Change (%RH) | | Bedroom Crack | Exterior Crack | Basement Crack |
|--|---------------------------|------|-----------------------|------|---------------|----------------|----------------|
| | int. | ext. | int. | ext. | | | |
| <i>Environmental Effects (peak-to-peak)</i> | | | | | | | |
| Max measured long-term response | 10 | 90 | 22 | 71 | 14,000 | 31,254 | 8,346 |
| Max 24-hour average response | 8 | 59 | 19 | 51 | 12,335 | 20,542 | 7,595 |
| <i>Vibration Effects (peak to peak)</i> | | | | | | | |
| Typical ground motion (PPV = 0.08 ips) | - | - | - | - | 66 | 207 | 235 |
| Max ground motion (PPV = 0.17 ips) | - | - | - | - | 114 | 444 | 687 |

Further comparison of long-term crack behavior with dynamic crack response can be illustrated by concentrating on a shorter time frame as seen in Figures 2.18, 2.19, and 2.20. The top of each figure represents two months of recorded crack displacements from March 1st to April 30th. In the middle is an enlarged display of eight days of crack displacement. Typical peak-to-peak dynamic crack motions are also shown on the eight day plot. Even though the peak-to-peak displacement of the dynamic crack motions are plotted as a red

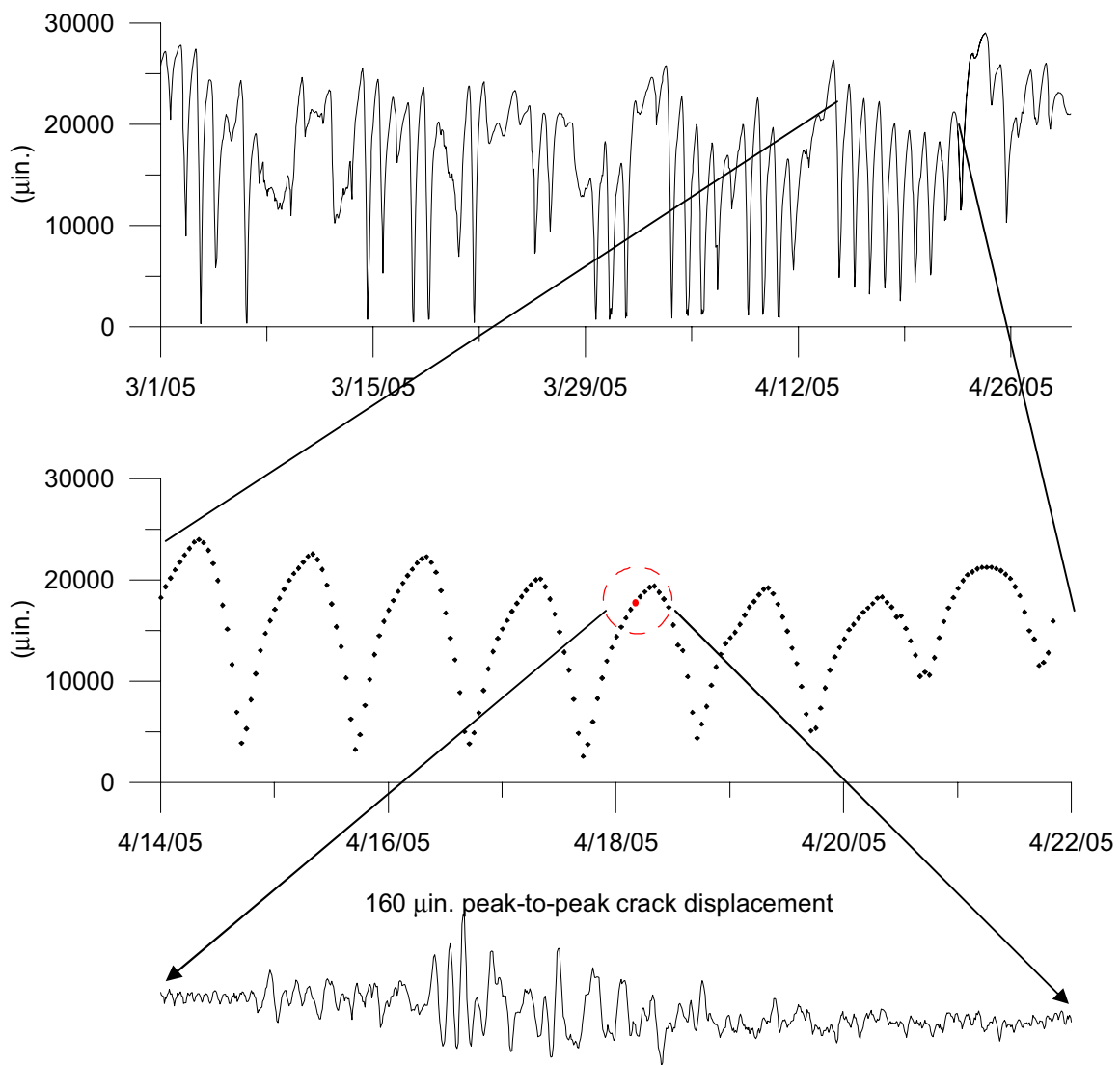


Figure 2.18 Long-term exterior crack behavior compared to blast response

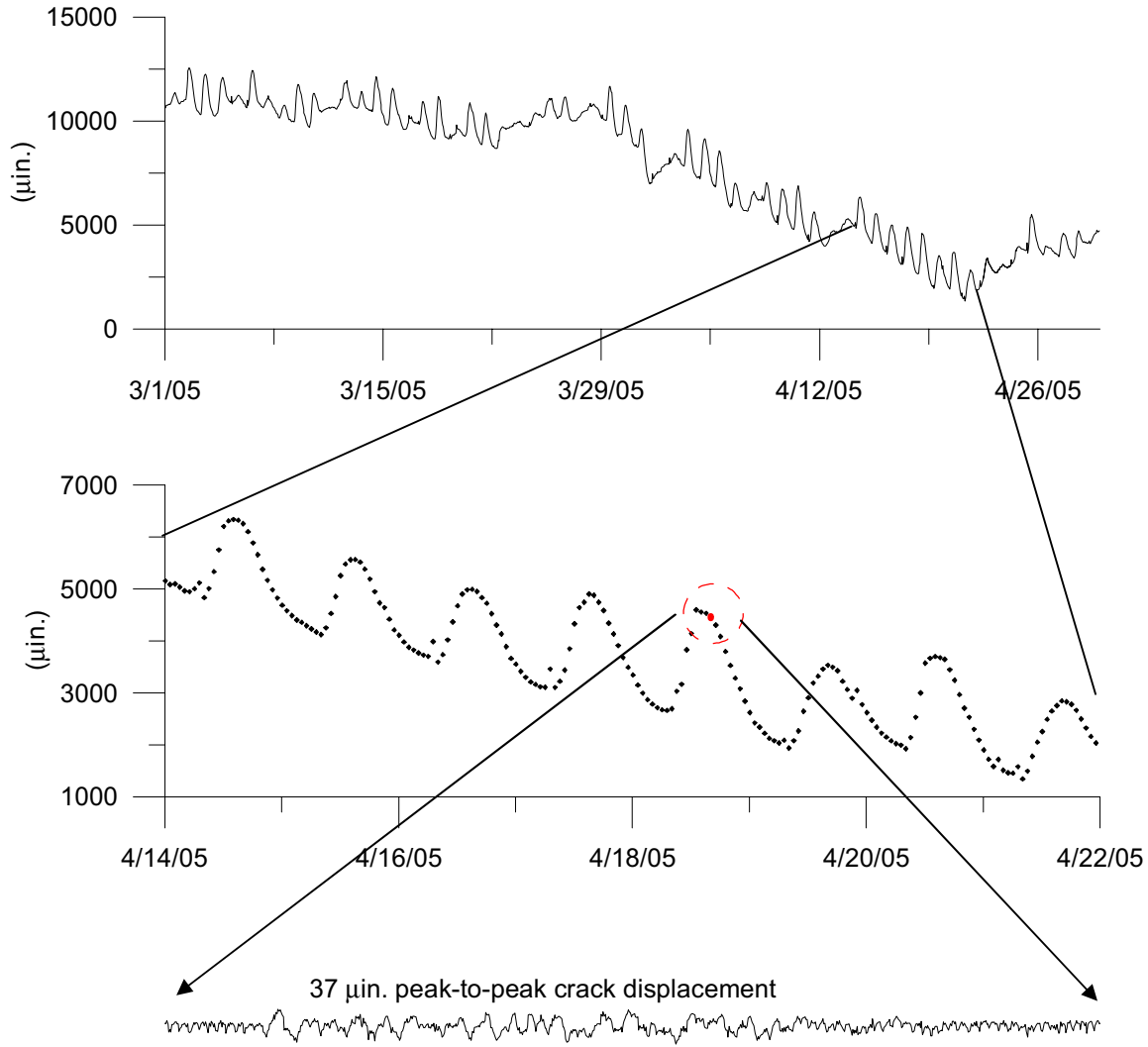


Figure 2.19 Long-term bedroom crack behavior compared to blast event

vertical line, they may appear as a barely visible red dot within the dotted circle. They are so miniscule because they are drawn at the same scale as the long-term behavior. The actual dynamic crack motion is shown as a time history at the bottom of the three figures along with the peak-to-peak displacements. The dynamic displacement time histories are shown at the same scale on all three figures.

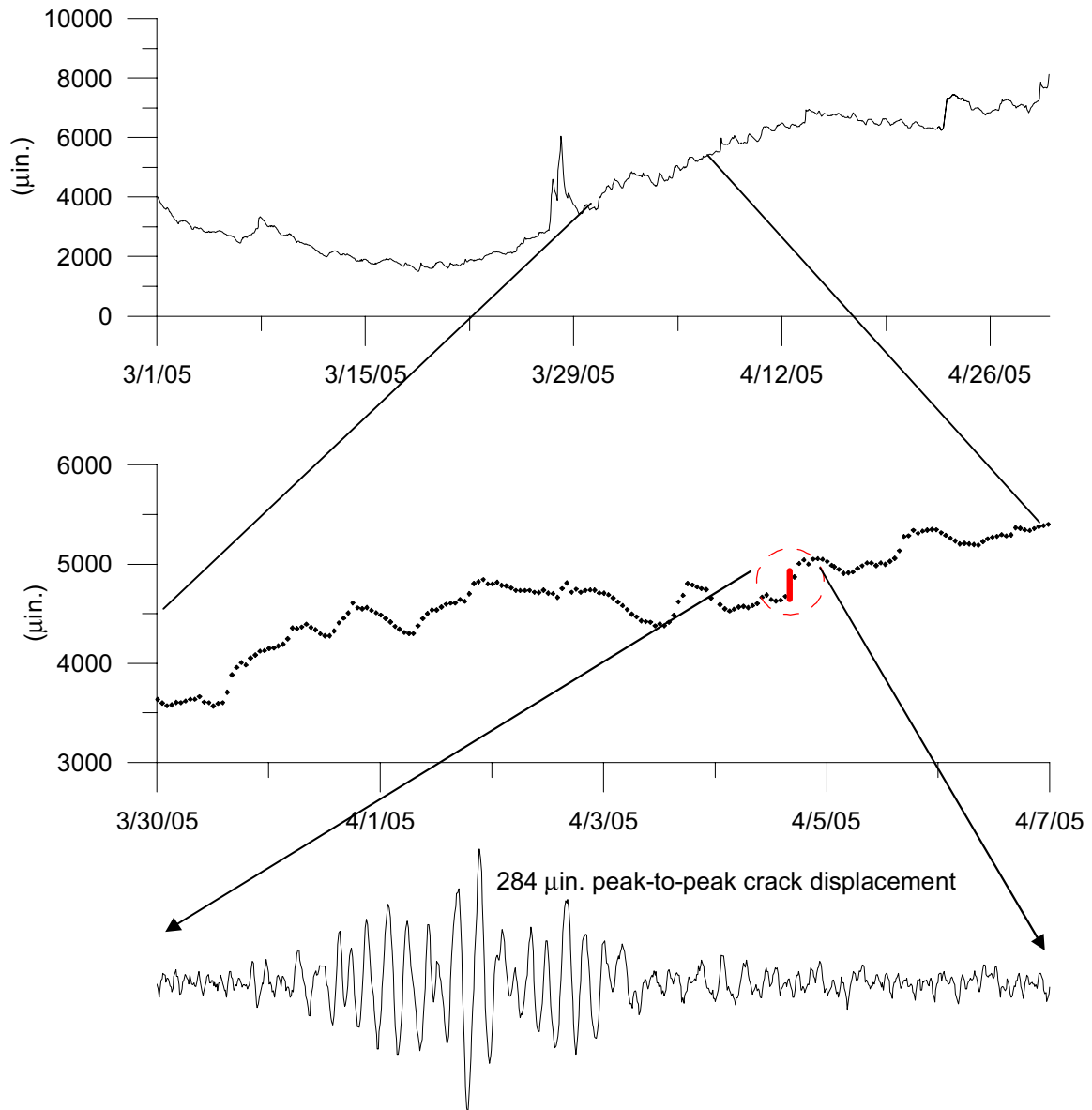


Figure 2.20 Long-term basement crack behavior compared to blast response

Dynamic Crack Behavior

This section describes dynamic response of cracks to blast induced ground motions producing peak-particle-velocities (PPV) greater than 0.04 ips. Each blast event contains three seconds of data for each of the three crack and null gauges and each of the three geophone directions longitudinal, transverse, and vertical. To ensure the full dynamic event is recorded, the three seconds includes one second of data prior to the triggering point and two seconds after the triggering point.

Table 2.3 summarizes all 37 recorded blast events that occurred between January 14th and June 2nd of 2005. Event histories from the gray highlighted blasts were employed to determine the sensitivity of the crack response to typical descriptors of ground motions. Listed are the maximum ground motions in all three directions, the maximum crack displacement response for each of the three cracks, and a Fast Fourier Transform frequency analysis of the longitudinal ground motions, which are usually the largest. As the table shows, the majority (all but 9) of the ground motions are less than 0.1 ips. All of the larger blast events (> 0.1 ips) occurred before March 7th, which is also the date of the largest blast (0.17ips).

Time histories of ground motions and crack response produced by the March 7th blast event are shown in Figure 2.21 producing the largest PPV of all recorded blasts. Shown are the three directions of ground motion and all three crack displacement responses. Listed with each ground motion is the PPV and with each crack displacement response is the maximum peak-to-peak displacement. The exterior brick and bedroom drywall cracks are in walls that are parallel to the longitudinal component of ground motion while the CMU basement crack is parallel to the transverse component. Even though the March 7th blast produced the largest

Table 2.3 Ground motion, frequency, and crack displacement for all blast events in Kentucky

| Shot Date | GROUND MOTION | | | | CRACK DISPLACEMENT | | |
|-----------|------------------|----------------|--------------|------------------------------|--------------------|----------------|---------------|
| | Longitudinal PPV | Transverse PPV | Vertical PPV | FFT Frequency (Longitudinal) | Exterior Crack | Basement Crack | Bedroom Crack |
| | (in/sec) | (in/sec) | (in/sec) | (Hz) | (μ in.) | (μ in.) | (μ in.) |
| 01/18/05 | 0.11 | 0.08 | 0.05 | 45 | 414 | 316 | 79 |
| 01/20/05 | 0.15 | 0.08 | 0.14 | 35 | 444 | 379 | 104 |
| 01/25/05 | 0.14 | 0.08 | 0.06 | 55 | 165 | 421 | 89 |
| 01/26/05 | 0.12 | 0.09 | 0.07 | 45 | 293 | 386 | 74 |
| 02/02/05 | 0.14 | 0.06 | 0.05 | 53 | 250 | 317 | 86 |
| 02/07/05 | 0.06 | 0.04 | 0.04 | 41 | 219 | 365 | 96 |
| 02/08/05 | 0.13 | 0.07 | 0.08 | 55 | 302 | 271 | 90 |
| 02/15/05 | 0.14 | 0.10 | 0.09 | 43 | 143 | 396 | 114 |
| 02/16/05 | 0.14 | 0.12 | 0.10 | 43 | 355 | 476 | 82 |
| 02/22/05 | 0.05 | 0.04 | 0.03 | 31 | 347 | 236 | 93 |
| 03/01/05 | 0.08 | 0.06 | 0.06 | 54 | 192 | 227 | 70 |
| 03/03/05 | 0.09 | 0.06 | 0.06 | 44 | 216 | 417 | 96 |
| 03/07/05 | 0.17 | 0.13 | 0.06 | 45 | 348 | 687 | 82 |
| 03/10/05 | 0.04 | 0.03 | 0.03 | 36 | 159 | 107 | 56 |
| 03/15/05 | 0.07 | 0.05 | 0.05 | 48 | 214 | 163 | 60 |
| 03/16/05 | 0.05 | 0.05 | 0.04 | 45 | 244 | 163 | 71 |
| 03/22/05 | 0.06 | 0.06 | 0.06 | 31 | 248 | 176 | 59 |
| 03/24/05 | 0.06 | 0.05 | 0.04 | 33 | 176 | 125 | 60 |
| 04/04/05 | 0.06 | 0.06 | 0.05 | 32 | 35 | 166 | 61 |
| 04/04/05 | 0.07 | 0.04 | 0.04 | 35 | 36 | 284 | 74 |
| 04/06/05 | 0.07 | 0.05 | 0.03 | 34 | 152 | 132 | 41 |
| 04/11/05 | 0.06 | 0.05 | 0.03 | 47 | 164 | 187 | 56 |
| 04/12/05 | 0.07 | 0.06 | 0.05 | 36 | 264 | 221 | 63 |
| 04/14/05 | 0.05 | 0.06 | 0.03 | 36 | 208 | 175 | 44 |
| 04/18/05 | 0.05 | 0.04 | 0.03 | 41 | 160 | 136 | 35 |
| 04/25/05 | 0.06 | 0.05 | 0.04 | 43 | 162 | 164 | 52 |
| 04/27/05 | 0.05 | 0.04 | 0.03 | 41 | 208 | 104 | 52 |
| 04/28/05 | 0.06 | 0.04 | 0.03 | 43 | 138 | 135 | 43 |
| 05/02/05 | 0.06 | 0.07 | 0.04 | 34 | 187 | 169 | 61 |
| 05/03/05 | 0.04 | 0.04 | 0.03 | 43 | 106 | 116 | 33 |
| 05/04/05 | 0.04 | 0.06 | 0.05 | 41 | 169 | 162 | 47 |
| 05/05/05 | 0.06 | 0.07 | 0.05 | 34 | 197 | 169 | 51 |
| 05/09/05 | 0.05 | 0.08 | 0.05 | 42 | 180 | 170 | 63 |
| 05/11/05 | 0.06 | 0.04 | 0.05 | 43 | 171 | 126 | 53 |
| 05/13/05 | 0.07 | 0.05 | 0.04 | 43 | 258 | 158 | 60 |
| 05/17/05 | 0.05 | 0.04 | 0.04 | 58 | 147 | 142 | 36 |
| 05/26/05 | 0.04 | 0.05 | 0.04 | 42 | 140 | 133 | 65 |

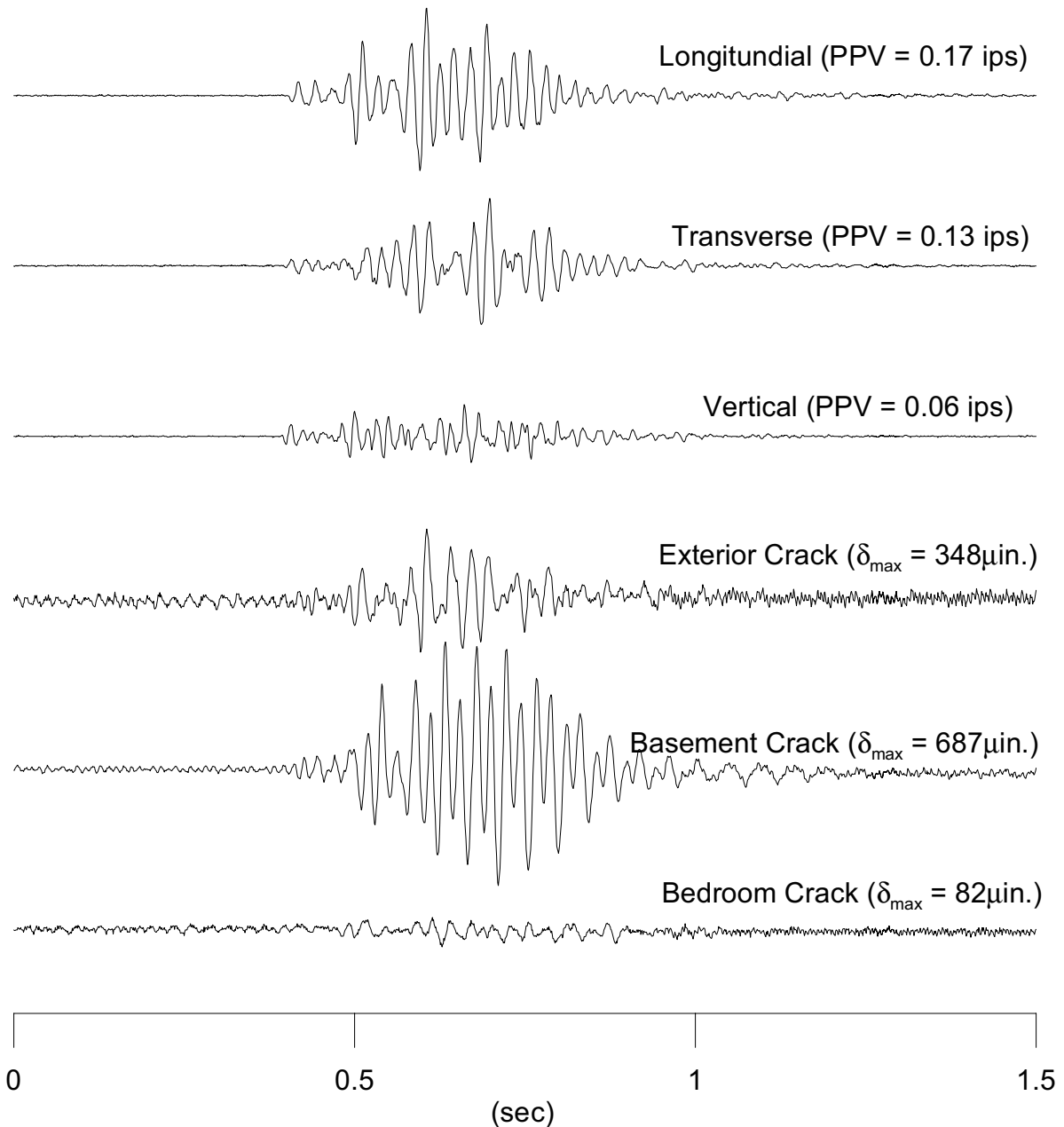


Figure 2.21 Ground motions and crack response for the March 7th blast

PPV, it is considered typical in that the longitudinal direction is generally the largest ground motion direction for this site and the bedroom crack was always the least responsive. The exterior and basement cracks, in exterior brick and between CMU blocks respectively, both respond more than the bedroom drywall crack. The peak-to-peak amplitudes of exterior and basement cracks often exceed 300 micro-inches while the bedroom crack typically responds

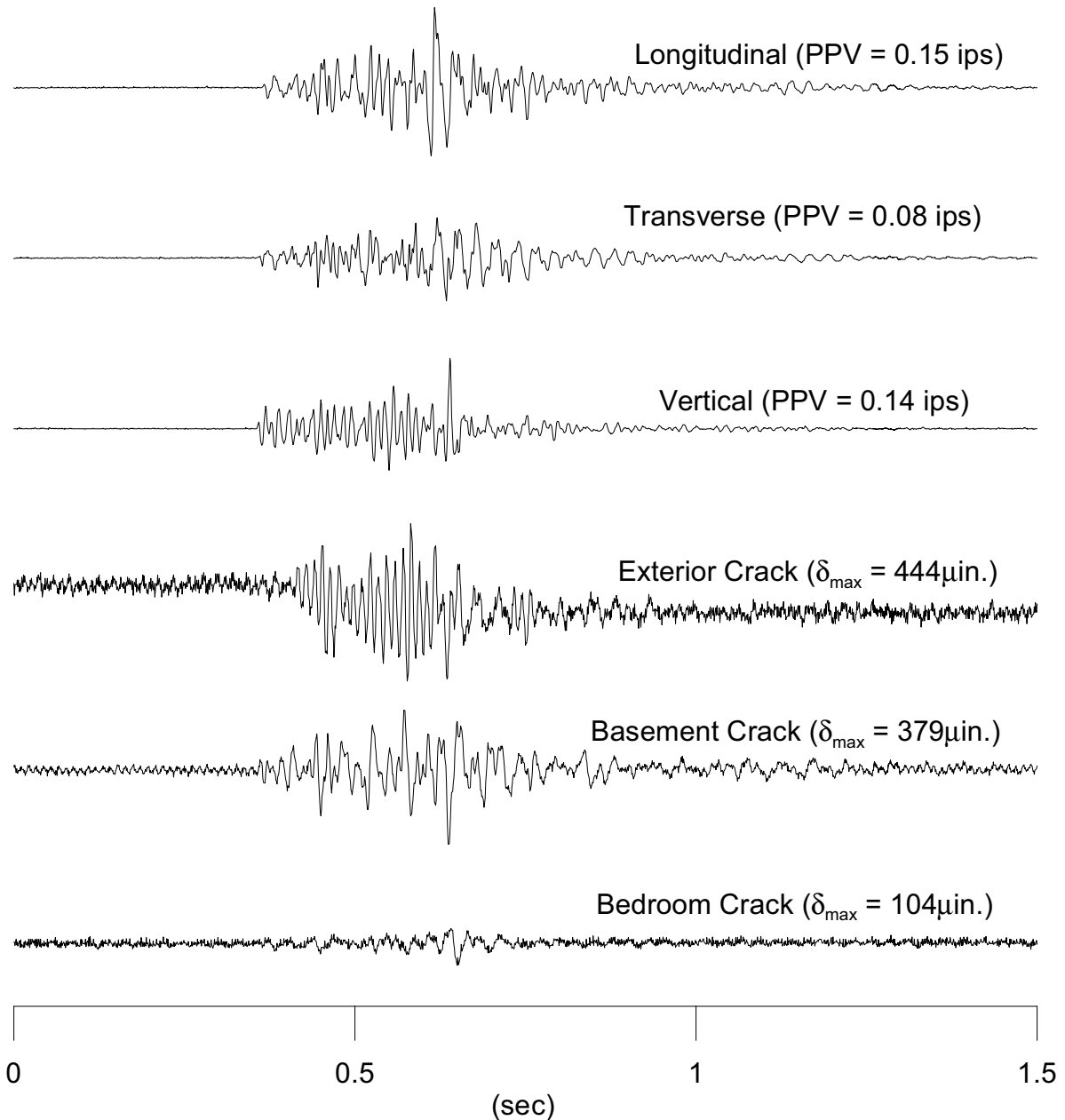


Figure 2.22 Ground motions and crack response for Comp the January 20th blast

less than 100 micro-inches peak-to-peak. However, these dynamic responses are much smaller than the long-term displacements discussed in the previous section. Three more comparisons of ground motion and crack response are shown in Figures 2.22, 2.23 and 2.24 to provide pairs of events with different dominant longitudinal frequencies, yet similar

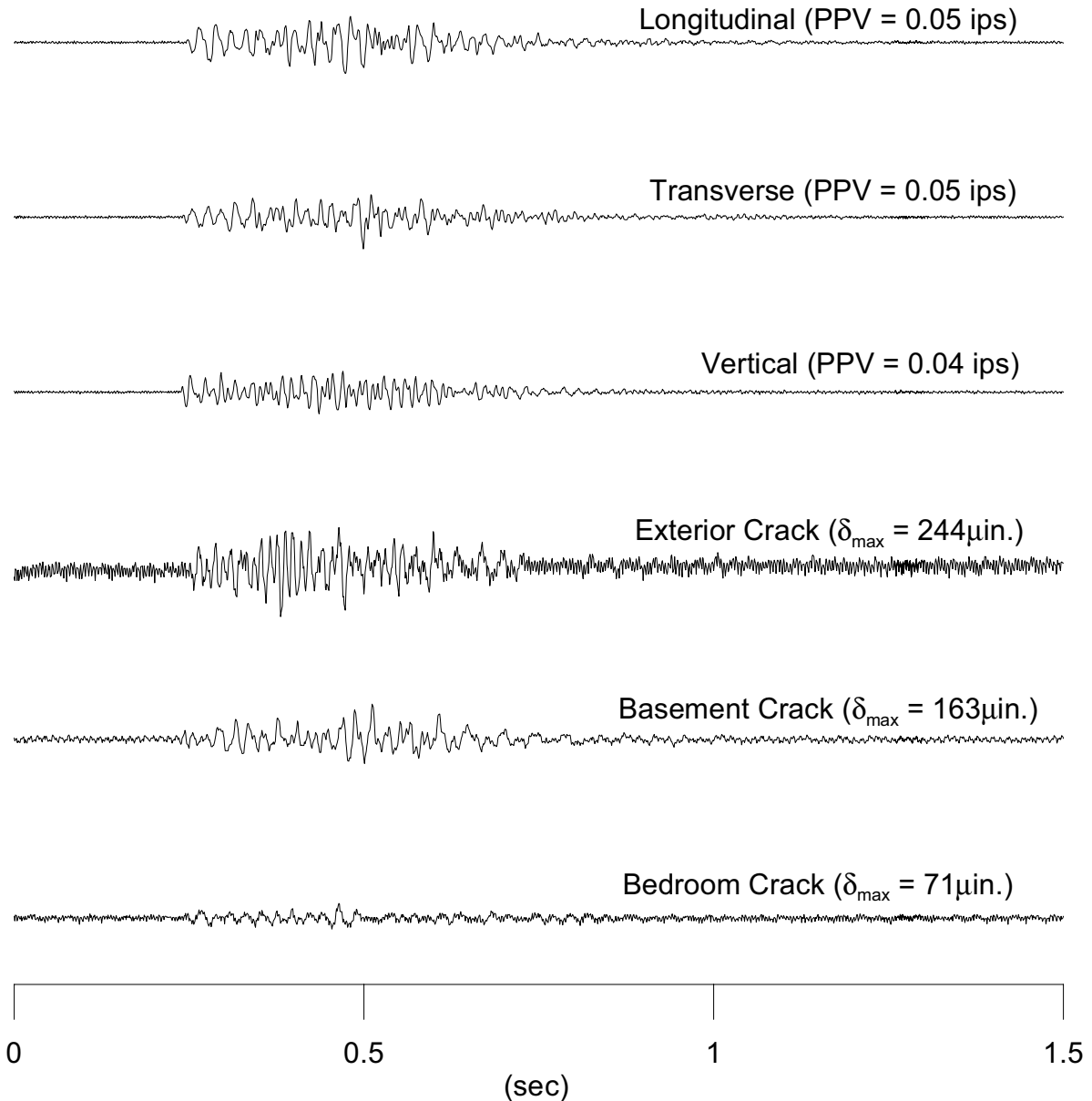


Figure 2.23 Ground motions and crack response for the March 16th blast

PPV's. Each pair consists of a high and low dominant frequency. The dominant frequencies for January 20th and March 7th pair with high PPV's are 35 Hz and 45 Hz respectively; those for the lower PPV pair March 16th and May 17th are 45 Hz and 58 Hz respectively. The January 20th blast, which produced the lower dominant longitudinal frequency of 35 Hz,

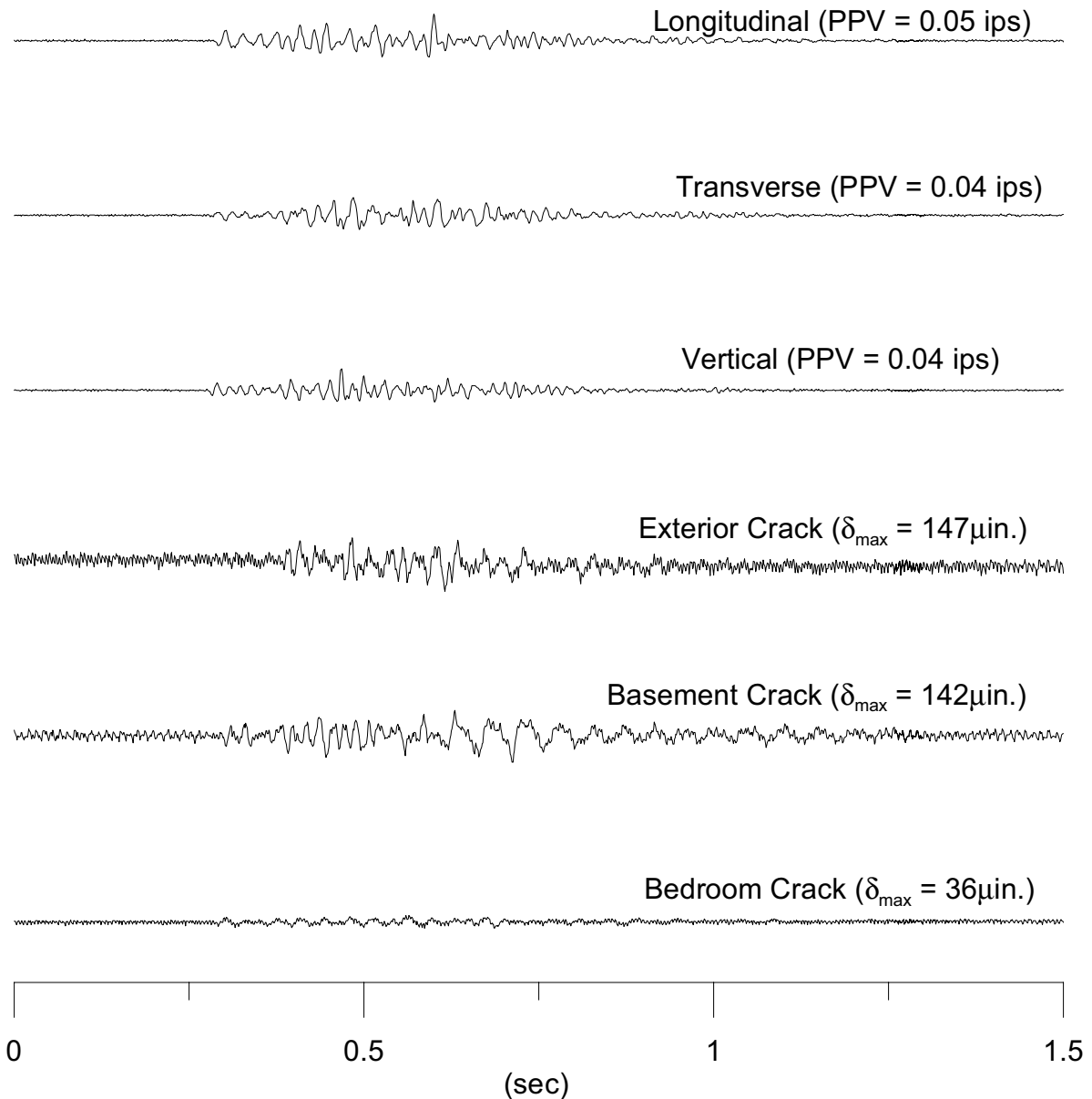


Figure 2.24 Ground motions and crack response for the May 17th blast

induced larger crack displacements for both the exterior and bedroom cracks and a lower crack displacement for the basement crack in comparison to the other, high PPV blast with a higher excitation frequency. The March 16th blast, which contained the lower dominant frequency of 45 Hz of the low PPV pair, produced larger crack displacements for all three

cracks than did the event with similar PPV but higher dominant excitation frequency. The trend of the lower dominant frequency blasts causing greater crack displacement is expected since the natural frequency of a one-story structure is usually 5-10 Hz and that of walls and floors is 10-20 Hz. A greater response is expected when excitation frequencies are closer to the natural frequency of the superstructure or structural components.

Effects of excitation frequency can be investigated by considering the ratio of the crack displacement to the sinusoidal displacement approximation as shown in Equation 2.2. The sinusoidal approximation is calculated by dividing the measured parallel (to the wall which contains the crack) PPV, or V_{ground} , of the incoming ground motions by the circular dominant frequency of the same wave ($2*\Pi*f$). The displacement ratio is greater in the exterior brick crack for the lower dominant frequency for both the high and low PPV comparisons as seen in Table 2.4. For the basement crack, the higher dominant frequencies for both the high and low PPV comparison result in larger displacement ratios. The lower

$$Displacement\ ratio = \frac{\delta_{crack}}{V_{ground} * \left(\frac{1}{2 * \Pi * f}\right)} \quad (2.2)$$

Table 2.4 Comparison of ground displacement to crack displacement ratios

| crack | Lower PPV | | Higher PPV | |
|----------|--|---|--|--|
| | Low frequency (45 Hz) <i>March 16th</i> | High frequency (58 Hz) <i>May 17th</i> | Low frequency (35 Hz) <i>January 20th</i> | High frequency (45 Hz) <i>March 7th</i> |
| Exterior | 1.38 | 1.07 | 0.65 | 0.58 |
| Basement | 0.92 | 1.29 | 1.04 | 1.49 |
| Bedroom | 0.50 | 0.33 | 0.16 | 0.39 |

dominant frequency produces a larger displacement ratio for the low PPV, yet a smaller ratio for the high PPV for the bedroom crack. This displacement ratio analysis is not consistent and therefore makes no useful correlation for this particular study.

Correlations can be made between crack displacements and various descriptors of ground motion to determine which descriptor could be employed as the best descriptor. Figure 2.25 presents correlations for all three cracks with parallel PPV, peak ground displacement, and peak relative displacement calculated from the pseudo velocity response spectrum of the ground motions. The fifteen blasts (highlighted in gray) in Table 2.3 that were employed in this correlation were chosen to include five blasts producing high and low PPV's and five intermediate PPV's. When assessing each correlation, only ground motion in the direction parallel to the wall containing the crack was considered, since crack displacement was measured in the plane of the wall. The bedroom and exterior cracks are associated with the longitudinal ground motions and the basement crack with the transverse direction.

Peak crack displacements can be compared directly to PPV as shown in Figure 2.21. Here, the exterior crack peak displacement occurred just after the peak PPV in the longitudinal direction. The longitudinal and transverse ground particle velocity time histories were integrated to produce ground displacements time histories in the respective directions and compared to the crack displacements as shown in Figure 2.25*b*.

Relative displacements between the ground and the structure can be estimated by calculating a single-degree-of-freedom (SDOF) response for this structure. Since the natural frequency for this structure is unknown, the average response in the 10 to 16 Hz range with 5% damping is employed as an estimate of the relative displacement. This frequency range

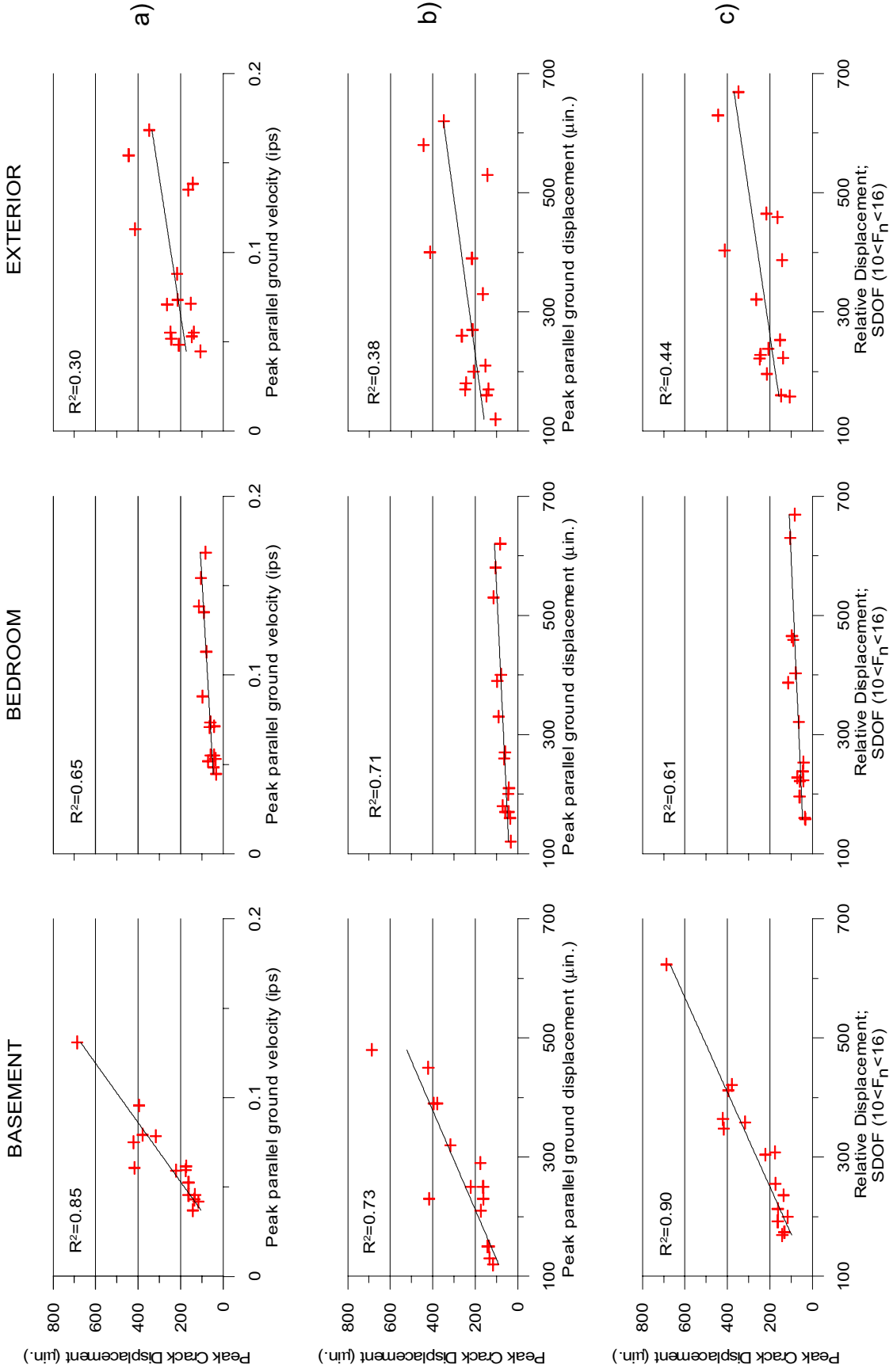


Figure 2.25 Correlations between measured crack displacement and computed displacements and peak ground velocities

was employed because the cracks were located on walls (which might have natural frequencies in the 10-20 Hz range) and were expected to respond to wall as well as superstructure motions, whose natural frequency would be closer to 5-10 Hz. Figure 2.26 shows the response spectra for longitudinal motions for the four example events. Figure 2.27 compares relative displacement time histories of a structure in the longitudinal and transverse direction for the March 7th ground motions. The relative displacement time histories were obtained by computing single degree of freedom response of a system with a 5% damping ratio and a natural frequency of 12 Hz to ground motions produced by the March 7th blast.

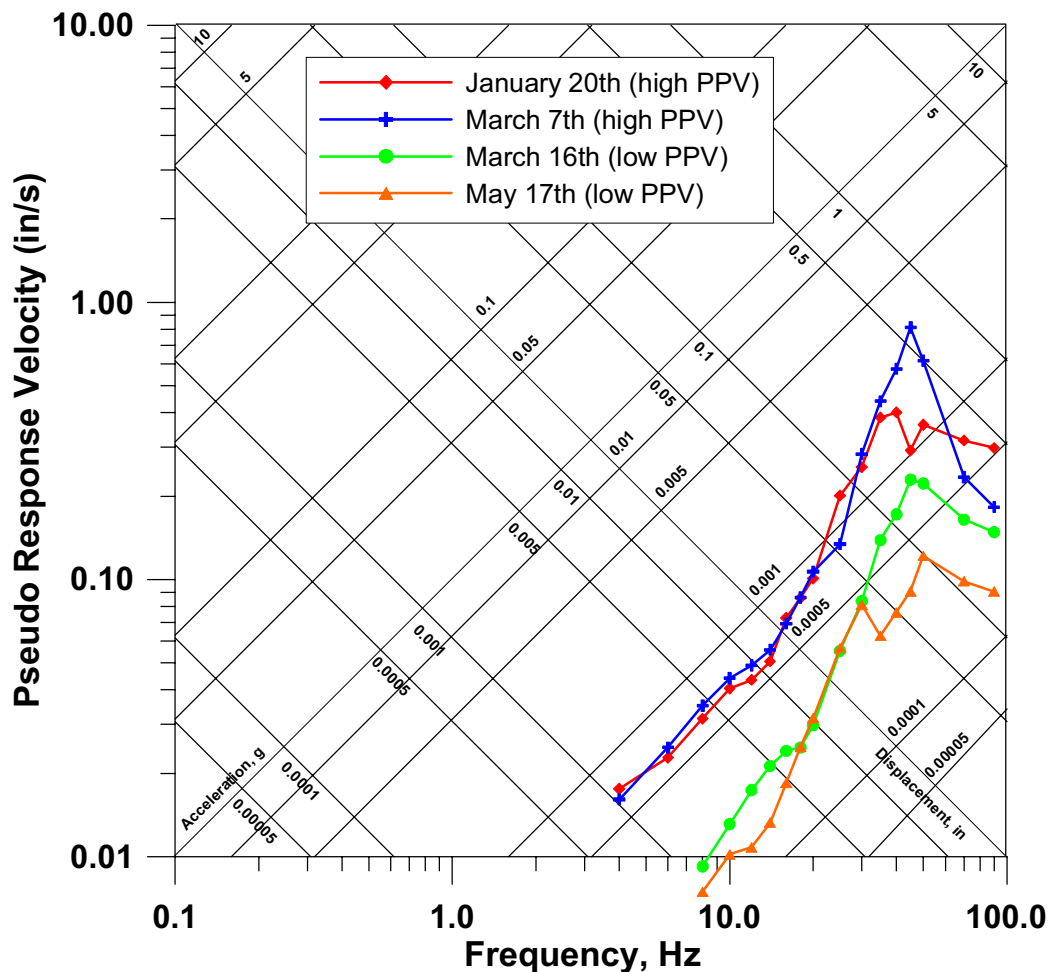


Figure 2.26 Pseudo-velocity response spectra of the longitudinal excitation ground motions for the four example events

With the assumed damping and frequency values, both the transverse and longitudinal relative displacements computed to be approximately 1200 micro-inches peak-to-peak as seen in Figure 2.27.

Figure 2.25 shows that for all three cracks, crack displacement increases with all three estimators. Each of the graphs include a regression coefficient (R^2) as listed in each plot in Figure 2.25. The basement crack exhibited the highest regression coefficients ($R^2 = .85-.90$) for all three of the correlations. The exterior crack exhibited the lowest regression coefficients ($R^2=.30-.44$) for all three of the correlations. Except for the bedroom, the SDOF correlations result in the highest regression coefficients. In this thesis, the square of the

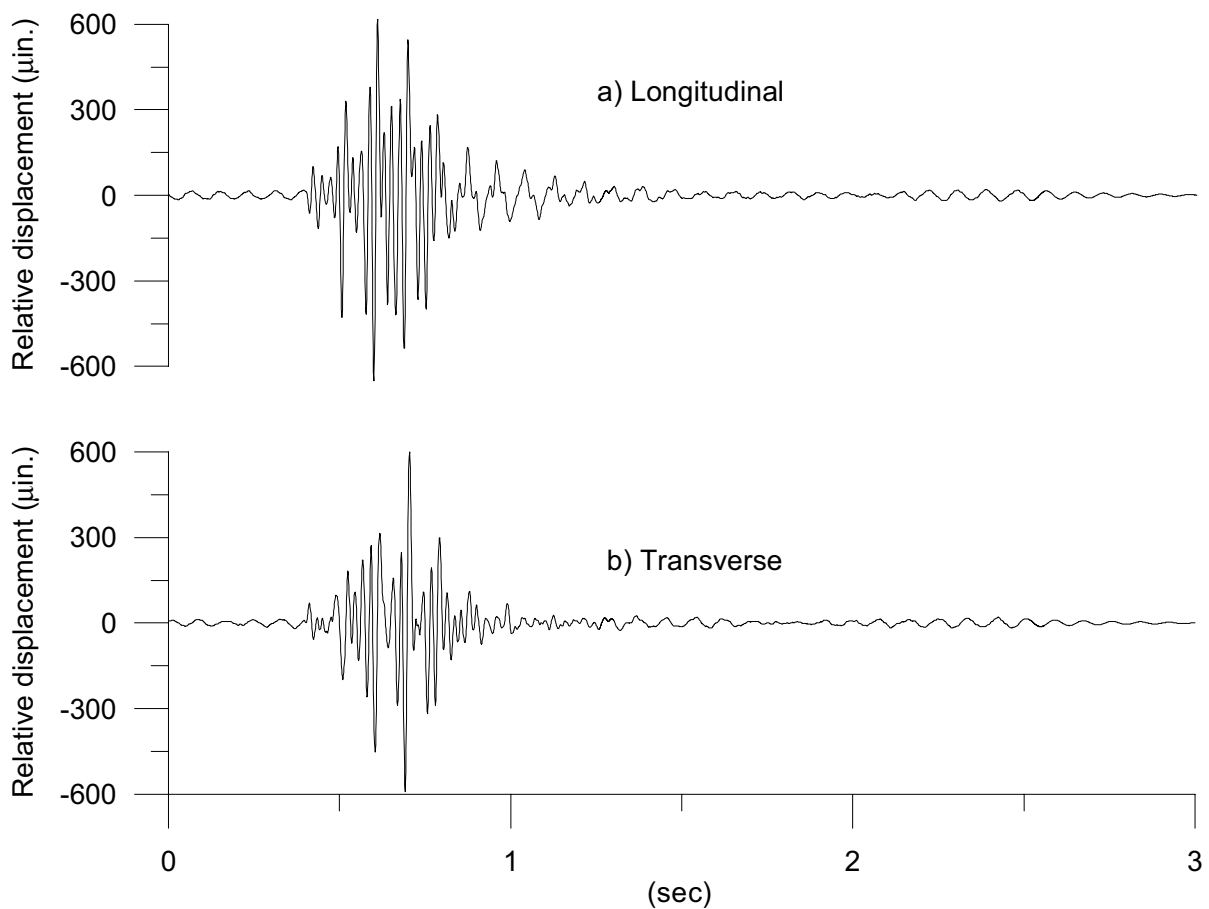


Figure 2.27 Relative displacement time histories of a 12 Hz structure with 5% damping to the March 7th ground motions.

regression coefficient, R^2 , was employed to describe the tightness of data to a best-fit trendline. The R^2 value is defined herein as the square of the Pearson product moment correlation coefficient, which is the proportion of the variance in y, depending on the variance in x. A larger regression coefficient implies more tighter fit of the data to the trendline.

Underground vs. Surface Quarries

There are several differences in the excitation environment in this case when compared to others that have been studied. The first difference lies in the high excitation frequency. As shown in Table 2.3, the average dominant excitation frequency is 42 Hz with a range of 31 to 58 Hz. There appears to be no surface wave excitation as well as an absence of an air pressure excitation to the structure.

The significance of these differences is shown in Figure 2.28. This figure compares the excitation environment and crack response of this Kentucky site with that of the Milwaukee test house. The instrumented crack in Milwaukee is located in an overly flexible ceiling as described by others (McKenna, 2002 and Louis, 2000). This test house is located approximately 1500 ft. from a surface limestone quarry. The displacements listed near each crack response are peak-to-peak values. The time scale of all plots in Figure 2.28 is three seconds.

As shown in Figure 2.28, the air overpressure for a typical surface quarry produces a significant crack response, whereas the underground quarry produces no such excitation response. In addition, the ground motion produced by the surface mine has a dominant

frequency of 13 Hz. Other measurements from the surface mine reveal frequencies ranging from 12 to 20 Hz.

Due to the nature of the geometry of the underground mine in Kentucky, blasting produces ground motions dominated by body waves with an absence of lower frequency surface waves. On the other hand, blasting in the surface quarry produces lower frequency waves, which are presumed to be surface waves. These lower frequency motions arrive after

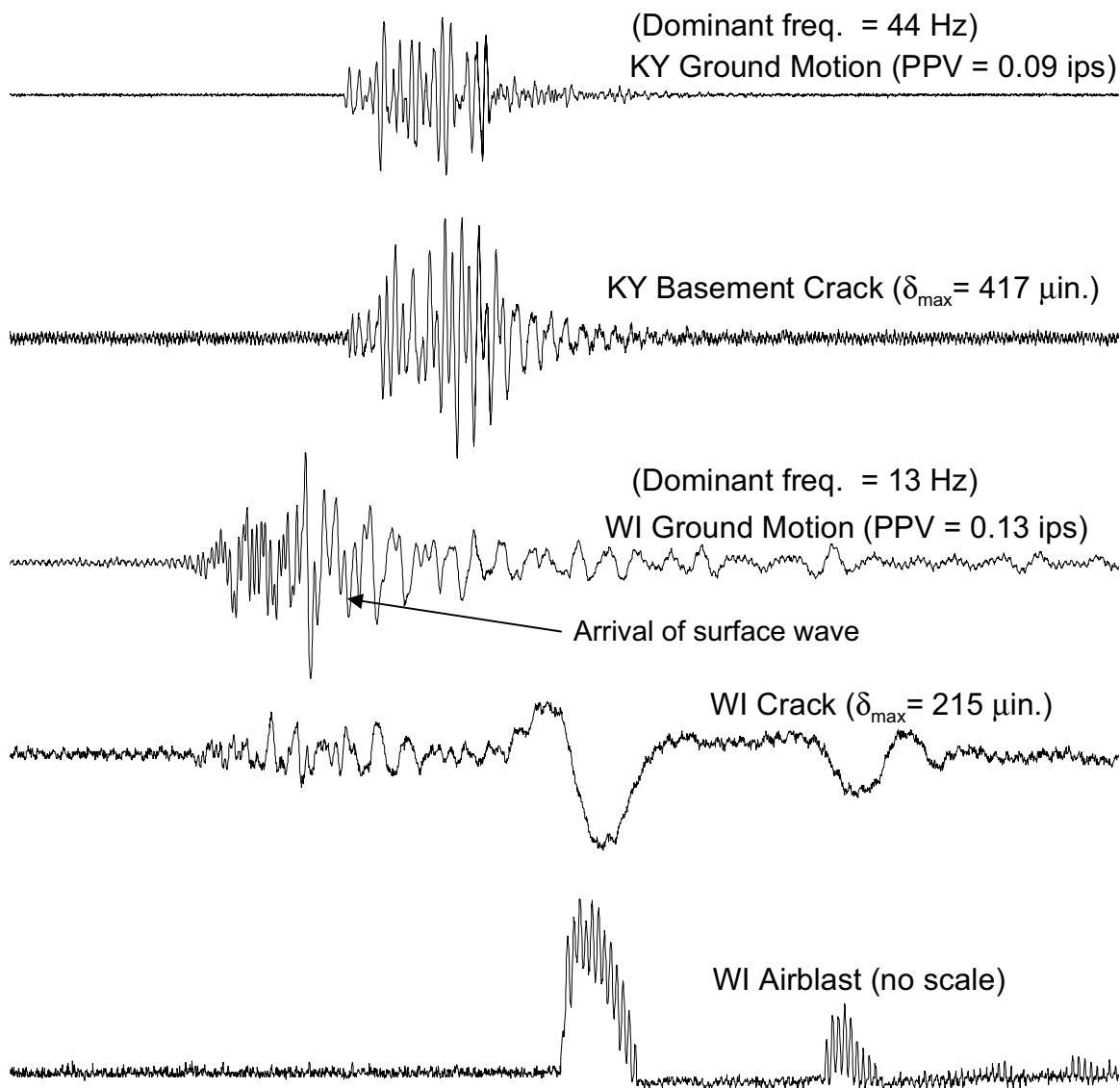


Figure 2.28 Comparison of ground motions and crack response between Kentucky and Wisconsin test structures

the higher frequency body waves, are lower in amplitude, and extend for longer durations of time. Air over pressures from the surface quarry produced the largest response for this particular crack. For other cracks in this house, the influence is smaller (McKenna, 2002). It is evident in Figure 2.28 that the two air pressure pulses are responsible for the large low frequency crack displacement responses.

Attic Response

In attempt to measure structural response to ground vibrations, a tri-axial geophone block was attached to the attic of the structure by another party (Revey, 2005). The trigger level was set to begin recording at 0.05 ips. The block was placed between the rafters on the upper side of the ceiling drywall as shown in Figure 2.29, so that the longitudinal direction was parallel to the short-axis of the structure. It was assumed that if the drywall is relatively stiff between the rafters, the drywall response in the transverse and longitudinal directions would be similar to the superstructure response in those directions. In the vertical direction, however, the drywall between the rafters may respond independently of the structure.



Figure 2.29 Picture showing the placement of the velocity transducer near the attic rafters

The attic geophone block was present for a little over a month during the period February 20th until March 31st. During this time, only five events exceeded the trigger level and were recorded. In the same time period, nine blasts were recorded by the ground geophones. As seen in Table 2.5 only one of the five attic responses occurred on the same date as a recorded blast, March 22nd. The largest blast ever recorded during the monitoring period occurred on March 7th and produced ground vibrations more than 3 times the trigger level at 0.17 ips. As Table 2.5 shows, an attic response was not recorded on this date. If the largest blast recorded did not trigger the attic transducers, it is likely then that no blast would cause enough structural response to trigger the attic transducers.

Table 2.5 Summary of recorded attic vibrations compared to recorded blast vibrations for the period in which the attic velocity transducer was installed

| Recorded Attic Vibrations | | Recorded Ground Vibrations due to Blasting | | Max. PPV (ips) |
|---------------------------|--------------|--|--------------|----------------|
| Date | Time | Date | Time | |
| Feb. 20 | 12:32 | Feb. 22 | 16:23 | .05 |
| | | March 1 | 16:22 | .08 |
| | | March 3 | 16:16 | .09 |
| | | March 7 | 16:20 | .17 |
| | | March 10 | 16:22 | .04 |
| | | March 15 | 16:26 | .07 |
| | | March 16 | 16:26 | .05 |
| March 22 | 16:11 | March 22 | 16:31 | .06 |
| | | March 24 | 16:17 | .06 |
| March 27 | 22:25 | | | |
| March 31 | 9:44 | | | |
| March 31 | 9:45 | | | |

Figure 2.30 compares the attic motions and the ground motions for March 22nd. It is seen that the recorded attic response is a series of six quick independent vibrations. Therefore it is not a result of the blast induced motion, which consists of one longer vibration.

Furthermore, every attic response recorded was triggered by the vertical direction, whereas every blast vibrations always triggered the buried geophone in either the transverse or longitudinal direction. The March 27th attic vibration was the only one which even produced amplitudes either transverse or longitudinal large enough (>.05 ips) to trigger an event, yet the vertical direction still governed that response. These attic vibrations probably result from some other phenomena other than the mine blasting, such as someone walking around in the attic or other domestic activity.

Vibrations produced by the mining operations do not induce a detectable structural response when the trigger level is set at 0.05 ips. Typical one-story structures have a natural frequency on the order of 5-10 Hz. The ground vibrations measured have relatively high

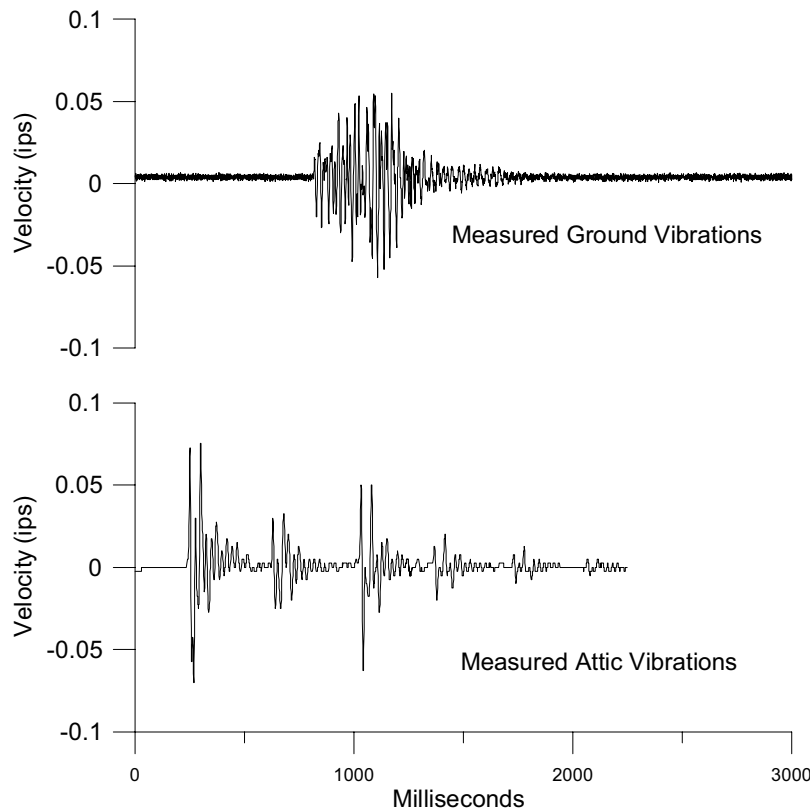


Figure 2.30 Plot of blast ground vibrations and measured attic movements on the same date of March 22nd

frequencies ranging 31-58 Hz, which may be too high to excite significant response for a structure with a natural frequency between 5 and 10 Hz.

Occupant Activity

It is important to understand how cracks respond to dynamic events other than blast vibration effects. During the installation of the equipment, researchers intentionally initiated typical household or occupant activities and recorded appropriate resulting crack behavior. Crack response was recorded while a person leaned on walls, pounded walls, and walked through doorways. The recording channels were set to collect data every millisecond (~1000 Hz) during all three tests to accurately capture the crack response and be able to correlate it to the performed activities. Table 2.6 presents measured crack displacement corresponding to induced occupant activity events. The measured crack displacements caused by the largest blast event are presented as well in Table 2.6. Approximate distances between the

Table 2.6 Measured crack displacements associated with dynamic events

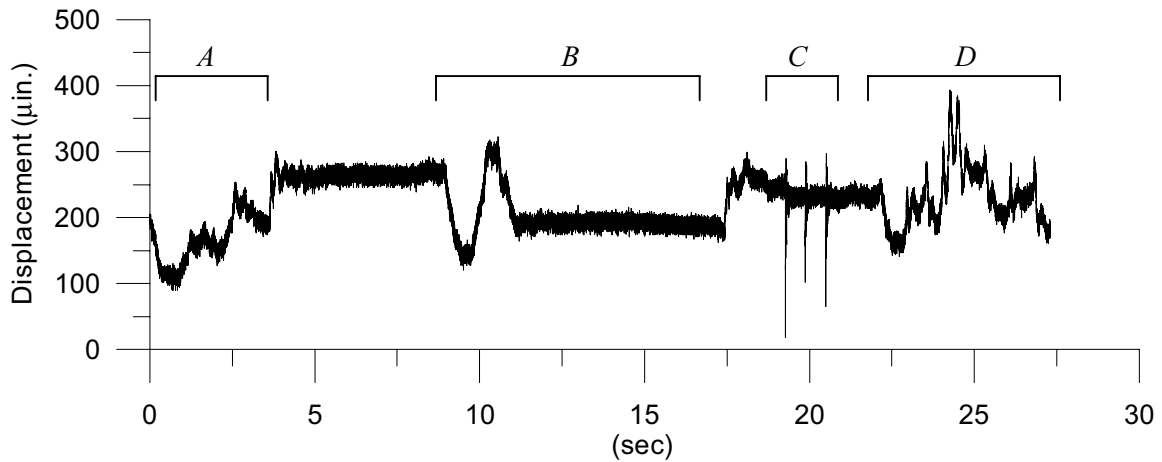
| Crack | Activity | Description | Approximate Distance from crack (ft) | Peak-to-Peak crack Displacement (µin.) |
|--------------|-----------------------|--------------------|---|---|
| Bedroom | lean on near doorjamb | with shoulder | 2 | 200 |
| | lean on far doorjamb | with shoulder | 4 | 175 |
| | pound wall | gentle with fist | 1 | 250 |
| | walk through doorway | typical walking | 2 to 6 | 250 |
| | largest blast | 0.168 ips | 1650 | 82 |
| Exterior | pound wall | moderate with fist | 0.5 | 450 |
| | push on wall | moderate with hand | 2 | 325 |
| | largest blast | 0.168 ips | 1650 | 348 |
| Basement | pound wall | moderate with fist | 3 | 350 |
| | largest blast | 0.168 ips | 1650 | 687 |

location of the activity and the crack are also included in the table.

Bedroom and exterior cracks responded more to typical household activities than to the highest ground motion from blasting. The basement wall crack responded more to blast motions than to moderate pounding on the wall near the crack. Pounding on the walls produced the largest response for occupant activities ranging in peak-to-peak displacements of 250-450 micro-inches as seen in Table 2.6. However, simply walking through the bedroom doorway into the bathroom produced a crack displacement of 250 micro-inches. As described in the previous section, the largest blast of 0.168 ips produced crack displacements ranging from 82-687 micro-inches peak-to-peak depending on the crack location and material.

Figure 2.31 illustrates the occupant activity response of the bedroom crack to deliberate household activity. Bedroom crack response was recorded for 30 seconds while the far doorjamb (A) and then the near doorjamb (B), which is closest to the door, was leaned upon. Then the wall was gently pounded on (C) and finally a 185 lb person walked back and forth through the doorway (D). Part A was recorded while the person was ending a lean on the far doorjamb as shown in the picture. At the beginning of the lean on the near doorjamb labeled as B, an abrupt crack displacement occurs but then remains constant while the person applies steady pressure to the wall. Upon release of this second lean, the crack almost returns to its original position. Part C displays a person gently pounding on the wall approximately one foot from the crack and is also shown in picture form. Lastly, part D contains the most dramatic crack response while a person simply walks back and forth through the doorway resulting in amplitude of 250 micro-inches crack displacement. During other monitoring times, crack responses similar to part D were recorded frequently, sometimes up to five to

eleven times daily. These occurrences are believed to be the result of the resident walking in and out of the master bathroom. Further discussion regarding this comparison is included in a later section.



| Event | Description | A | C |
|-------|-----------------------------|---|---|
| A | Ending lean on far doorjamb | | |
| B | Leaning on near doorjamb | | |
| C | Pounding on wall | | |
| D | Walking through doorway | | |

Figure 2.31 Induced occupant activity for bedroom crack

Figure 2.32 illustrates the occupant activity tests performed in the basement and outside the structure along with resulting respective crack responses. The exterior and basement crack responses were produced by moderately pounding on the wall near the crack. The exterior crack responses to pounding were larger than the basement crack. The greater

brick response is understandable given the flap of brick loosened from the structure by the cracking as shown in Figure 2.33. The sensor is placed directly above a triangle or “flap” of brick that seems disconnected from the rest of the brick mass. The crack in the basement CMU does not isolate a similar zone of disconnected mass. Thus, the smaller exterior brick mass can respond more to the pounding than the CMU mass. This concept can also be described by the stiffer response of the basement crack noticed in Figure 2.32. While the exterior crack requires about a ¼ second to equilibrate back to its baseline position before pounding, the basement crack appears to return to its original position instantaneously. For the basement crack, further occupant tests were performed during instrumentation removal in an effort to simulate unusual crack response noted to occur throughout durations of the monitoring period. This induced occupant activity included stomping on the first floor above

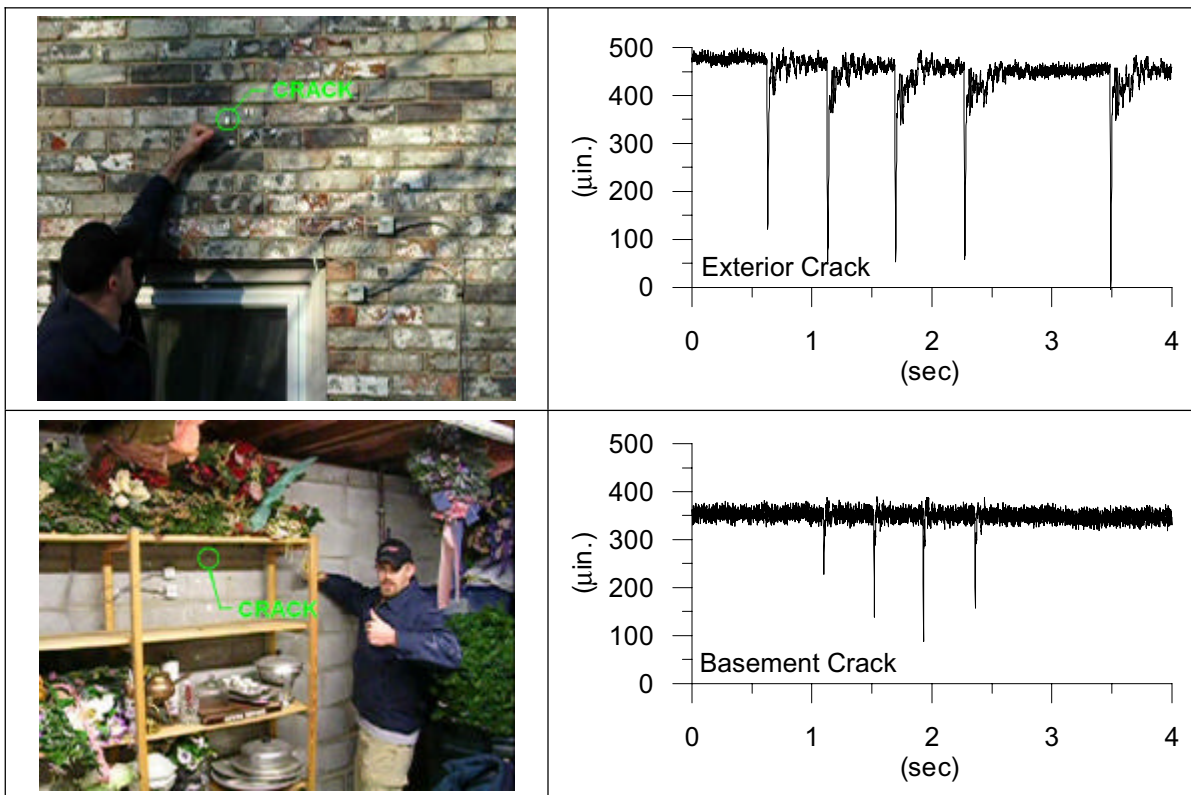


Figure 2.32 Induced occupant activity for exterior and basement cracks

the crack, opening and closing the front door which is located above the crack, and stomping on the floor in the basement in the general vicinity of the crack. None of the activities mentioned produced any significant basement crack response.

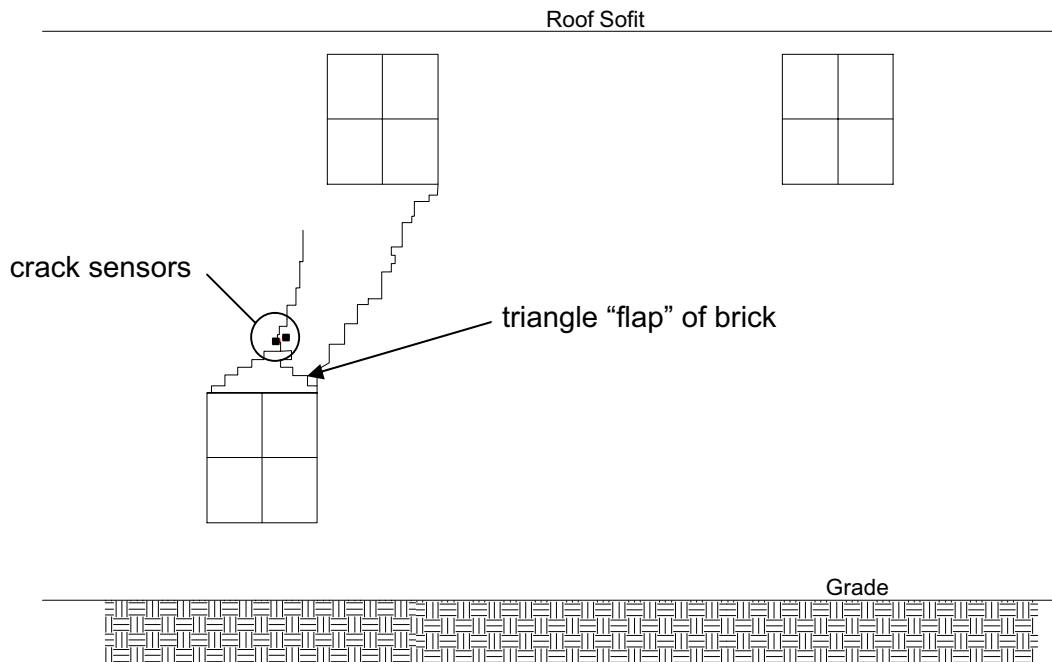


Figure 2.33 Elevation view of the brick wall which contains the exterior crack

From the figures and data provided, it is evident that daily household events such as walking through doorways and leaning on walls and other potential events such as pounding on walls can cause greater crack displacements than effects due to blast induced ground motions.

Detection of Unusual Behavior

High winds and domestic human occupant activities were suspected to influence crack behavior. These events are important as they are not detected or if detected, not identifiable during the normal operation of the ACM system. To detect these sporadic events, crack displacement responses were continuously recorded at fifty samples per second (~ 50 Hz) for extended periods of time ranging from two to seven days. Although one-thousand samples per second is the normal sampling rate for blast triggered events, it is impractical to sample at such a high frequency for extended periods because doing so would produce extraordinarily large data files. Fifty samples per second (~ 50Hz) was selected because it was believed to be sufficient to capture any unanticipated dynamic events, yet small enough to produce manageable data files, which still produced 4.32 million data points per day.

Exterior brick crack responses were collected for four days between March 4th and March 7th. For the majority of this time, the exterior crack showed no signs of odd or unusual behavior and time histories closely match typical long-term data collected hourly as shown in Figure 2.34. As expected, the 50 Hz data exhibits higher resolution and more accurately depicts the actual crack behavior. The only unusual behavior detected occurred towards the end of March 7th, which is seen in Figure 2.35. During this time, the exterior crack response was erratic and atypical, yet further investigation and analysis failed to reveal the cause of this behavior. A blast occurred at 4:20pm on March 7th, yet was undetectable and relatively insignificant when compared to the crack response seen during the entire twenty-four hour period. As seen in Figure 2.35, the exterior crack experiences larger displacements during a random time frame of four seconds in which no blast occurred with a peak-to-peak displacement exceeding 800 micro-inches than when subjected to a geophone triggered blast

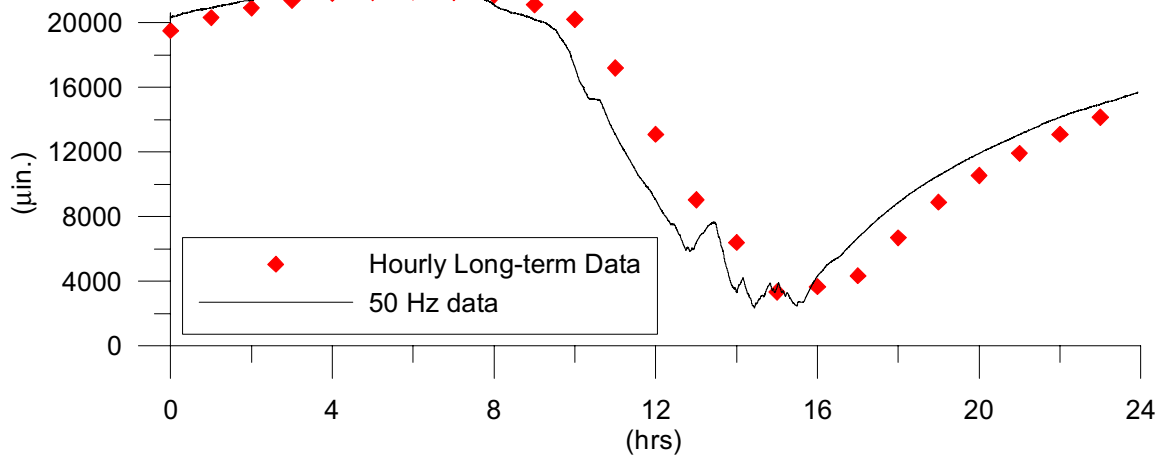


Figure 2.34 Comparison of hourly data and 50 Hz data for the exterior crack (March 4th)

event. As listed in Table 2.3, the March 7th blast induced the largest ground motions of 0.168 ips of any recorded blast, which produced a peak-to-peak displacement of 348 micro-inches in the exterior crack. For comparison, the exterior response of the February 8th blast is shown at the bottom (part b) of Figure 2.35.

Basement crack response was recorded continuously next between March 8th and March 9th. Although slightly difficult to see when viewing the entire twenty-four hour period, the basement crack response included unusual behavior in the form of “spikes” as shown in Figure 2.36. These spikes occurred consistently throughout both days of testing at irregular times. Figure 2.36 consecutively magnifies these spikes to illustrate the amplitude and duration of this atypical dynamic crack behavior. It was believed these spikes were result of domestic activities; therefore potential domestic activities were purposely performed and recorded in attempt to induce similar behavior in the basement crack. The activities performed included stomping around the basement, walking in and out the front door (which is located on the first floor above the crack), opening and slamming shut the front door, and stomping around in the garden in the proximity of the crack. All of these activities failed to

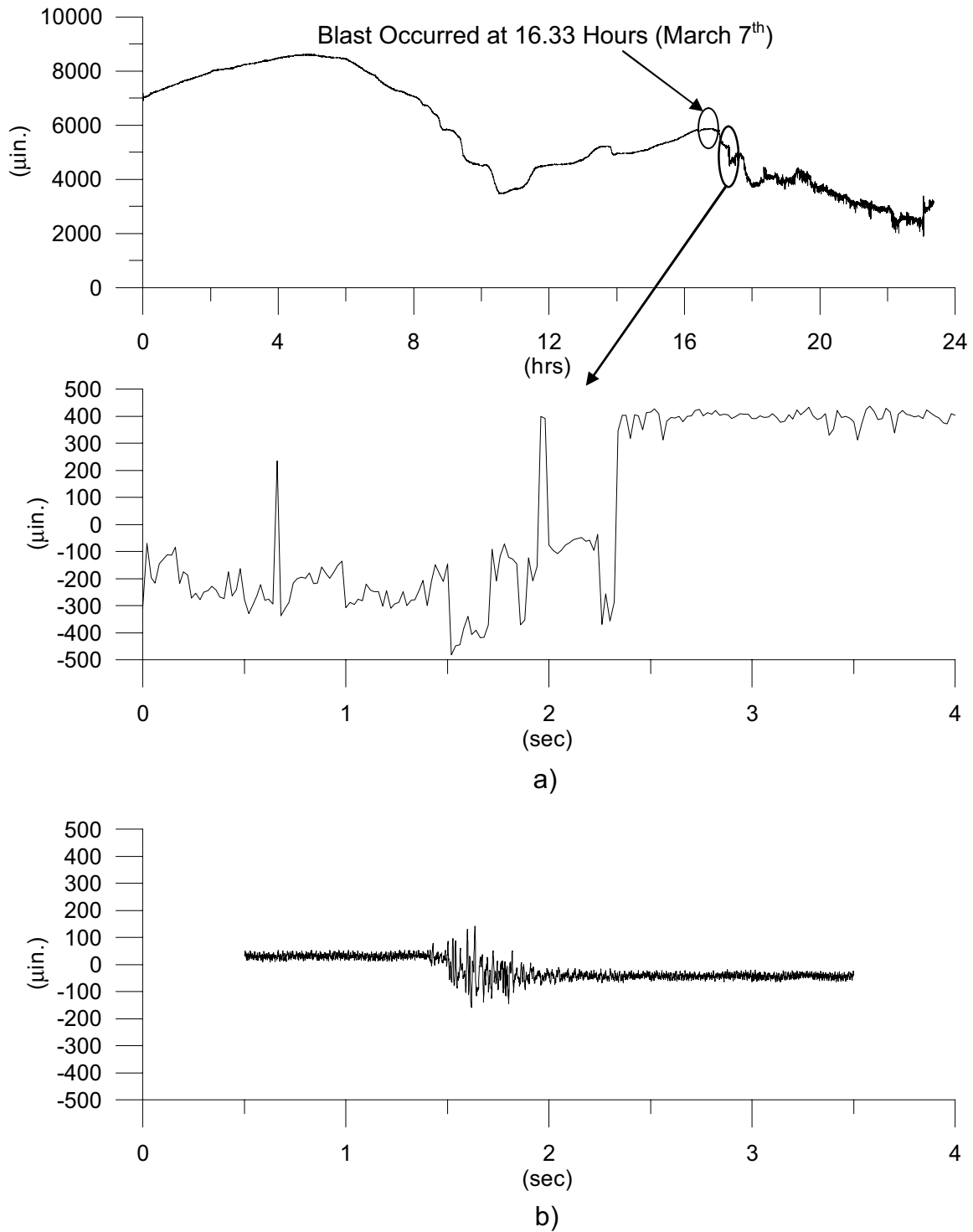


Figure 2.35 Exterior crack behavior during a non-blast period compared to a blast event a) 24 hour crack behavior recorded during 50 Hz testing with 4 second time window expanded below b) exterior crack response to blast event (Feb. 8th)

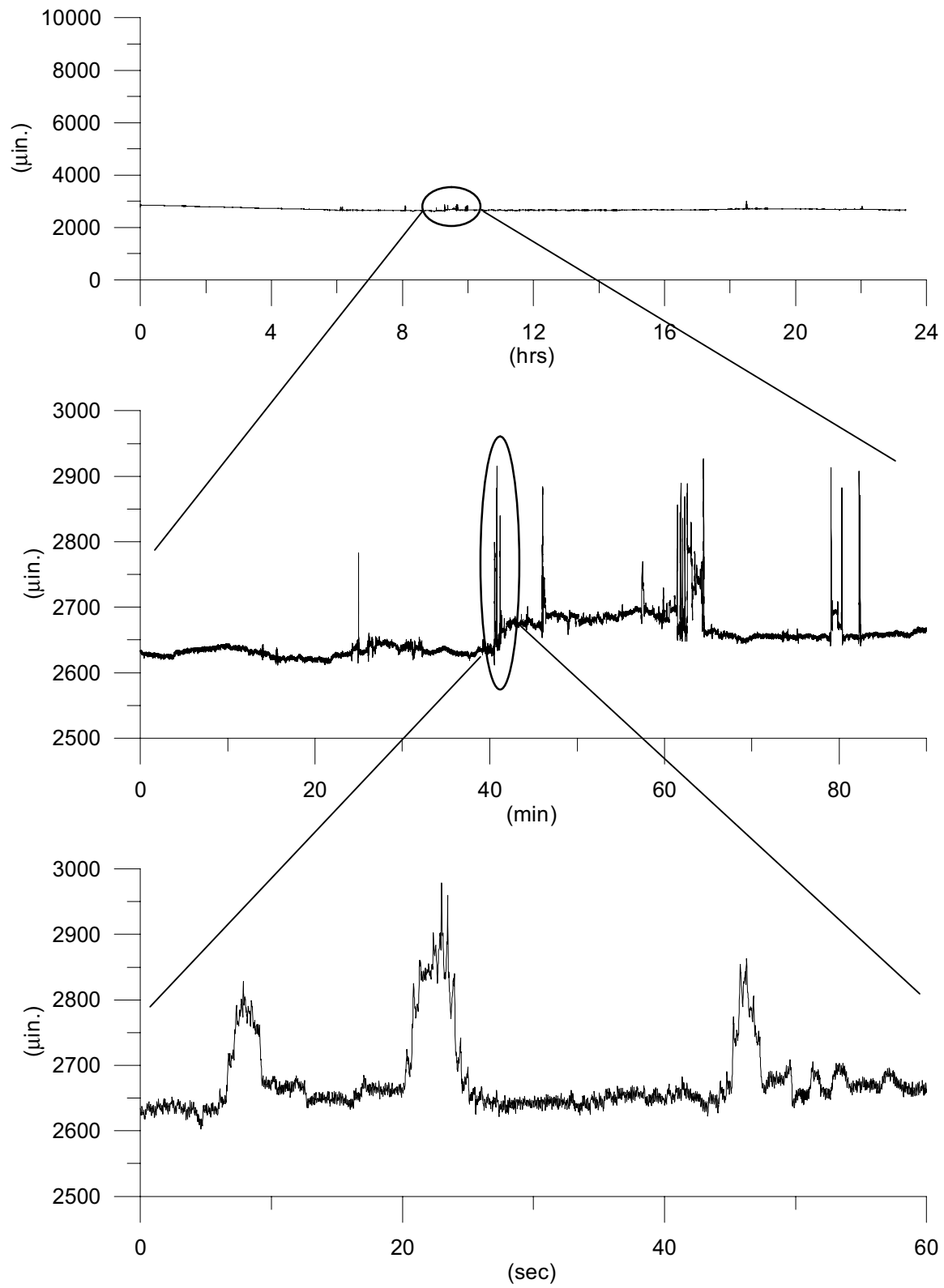


Figure 2.36 Basement crack response during recorded 50 Hz testing

produce similar spikes often seen in the basement crack behavior. It remains unclear the source of these spikes in crack displacement, however the amplitudes can be in excess of 300 micro-inches.

Finally, the bedroom crack response was recorded continuously at 50 Hz for seven days between March 10th and March 16th. As expected, the general response was representative of the regular long-term data collected hourly; however, as discussed in the previous section, spikes were noticed to occur throughout all seven days of testing similar to those in the basement. The bedroom crack response includes some five to eleven spikes daily during the seven days of observation as shown in Figure 2.37 and again were presumed to be the result of domestic activity. In Figure 2.37, two spikes from the 50 Hz study are compared to a previously recorded induced domestic activity of simply walking back and forth through the master bathroom doorway. From the similarity of these crack responses and the number of daily occurrences, it is believed that these spikes seen in the bedroom crack response are produced by the resident walking in and out of the master bathroom. The amplitude of the spikes seen in the bedroom crack can be in excess of 400 micro-inches.

Figure 2.38 compares the spikes seen in the basement crack displacement to the spikes seen in the bedroom crack displacement during the 50 Hz investigation. The spikes selected for the comparison are typical in that the bedroom spikes are usually longer in duration and exhibit slightly larger amplitudes than the basement spikes. Even when considering their differences in response, the spikes in the different crack locations appear fairly similar. Although already mentioned, occupant activities immediately above did not produce similar responses like walking through the master bed/bath door; thus some other, yet undefined, activity must have produced these basement crack responses.

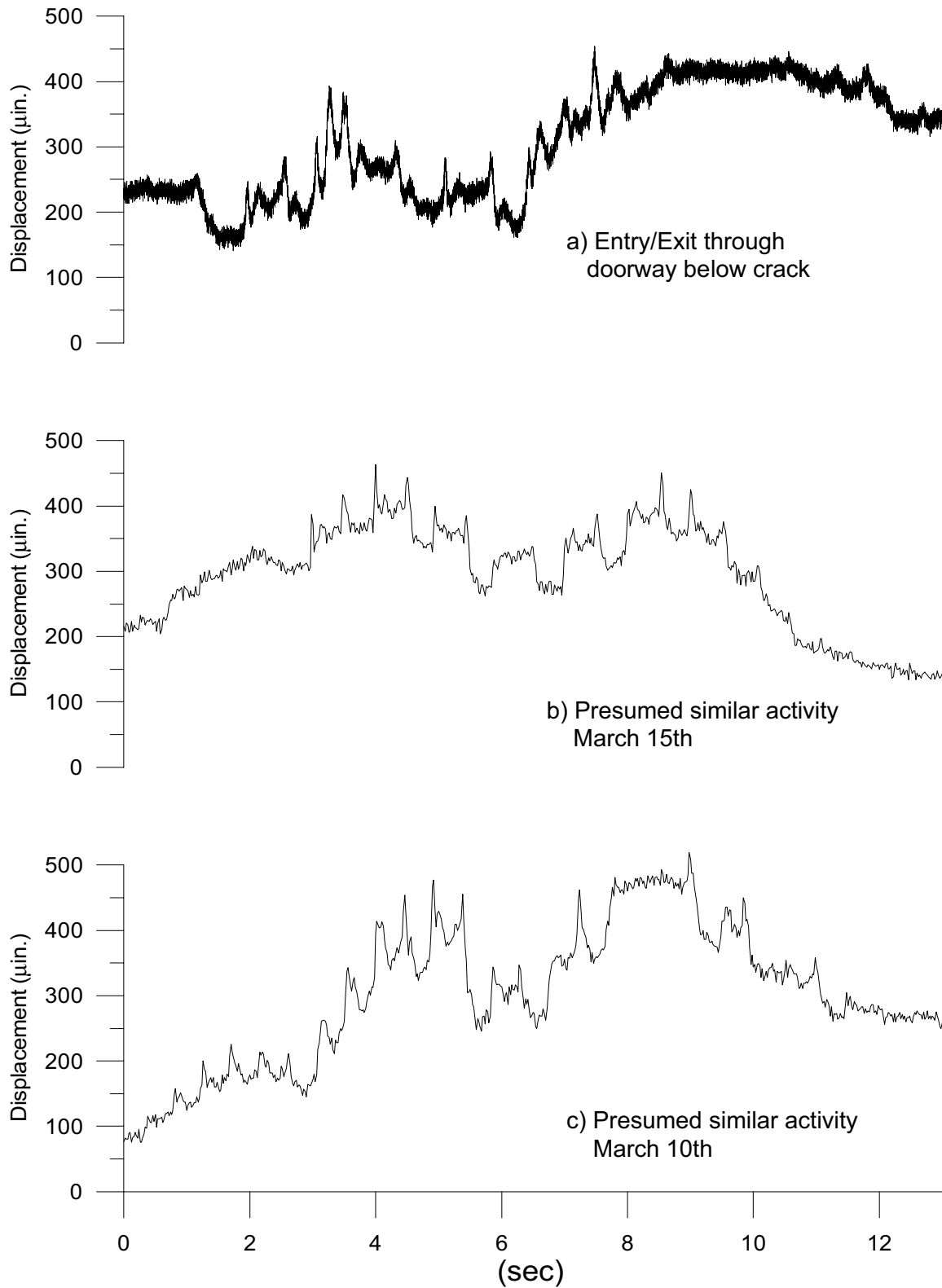


Figure 2.37 Comparison of deliberate and presumed occupant activity bedroom crack response a) induced response during installation of equipment b) & c) presumed response recorded during 50 Hz data collection on respective dates

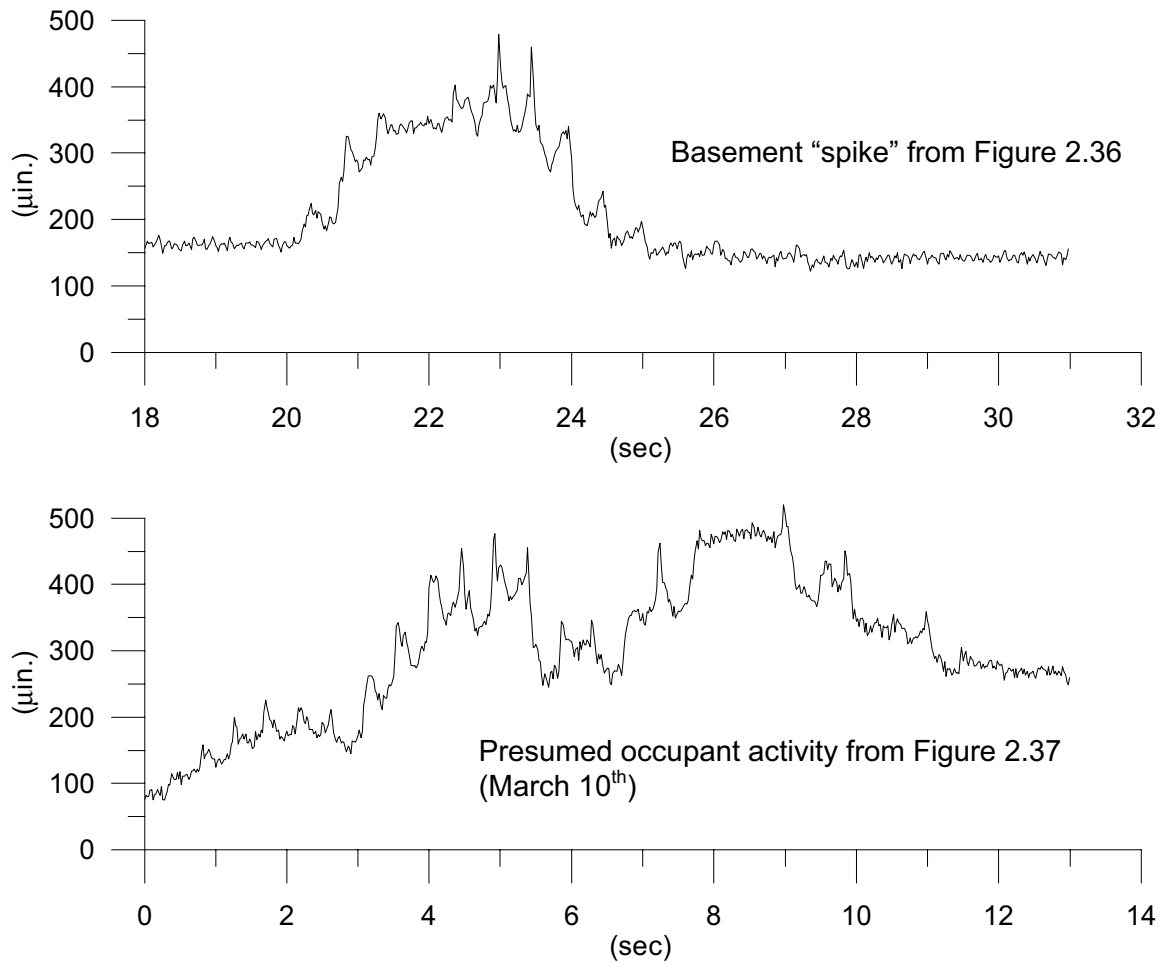


Figure 2.38 Comparison of basement and bedroom spikes seen during 50 Hz testing

It is important to assess the significance of these spikes and other unusual crack behavior relative to responses due to blasting events. Figures 2.39, 2.40, and 2.41 show in-depth more examples of the 50 Hz analysis for each of the three cracks. Each figure progressively zooms in on detected odd behavior and then is compared to a blast induced crack response. Blast induced response is at the bottom (part b). The time scale of the lowest of the four graphs of the 50 Hz data (part a) is 1 hour (3600 seconds). The three plots above have times scales of 600, 60, and 4 seconds respectively. The x and y scales for the top graph

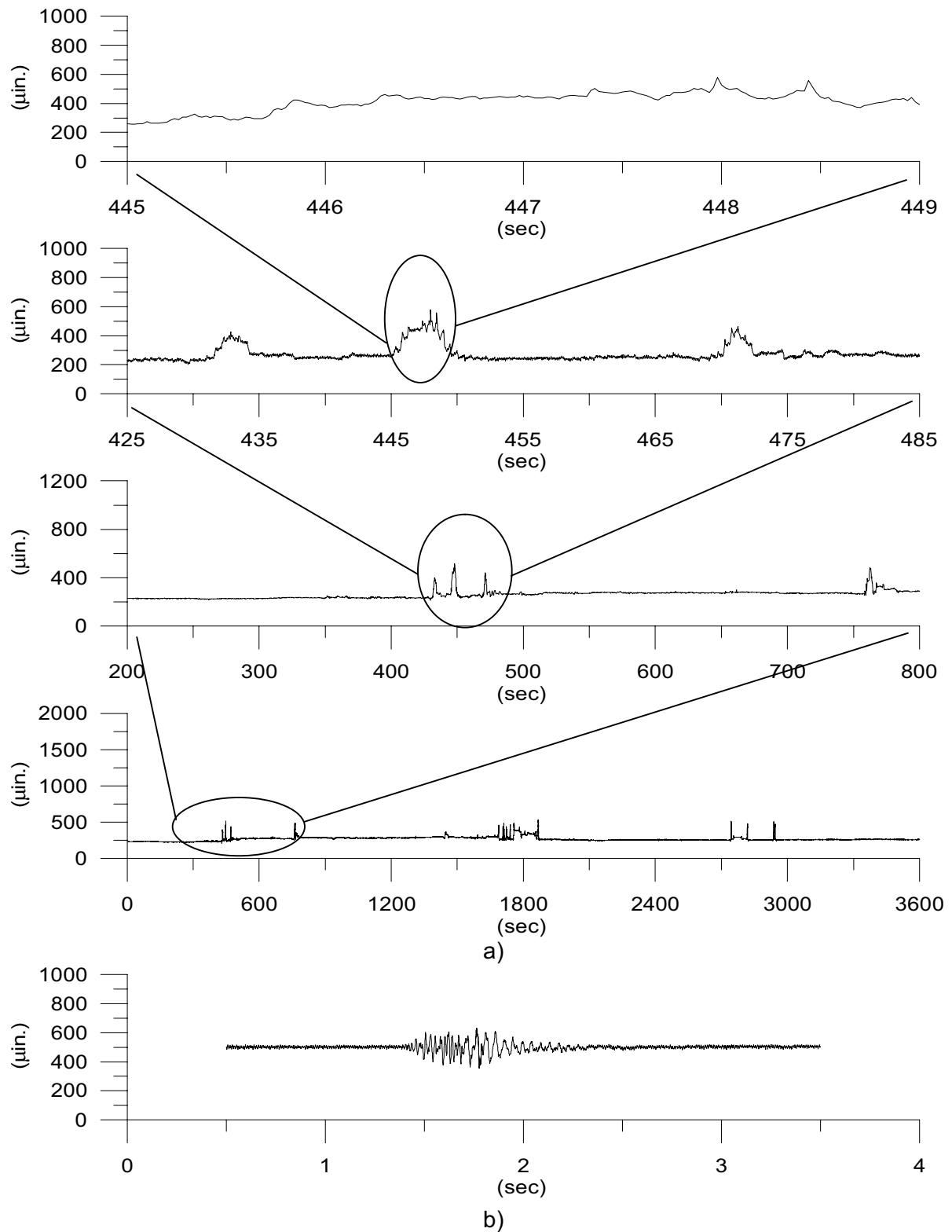


Figure 2.39 Comparison of basement crack displacement for blast and non-blast responses a) 50 Hz data collected during a time period when no blasting occurred (March 9th) b) basement crack response to blast (Feb. 8th)

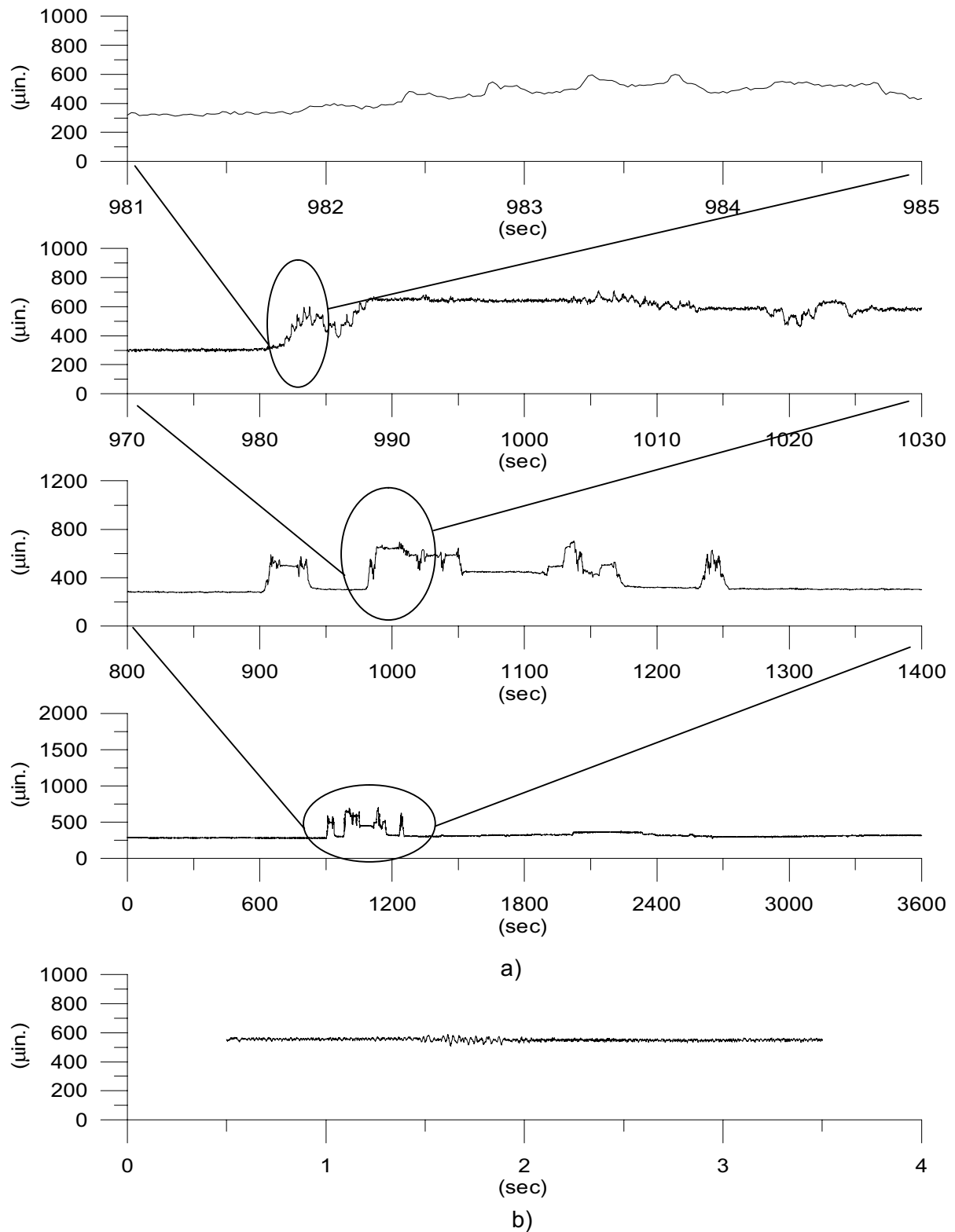


Figure 2.40 Comparison of bedroom crack displacement for blast and non-blast responses a) 50 Hz data collected during a time period when no blasting occurred (March 10th) b) bedroom crack response to blast (March 7th)

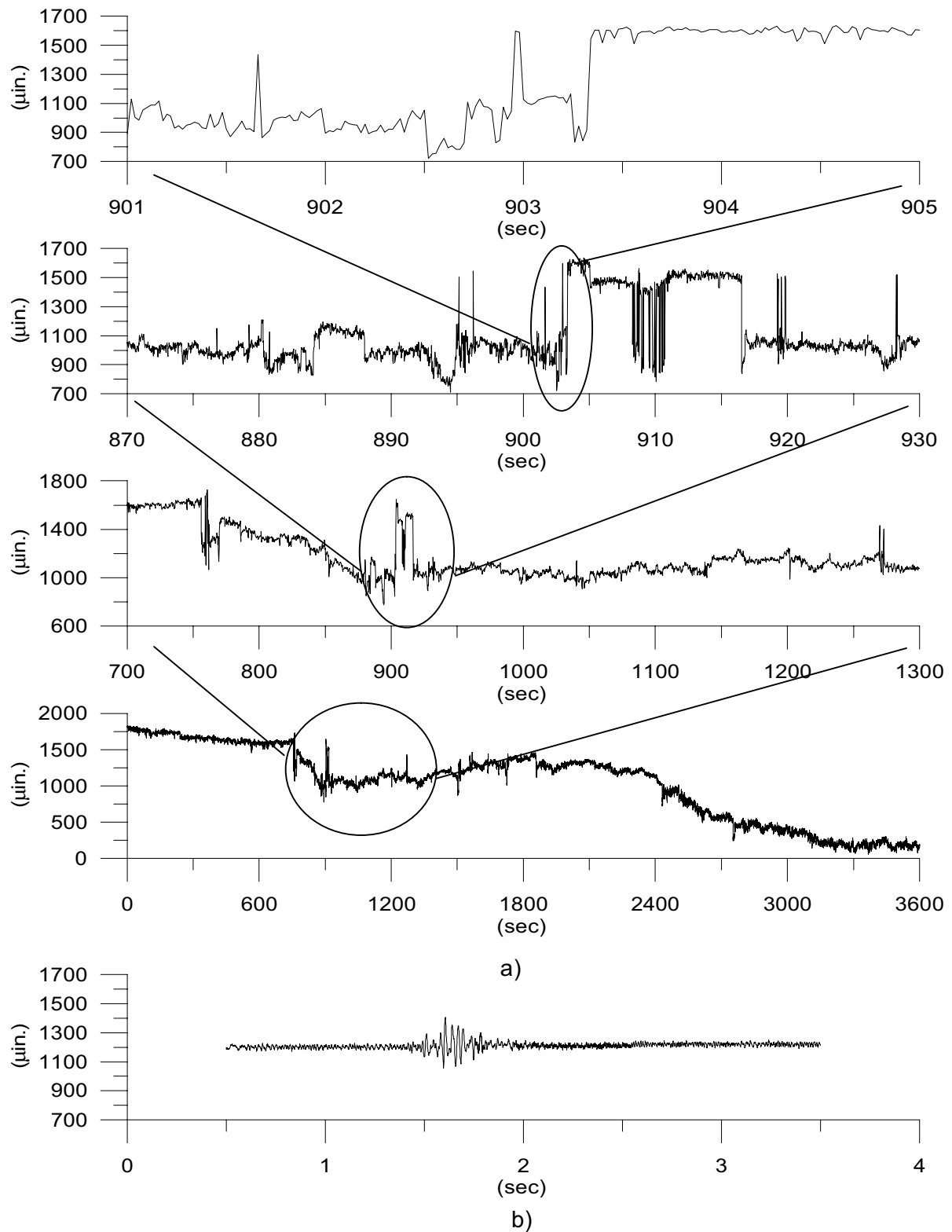


Figure 2.41 Comparison of exterior crack displacement for blast and non-blast responses a) 50 Hz data collected during a time period when no blasting occurred (March 7th) b) exterior crack response to blast (March 7th)

of part a) and the blast response shown in part b) on the bottom are the same.

Figure 2.39 compares the basement crack displacement response during the 50 Hz sampling period to the same crack responding to a blast. The spikes seen in the basement during a non-blast time period such as in Figure 2.39a can exceed 300 micro-inches. The comparative blast response has a peak-to-peak displacement of 348 micro-inches, which is considerably larger than the average basement crack response of 234 micro-inches.

Figure 2.40 compares the bedroom crack displacement response during the 50 Hz sampling period to the same crack responding to a blast. The spikes seen in the bedroom during the non-blast time period such as in Figure 2.40a can exceed 400 micro-inches. The comparative blast response has a peak-to-peak displacement of 82 micro-inches, which is larger than the typical bedroom crack response of 66 micro-inches.

Figure 2.41 compares the exterior crack displacement response during the 50 Hz sampling period to the same crack responding to a blast. The erratic crack behavior noticed during a time when no blasting occurred portrayed in part a) is shown to exceed 1700 micro-inches over 1 hour and exceed 900 micro-inches over 4 seconds. The comparative blast response has a peak-to-peak displacement of 348 micro-inches, which is larger than the average exterior crack response of 207 micro-inches.

A comparison of blast and environmental response is shown in Figure 2.42 with one hour of regular long-term hourly data that encompasses the 9:31am morning blast of May 13th. Single points at either end of each plot represent the measured displacements from the long-term data. The crack responses to the blast event are shown to scale (vertically) at the respective time relative to the hourly data. The horizontal scale of each blast response has been exaggerated 50 times to allow for the one-half second event to be seen. Table 2.7

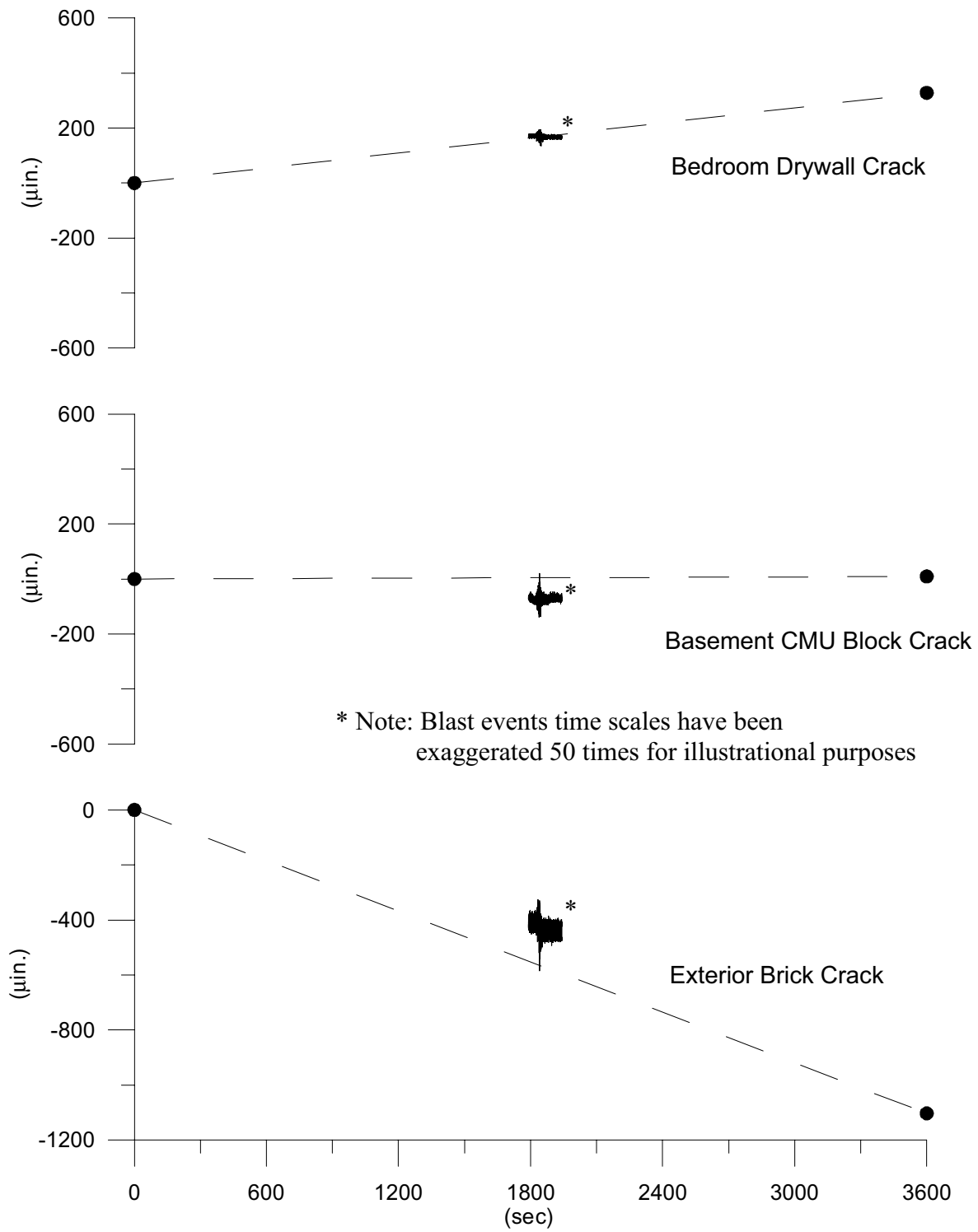


Figure 2.42 Respective crack behavior from blast event compared to crack displacement measured each hour

summarizes the hourly measurements and dynamic displacements associated with Figure 2.42. Not only do the cracks expand and contract in response to environmental conditions over long periods of time far greater than to dynamic responses as discussed previously, but they can displace more during as little as one hour of time than to dynamic responses as shown in Figure 2.42.

Table 2.7 Summary of results from Figure 2.42

| | Bedroom Crack | Exterior Crack | Basement Crack |
|--|---------------|----------------|----------------|
| <i>Displacement from hourly measurements</i> | 328 | 1103 | 9 |
| <i>Displacement to dynamic blasts (peak-to-peak)</i> | 60 | 258 | 158 |

Noise Considerations

When measuring displacements (and thus voltage changes) of such small magnitudes as with the ACM systems, resolution and electronic noise become critical factors. High system resolution does not necessarily produce highly resolved response data if the electrical components of the system produce large amounts of “noise”. Inherent noise of a measuring system is produced by a number of factors such as type of sensors, type of wires, data collection system, and ambient electromagnetic interference (EMI). To obtain adequate response data, the noise level must be minimal relative to the displacement induced voltage changes, otherwise the noise levels can mask the measured displacements.

Figure 2.43 presents a comparison of noise levels. Both systems were very similar in design with the only difference lying in the type of wiring and connections used to transmit data from the sensor to the data acquisition system. Both systems used Kaman eddy-current crack gauges wired to an eDAQ to measure changes in crack width. The Kentucky study

used shielded CAT5 wires and a shielded RJ45 jack as a connection. Petrina (2004), on the other hand, used shielded 22-gauge instrumentation cable with polyvinyl chloride (PVC) as the jacket material and foil as the shielding material. Connections were made by soldering in the Petrina study. As shown in Figure 2.43, the noise level in Petrina’s system approximates to 10 micro-inches, whereas the noise level in the Kentucky system approximates to 30 micro-inches.

The comparison discussed indicates more work is necessary to isolate all of the causes of the variability in noise levels. As seen throughout this chapter, the Kentucky study revealed noise levels could be seen to differ within the same recording system as well.

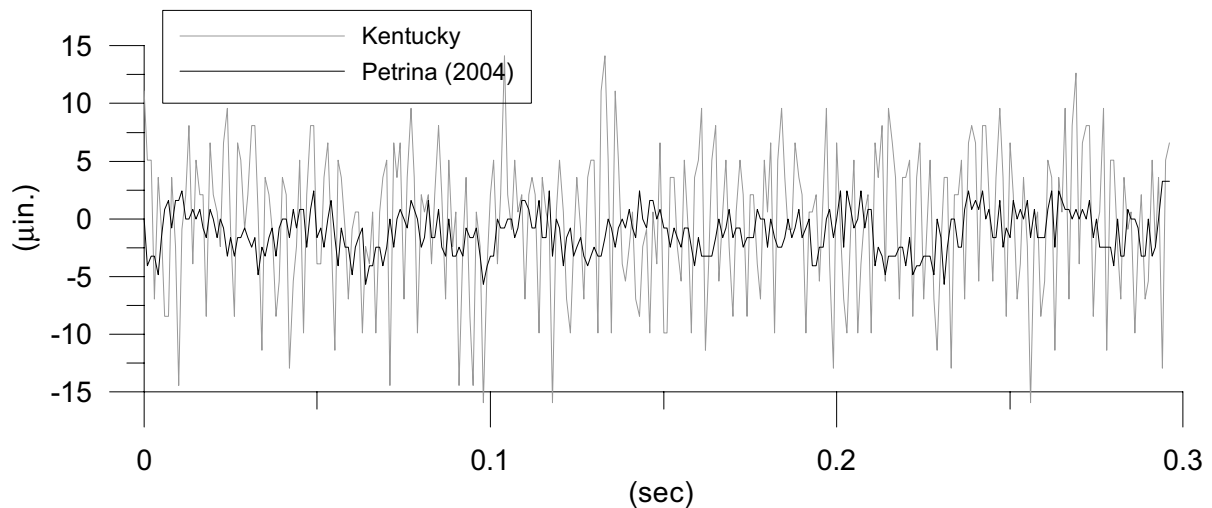


Figure 2.43 Comparison of noise levels for different ACM systems. Shielded CAT5 cables were employed in Kentucky while Petrina utilized instrumentation cable

Wind Effects

Another less “spikey” anomaly appeared in the exterior crack responses as shown in Figure 2.44. These longer period ($\frac{1}{4}$ to $\frac{1}{2}$ sec) excursions, although smaller in amplitude, have been observed in situations to be related to wind excitation. This particular event was recorded when the system was triggered by an electrical noise event. Since this ACM system

is triggered to record when ground particle velocity exceeds 0.04 inches per second (ips), no response to wind gusts (which produce air pressure pulses) could be recorded. It may be that there were significant wind events but were not recorded because the system was not sensitive to these types of events.

Weather records of the Frankfort Capital City Airport were consulted to see if the data of the records during this event (16 February 2005) suggested windy conditions. These records (NCDC, 2005) indicate that February 16th was the windiest day of the month with a maximum 5-second wind gusts of 31 miles per hour, but not at the time of the recorded response. Differences between the location of the site and the airport could suggest wind gusts appear at different times at the two locations. Furthermore as described above, there may have been significant wind responses that were undetected.

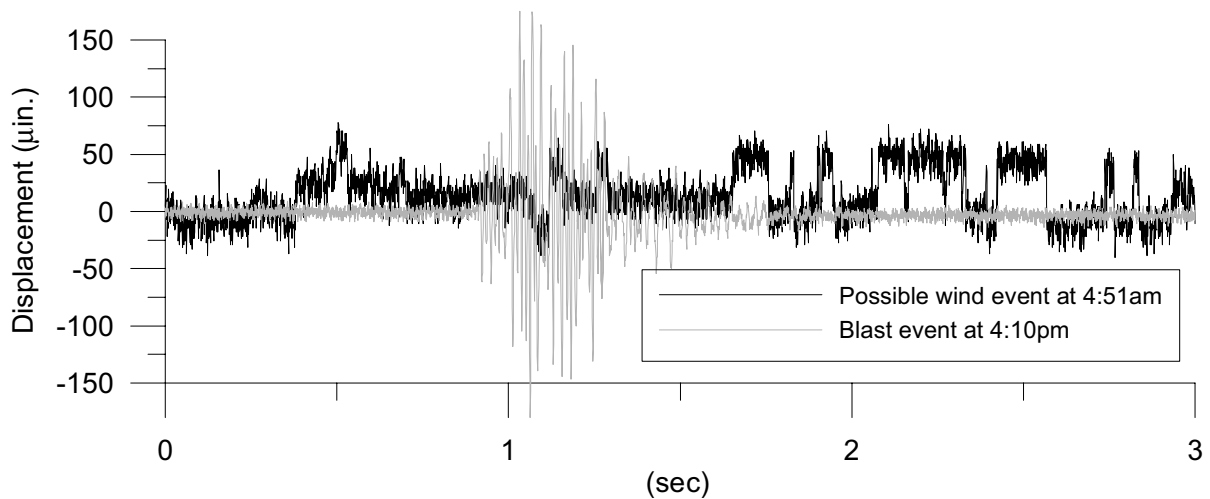


Figure 2.44 Exterior crack displacement due to unknown event recorded during electrical noise spike and a blast event (February 16th, 2005)

The “wind” crack movements are shown by a black line in Figure 2.44. For comparison, a blast that occurred later that same day has been plotted in gray. The changes in

crack displacement seen during the electrical noise spike approximate to 75 micro-inches whereas the crack displacement to the blast response (0.14 ips) exceeds 300 micro-inches peak-to-peak. Even if the motions detected during the electrical noise spike are in fact due to wind, they are less than the blast induced response.

Further wind studies include an attempt to correlate the spikes seen in the basement crack during the 50 Hz study previously shown in Figures 2.36 and 2.39. March 8th had a 5-sec maximum of 30 mph and March 9th had a 5-sec maximum of 18 mph. The largest 5-sec maximum occurred on March 7th and was 37 mph. The hourly data revealed values ranging from 0 to 21 mph over both days, yet due to the hourly data providing values to the nearest minute and having hour gaps of time between values, it is impossible to directly tie any changes in basement crack motion to wind gusts.

The last wind study performed for the Kentucky site involved an attempt to correlate the erratic behavior occurring towards the end of March 7th as seen in Figures 2.35 and 2.41. As mentioned, the windiest day in March happened to be on the 7th with a 5-sec maximum of 37 mph. Yet, upon an hourly evaluation, higher values were reported earlier in the day than were reported at times of the erratic crack behavior.

In conclusion, it is very difficult, if not impossible, to accurately correlate changes in crack displacement to outdoor wind conditions given the triggering system in the Kentucky installation. In order to properly assess potential wind induced crack changes, the system should include air pressure sensors for triggering as well as the traditional geophone triggering. Such systems are under development and should be able to detect wind induced responses.

Summary

As seen above crack responses vary widely in magnitude and can be induced by a variety of factors including blasting events, environmental effects, human activities, and wind. These crack responses can be compared in two ways, zero-to-peak or peak-to-peak as shown in Figure 2.45. The zero-to-peak method corresponds to the maximum potential to further propagate the crack, or extend its length. This thesis presents crack responses in a peak-to-peak fashion without regard to time of the peaks as shown in Figure 2.45 by “reported”. As seen, regardless of where on the time axis the maximum and minimum measurements occur, the peak-to-peak value (reported) is simply the difference of these two values. While this “reported” analysis is more economical, it does not necessarily define the “true” peak-to-peak displacements, only the differences between the minimum and maximum responses. A true peak-to-peak displacement refers to one that occurs over one cycle of crack motion as labeled “true”. Depending on the crack response history, the “reported” peak-to-peak displacement may reflect the “true” peak-to-peak displacement. All measurements in

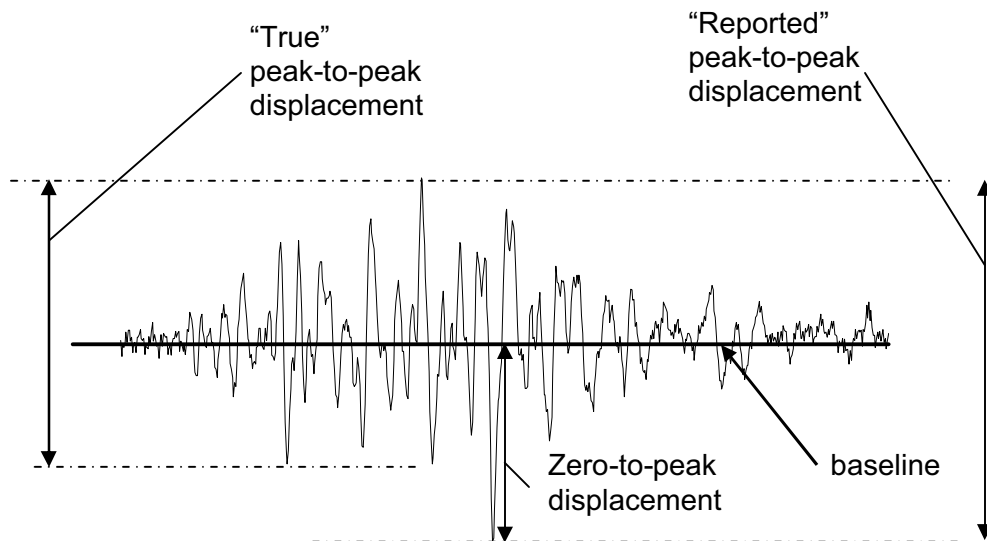


Figure 2.45 Possible ways to define crack displacement

this thesis, including dynamic and long-term, are “reported” as peak-to-peak displacements to maintain consistency.

A summary of all of the maximum peak-to-peak displacements measured due to various sources is provided in Table 2.8. Crack response to occupant activities is similar in magnitude to the crack response to blast-induced ground motions. Crack response to long-term environmental effects greatly exceeds both blast and occupant activity response by at least an order of magnitude in all cases.

Table 2.8 Maximum crack displacements measured from various sources

| Crack | Maximum measured peak-to-peak crack displacement (μin.) | | |
|---------------------|--|----------------------|--------------------------|
| | Blast | Environmental | Occupant Activity |
| Bedroom drywall | 114 (.14 ips) | 14,000 | 250 (walking) |
| Exterior Brick | 444 (.15 ips) | 31,254 | 450 (pounding wall) |
| Basement CMU mortar | 687 (.17 ips) | 8,346 | 350 (pounding wall) |

Chapter 3

Out-of-plane Crack Behavior

To fully define crack response, it is important to consider all three directions which a crack may displace as shown in Figure 3.1. To date autonomous crack monitoring (ACM) studies have focused on transverse crack response (or mode I) in the plane of the wall containing the crack; direction “A”. All previous work discussed in this thesis pertains to this commonly studied in-plane perpendicular direction “A”. Direction “B” (mode II) also lies in the plane of the surface containing the crack; however it is parallel to the long axis of the crack. At present no measurement of displacement in direction “B” has been made, as new mounting brackets would be needed to quantify crack response in this direction. This chapter describes the development of mounting brackets to measure out-of-plane crack; direction “C” (mode III).

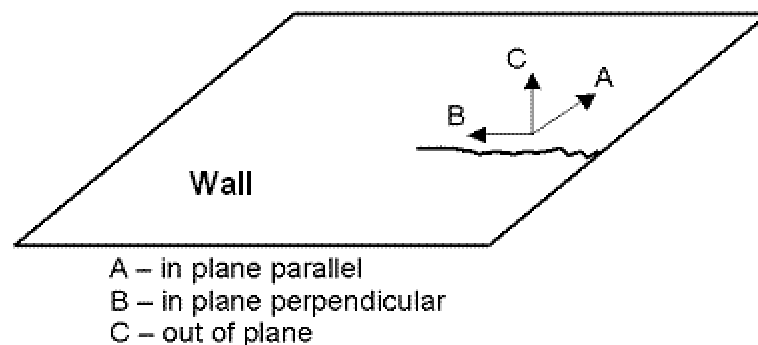


Figure 3.1 Three possible directions of crack response

To develop a measuring system to measure out-of-plane crack behavior (direction “C”), the following three steps were taken and are described in detail in this chapter: 1) design and construction of a new mounting system to measure out-of-plane crack movements 2) qualification of the system in the laboratory before field deployment 3) assessment of measured crack response in the field relative to that in-plane and perpendicular to the crack. Data gathered at a test site on a particular windy day are discussed in a separate section. For the remainder of the chapter, direction “A” will be simply referred to as *in-plane*, since direction “B” was not measured. Response in direction “C” will be referred to *out-of-plane* as it is the only out-of-plane direction.

Design and Construction

As with in-plane measurements, there are many considerations to design a system to measure both long-term and dynamic out-of-plane responses including type of transducer, mounting bracket, and test bed for laboratory qualification. To obtain reliable and comparative data relative to previous studies of in-plane crack behavior, it was decided to utilize the same Kaman sensors. In order to affix the crack sensor to a surface in the out-of-plane direction, glass with a low coefficient of thermal expansion (CTE) was selected for the mounting bracket. A bi-material test rig was developed for laboratory CTE qualification.

The chosen mounting bracket system is shown in Figure 3.2. As with all ACM applications, the system size should be minimized to be as inconspicuous as possible. These systems are often times installed in residences or other occupied structures and large, bulky testing equipment should be avoided. Geometry of the mounting bracket must accommodate

a null sensor as well as the crack sensor. The null sensor is necessary to measure long-term displacements associated with wall material and sensor changes.

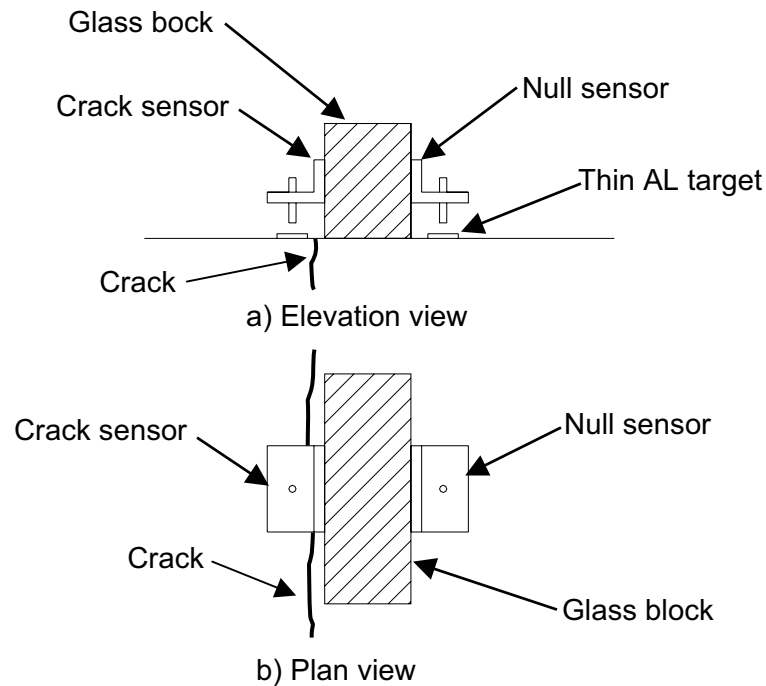


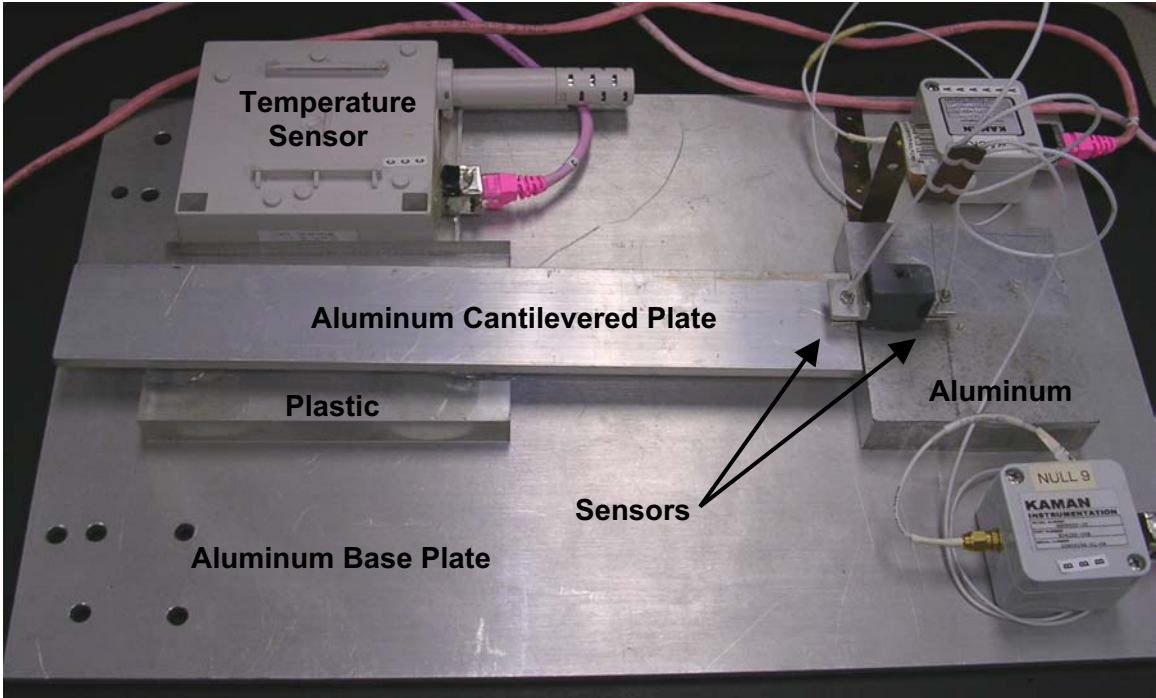
Figure 3.2 Mounting bracket design to measure out-of-plane crack response

The mounting bracket used to attach the crack sensors in the out-of-plane orientation will expand and contract with changes in temperature. It is important to select a material with a low CTE so that the material response to temperature changes is less than that of the crack that the system is intended to measure. It should be rigid and not deform during dynamic events. Thus, when the surface responds to a dynamic event, the affixed sensor should move concurrently so that the crack displacement is accurately measured. The mounting bracket should also be robust as to not easily break or deteriorate due to the elements if an outdoor application is required. During the installation of an ACM system, mounting brackets and sensors are transported and handled often, therefore a lighter weight, yet durable material is

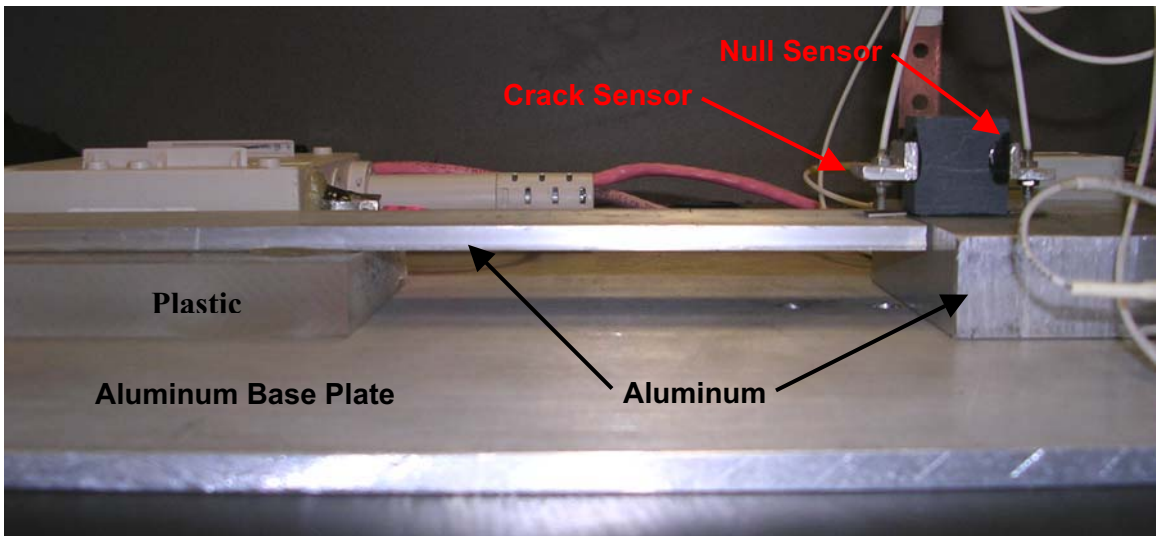
desired. Finally, cost is an important factor to add to the aforementioned concerns in selecting an appropriate system for out-of-plane crack measuring.

Taking into account all factors discussed, the final solution resulted in use of a pre-manufactured glass block of dimensions of 1”H x 2”W x 0.75” D to which the Kaman sensors could be affixed as shown in Figure 3.2. This solution to measure out-of-plane crack displacements almost seems intuitive when presented, but thought, research, and testing was required before a conclusion could be drawn. Photographs of the laboratory set-up used to qualify the system are shown in Figure 3.3. Before the glass block was chosen as a solution, other materials were considered and tested. Photographs in Figure 3.3 were actually taken while the crack sensors were attached to an aluminum silicate block, commonly referred to as LAVA. Both the glass and the LAVA have a low CTE (1.8 and 1.5 $\mu\text{in./in./}^\circ\text{F}$ respectively). However, the glass block was chosen over the LAVA for multiple reasons. LAVA arrives in sheets and requires fabrication to obtain a properly sized block whereas the glass can be ordered with the desired shape and size. Both materials are considered brittle, yet glass is actually more susceptible to cracking and breaking than the LAVA. However, the cost of the glass, at \$1.50 per block, is significantly lower than the LAVA. The breaking of glass blocks may occur upon removal, however considering the cost and ease of replacement, it is not detrimental to occasionally lose a glass block at the end of an installation.

The Kaman sensors require a metallic surface for a target. Aluminum angle brackets were mounted as targets near the sensor tip in the in-plane direction. A small thin aluminum plate, approximately 1/4” by 1/4” by 30 mils thick, was selected as a target and mounted directly below the sensor tip when measuring out-of-plane response. The minimum thickness of an aluminum target for the Kaman sensors used is fifteen mils. These plates were not



a) Overall View



b) Side View

Figure 3.3 Photographs showing the system used to test the out-of-plane crack measuring system a) an overall view showing the testing of the LAVA block b) a side view showing the testing of the LAVA block

necessary for the laboratory qualification system as the reflective surface was aluminum. However, the targets were necessary for mounting on the drywall ceiling.

As shown in Figure 3.3, multiple materials including aluminum and polycarbonate (plastic) were included in the construction of the testing apparatus for laboratory qualification. These materials have different CTE's, both of which are relatively large compared to glass. The difference in CTE's was essential for long-term testing in order to obtain differential displacements when subjected to cycles of temperature change. The aluminum cantilever just below the left side (crack) sensor tip was designed to produce dynamic responses in the laboratory by dropping weights onto the cantilever and measuring the response. An aluminum plate was used as a rigid base to support all the equipment and materials, which were attached to the base and each other with the same high strength 90-second epoxy used for all in-plane field applications. A temperature sensor was also mounted on the base plate to record temperature changes during the long-term testing.

Figure 3.4 presents dimensioned elevation and plan views of the out-of-plane testing apparatus. Since the cantilever arm was only needed for the dynamic testing, the plastic block was moved adjacent to the aluminum block for qualification for long-term temperature response. Figure 3.4 shows the plastic block in its modified location for long-term testing; dashed lines illustrate the location of the plastic for dynamic testing.

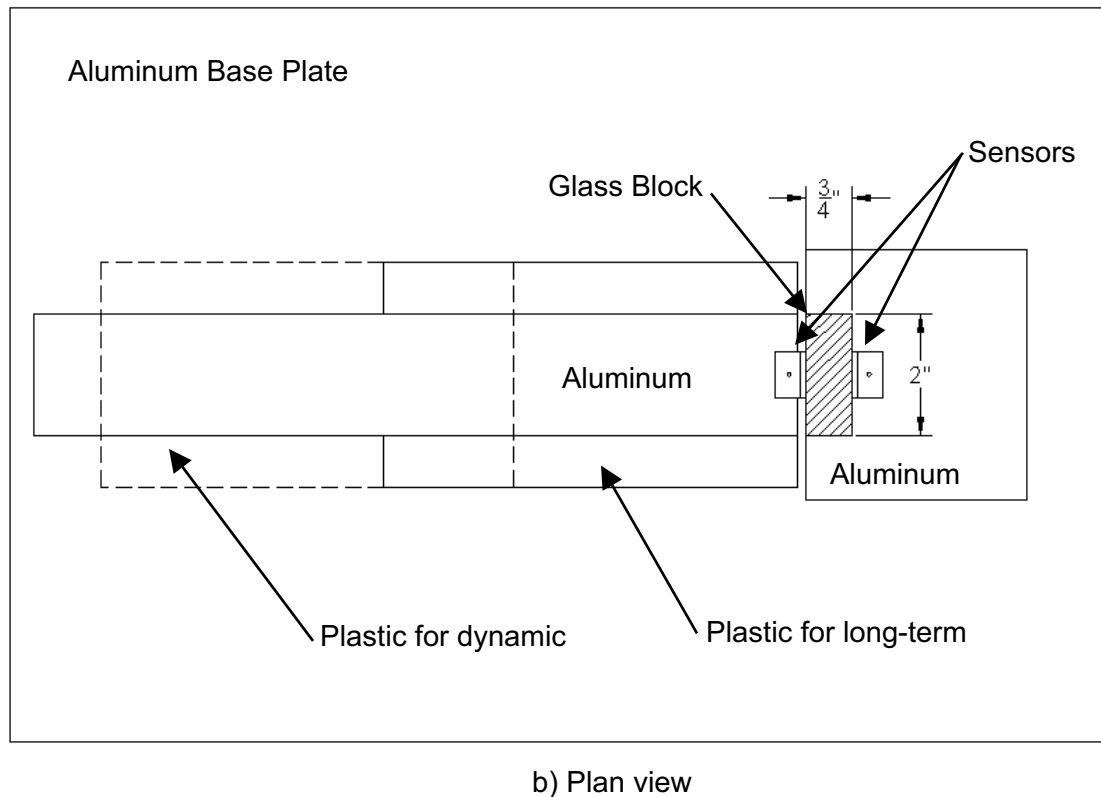
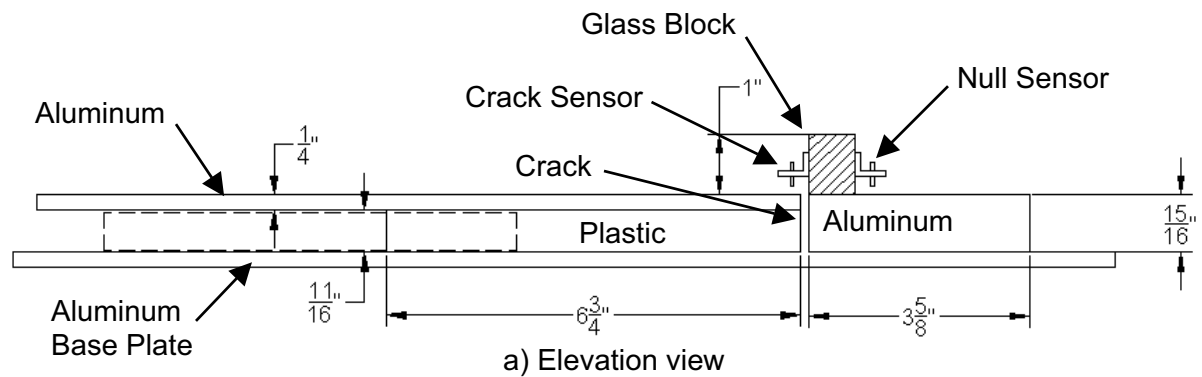


Figure 3.4 Drawing showing the dimensions of the out-of-plane displacement testing apparatus a) elevation view b) plan view

Laboratory Qualification

As with most prototypes, the out-of-plane crack measuring system was qualified in the laboratory before it was installed in a field application. Since the crack measuring system is intended to record long-term crack changes as well as capture dynamic events, both of

these displacements needed to be produced and successfully measured in the laboratory before deployed in a test structure.

Dynamic Qualification

To qualify the system dynamically, vibrations similar in both amplitude and frequency to those in the field were induced for measurement by the sensors in the new out-of-plane orientation. It was assumed that the out-of-plane crack response would be similar to in-plane behavior. Therefore measured responses from the underground quarry in Frankfort, Kentucky discussed in Chapter 2 were used as a comparison. Peak-to-peak in-plane crack displacements observed in Kentucky ranged from 33-687 micro-inches with averages of 66 and 234 micro-inches for the cracks in the bedroom drywall and basement CMU joint, respectively. The dominant longitudinal ground motions in KY consisted of frequencies ranging 31-58 Hz with an average of 42 Hz.

Dynamic responses were induced by dropping weights onto the aluminum cantilever arm from varying heights and distances from the sensor until a desired response was obtained. A small setscrew was dropped from a height of less than a few inches midway across the cantilever to produce the results shown in Figure 3.5. The two seemingly independent responses are actually one trial and represent the setscrew bouncing after its initial impact. The magnitude of response seen in Figure 3.5 ranges from about 600 micro-inches to less than 50 micro-inches which exactly matches the crack displacements observed in Kentucky. The frequency content is consistent at 220 Hz regardless of the height or distance from the sensor an object is dropped. 220 Hz is the natural frequency of the aluminum cantilever based on the section modulus and length of cantilever of the aluminum

arm. The system could have been altered to produce the lower frequencies that are anticipated in the field. However, it can easily be reasoned that if the system can accurately measure high frequencies, it can also measure lower frequencies at similar amplitudes.

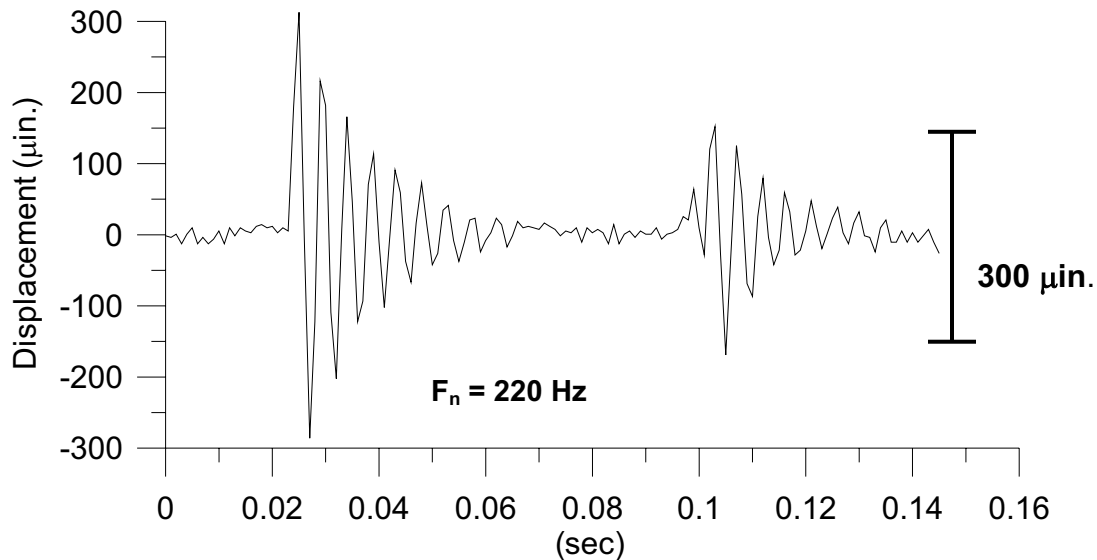


Figure 3.5 Dynamic testing of the out-of-plane displacement measuring system

Long-term Qualification

The goal in the long-term qualification of the system was to measure changes in out-of-plane displacement across a gap caused by differing CTE's of two different materials and then compare the measured changes to the theoretical, or computed, displacements. In the system shown in Figure 3.4, the plastic which has a CTE of $37\mu\text{in./in}^\circ\text{F}$ will expand and contract more for the same temperature changes than the aluminum having a CTE of $13.1\mu\text{in./in}^\circ\text{F}$. The glass block on which the sensors are mounted will also expand and contract in response to the same temperature changes. However, the CTE of the glass is much lower $1.8\mu\text{in./in}^\circ\text{F}$. Even though the thermal expansion of the glass is minimal by design, a null sensor was included on the backside of the block to account for the thermal

response of the glass as well as the sensor and aluminum mounting bracket that occurs even with no crack response.

$$\delta = \alpha * L * \Delta T \quad (3.1)$$

Equation 3.1 describes the theoretical relationship between displacement, δ , of a material subjected to temperature change ΔT . The coefficient of thermal expansion and length of the specimen subjected to expansion are defined by α and L . If the temperature of the system is increased, the aluminum on the right side of Figure 3.4 will expand as will the glass block that is mounted above. In order to compute the expected displacement measured by the left side (crack) sensor, the corresponding expansion of the plastic on the left side must be deducted from the sum of the aluminum and glass expansion. Equation 3.2 describes the calculation of theoretical displacement between the target (thinner aluminum plate on left) and crack sensor (left). This difference can be thought of as the expansion of the left side materials subtracted from the right side materials. Expansion of the equation with the respective lengths for each material is given in Equation 3.3.

$$\delta_{crack} = (Right) - (Left) = (\delta_{AL} + \delta_{GL}) - (\delta_{PL}) \quad (3.2)$$

$$\delta_{crack} = \alpha_{AL} * (11/16") * \Delta T - \alpha_{PL} * (11/16") * \Delta T + \alpha_{GL} * (1/2") * \Delta T \quad (3.3)$$

As seen in Equation 3.3, the 1/4" aluminum plate above the plastic has been ignored in the equation since aluminum is located on each side of the crack and its response cancels. Therefore, the only displacement difference across the gap (crack) is the result of the 11/16" of differing materials, plastic versus aluminum. The sensors are epoxied approximately

midway along the glass block which accounts for the 1/2" length for the glass block expansion in Equation 3.3. With all of the CTE's defined, the theoretical crack sensor displacement can be computed for any temperature change.

The out-of-plane testing apparatus was subjected to six cycles (days) of temperature change ranging 52-74 °F and Figure 3.6 shows the results. The solid red line shows the measured displacement. The black dashed line shows the computed displacement based upon Equation 3.3. The solid gray line shows the computed displacement neglecting the effects of the glass block (assuming a glass CTE of zero). Figure 3.6 shows that the effect of the glass block in computing displacements is negligible due to its low CTE and relatively small size. The computed displacements follow the same trend as the measured displacements, however the magnitudes of the measured changes are slightly larger than the calculated.

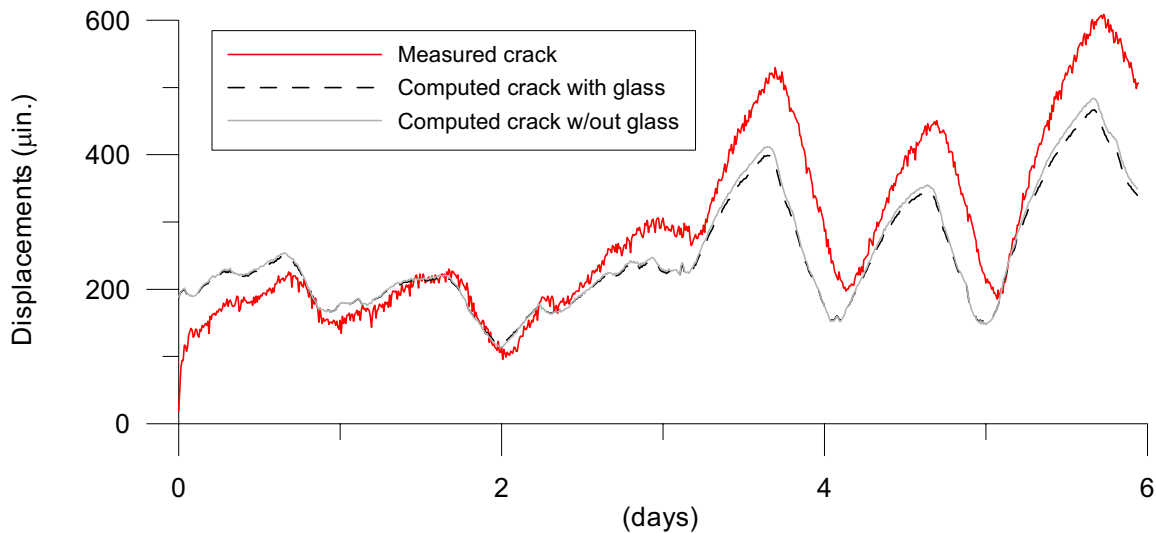


Figure 3.6 Comparison of measured and computed crack displacements for the out-of-plane testing laboratory qualification

The Kaman sensors are high precision displacement sensors. However, the combination of the sensor itself and the aluminum mounting brackets are affected by changes

in temperature. In long-term laboratory studies, the thermally induced displacements measured are relatively small compared to field studies and therefore thermal responses of the sensors and mounting brackets themselves can become significant (in the laboratory). This concept accounts for the difference between the measured and computed displacements seen in Figure 3.6 and is better illustrated in Figure 3.7.

Figure 3.7 compares the hysteresis response of two laboratory tests with the corresponding theoretical displacement changes. A hysteresis plot shows changes in displacement versus temperature over multiple cycles to illustrate the linearity and drift of a sensor. Further details on interpreting hysteresis loops can be found by referring to Baillot (2004).

On the left, part a) is the response of the out-of-plane testing apparatus when subjected to six temperature cycles as seen in Figure 3.6. The theoretical glass (G) displacements (black line) were computed using Equation 3.1 (with the CTE of glass) and indicate what the measured null response should be (black diamonds). The theoretical aluminum+glass-plastic (A+G-P) displacements (gray line) were computed using Equation 3.3 and indicate what the measured crack response should be (gray diamonds). As expected, the theoretical crack (A+G-P) response with a larger net CTE is sloped more steeply than the theoretical null (G) response. However, when tested, the measured crack and null responses were similar in slope to each other (and different than the respective theoretical responses).

On the right, part b) is the response of two sensors mounted in the in-plane orientation on an aluminum block to verify the long-term thermal response of the sensors. The theoretical thermal response of aluminum (red line) was computed using Equation 3.1

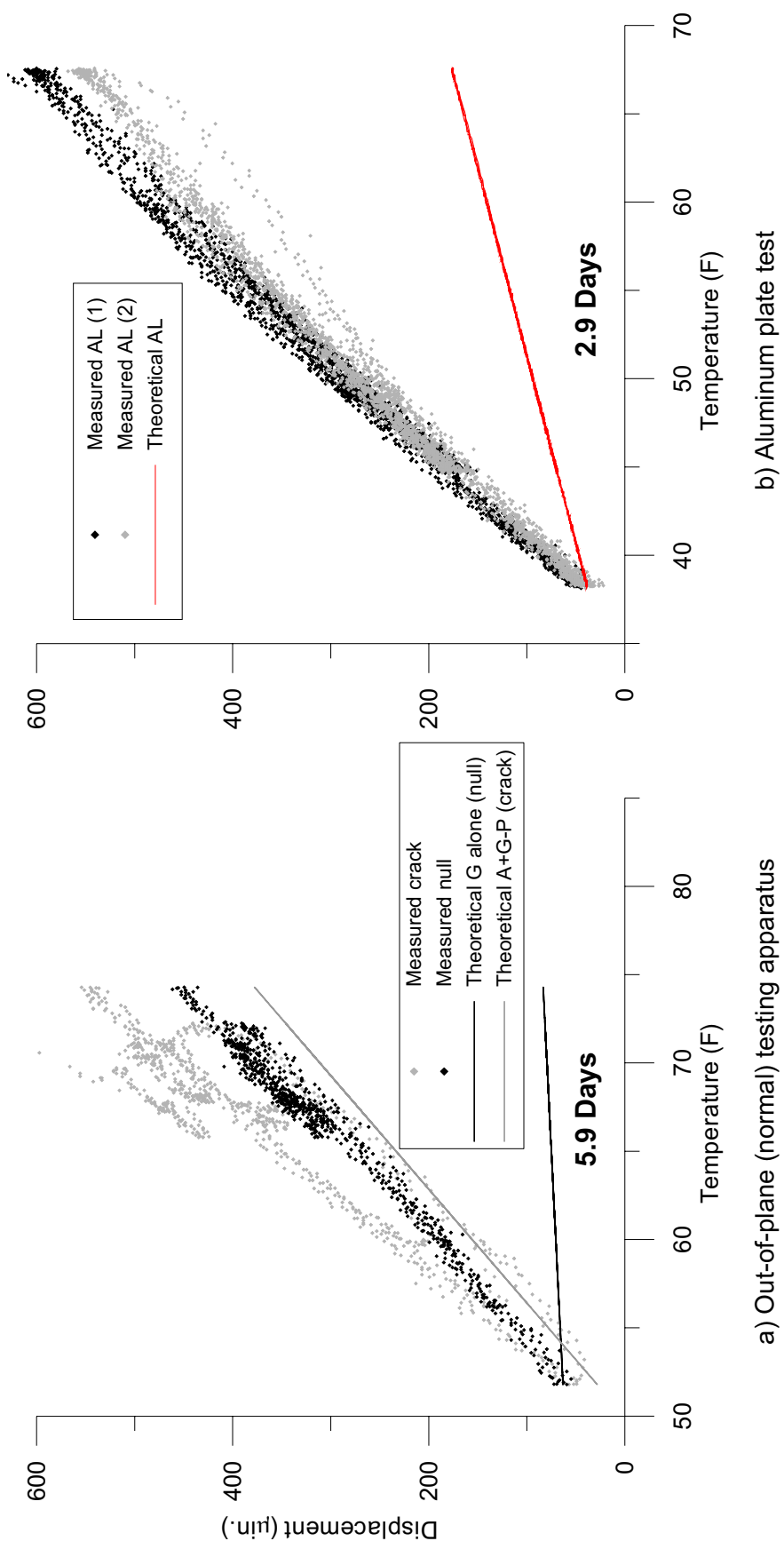


Figure 3.7 Hysteresis loops for out-of-plane (normal) system laboratory qualification tests a) two sensors mounted on glass block; null measures glass response only; crack measures difference between plastic, aluminum, and glass as shown in Figure 3.4 b) two sensors mounted on aluminum plate

and indicates what the measured responses (black and gray diamonds) should be. However, similar to part a), the measured responses are sloped more steeply than the theoretical thermal responses.

When comparing the measured responses of parts a) to those of part b), the slopes are similar regardless of the material in which they are mounted to measure the thermal response of (G, A+G-P, or AL). It is concluded that these measured responses in fact represent the thermal response of the sensors and aluminum mounting brackets and not of the material that was intended to be measured. This difference occurs because the sensor and aluminum mounting bracket thermal response is unexpectedly larger than the thermal response of the materials selected for the laboratory qualification.

Long-term crack displacements in the field are typically much larger than long-term laboratory responses and therefore the differences in measured versus computed displacements in the laboratory do not raise concerns regarding the validity of the system for the intended field applications. By comparing the slopes of the null sensors in Figure 3.7a, it is apparent that the measured null response (black diamonds) is far greater than the theoretical null response (black line) for the given temperature ranges. As already expressed, this difference is a result of the inherently large response of the sensor and aluminum mounting bracket themselves compared to the relatively low CTE of glass. The null sensor reports displacement values much larger than the actual glass response. As concerning as this may sound, the concept of the null sensor is valid in this case in that it records the sensor and material response which can then be subtracted from the measured crack response to obtain the actual, or net, crack response.

To show that the (larger than expected) measured null displacements are acceptable, measured null sensor responses in the laboratory are compared in Figure 3.8 to sensor responses mounted on three different uncracked materials at the Kentucky site. In Figure 3.8a, the laboratory null displacements (solid black line) are less than the Kentucky exterior null displacements but greater than the basement and bedroom null displacements. The effect of temperature change on the null can be seen by comparing the temperature changes in b)

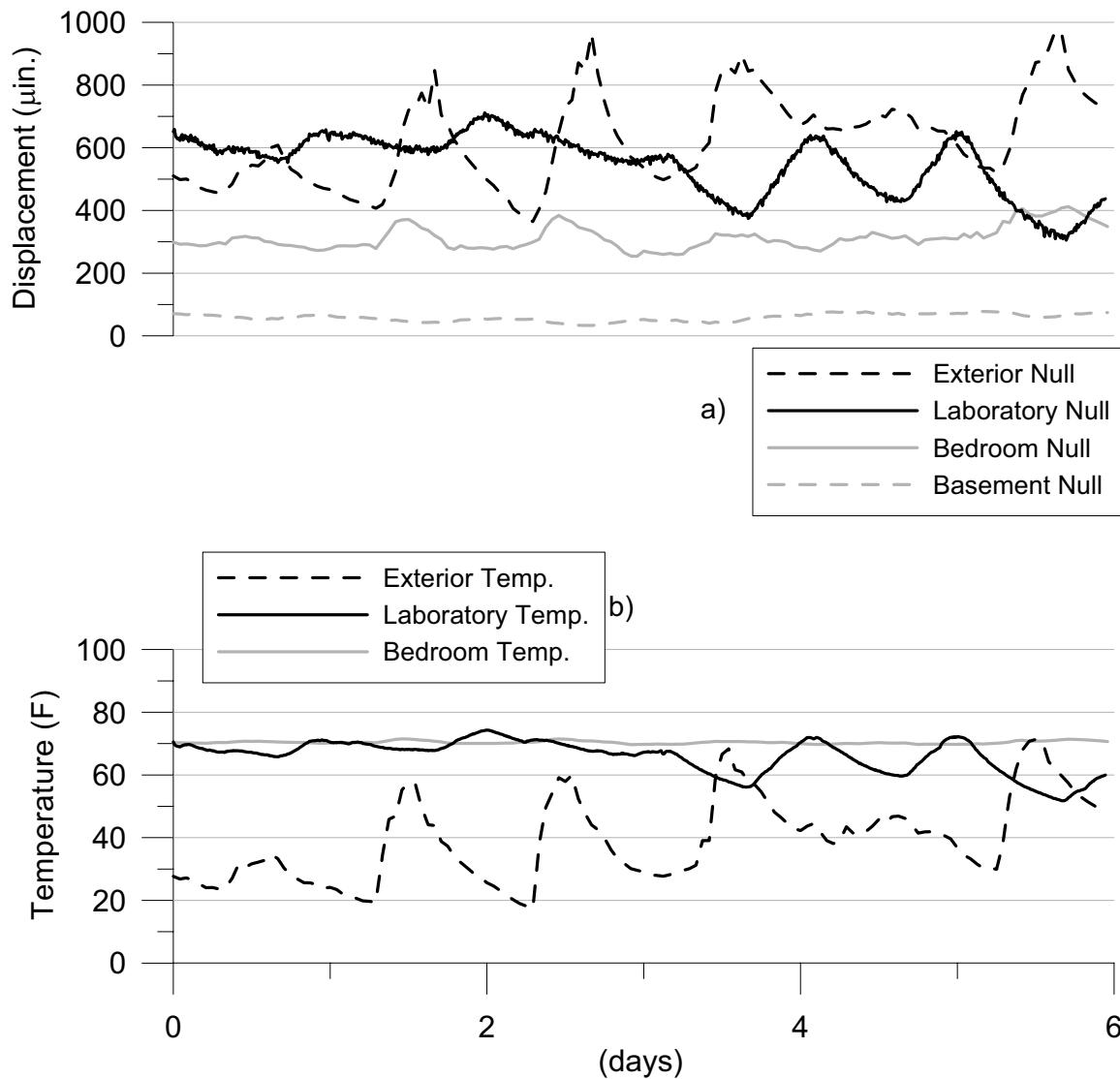


Figure 3.8 Comparison of field null sensors and laboratory null sensors a) null sensors displacements for a six-day period b) temperature conditions affecting null sensors for the corresponding six-day period

with the null response in a). Nulls respond the most with larger temperature changes, such as the exterior. The basement temperature was not measured; however, it is suspected to fluctuate even less than the bedroom temperature.

Inherent temperature response properties of sensors can cause measured null responses to be far greater than theoretically predicted on the basis of the glass block alone. However, if the crack displacement is much larger than the null displacement and the null response is linear, then this difference will not affect the technique of subtracting the null response from the crack response.

Field Qualification

The newly designed and laboratory qualified out-of-plane crack measuring system was installed on November 22nd 2005 on the ceiling at the Milwaukee test structure described in Chapter 2. The photograph in Figure 3.9 shows the placement of the glass block and out-of-plane sensors mounted adjacent to the already existing in-plane sensors. The glass block was epoxied near the in-plane sensors in effort to capture the same crack behavior, but in

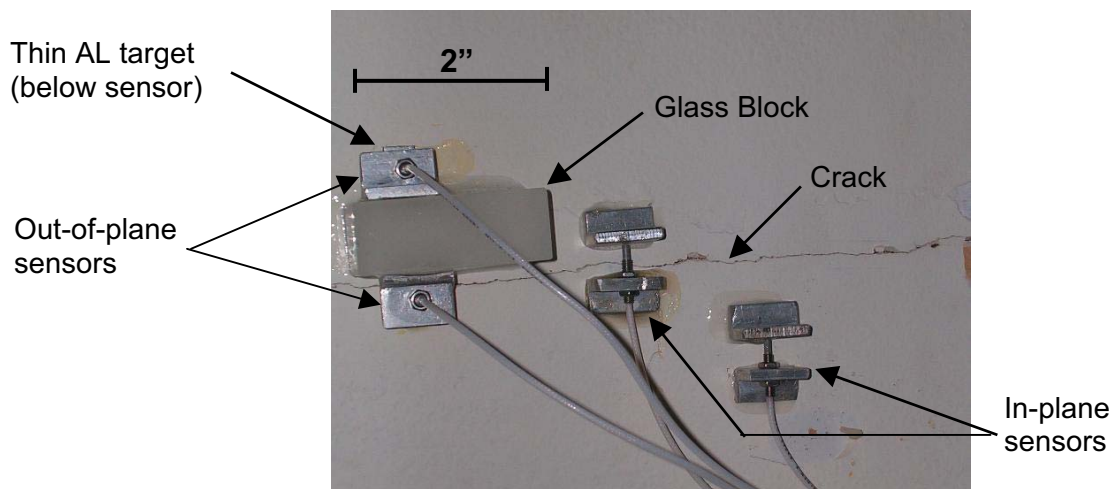


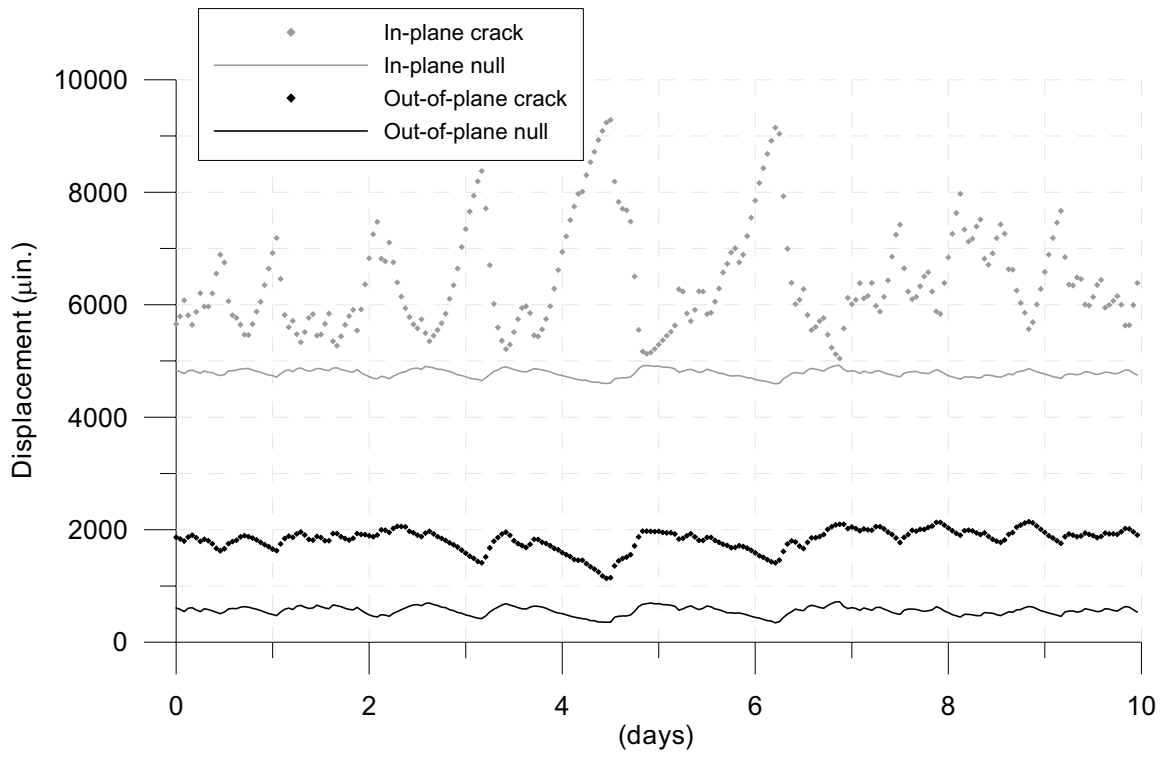
Figure 3.9 Picture of the out-of-plane system installed on a ceiling crack near previously installed in-plane sensors

different directions.

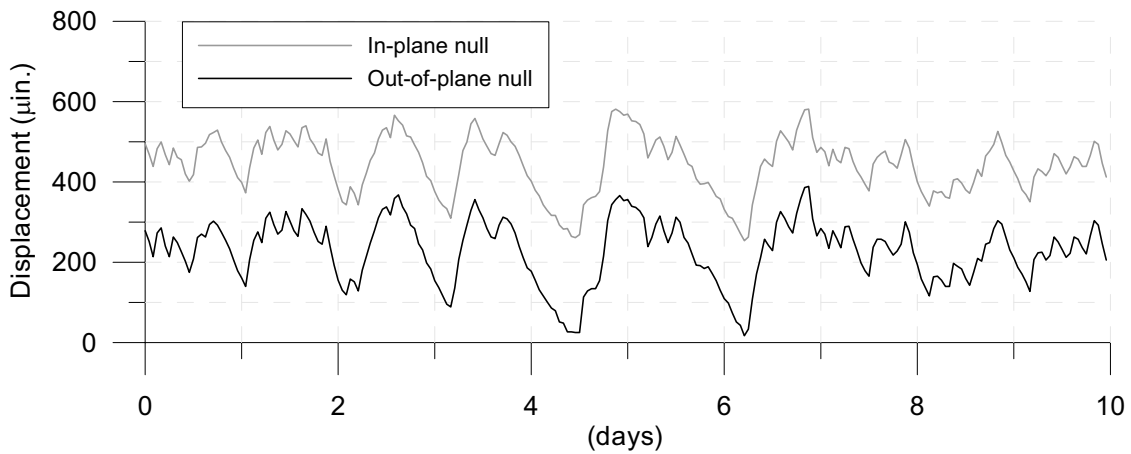
Long-term Response

In-plane and out-of-plane long-term crack displacements are displayed at the same scale for a ten-day period in Figure 3.10a by the hourly plotted gray and black diamonds respectively. As shown, the out-of-plane response is less than the in-plane movements for the same indoor environment conditions. Corresponding null sensor measurements are plotted below the respective crack displacements and are enlarged in b). Null responses are similar, even though they are measuring movements in different directions and on different materials, glass and drywall. Thus it seems most likely that null responses reflect the responses of the metal brackets and sensors with only slight effects from the material on which they are mounted.

For in-plane crack responses measured thus far, the null sensor responds far less than the crack sensor. Even though it would be numerically correct to subtract the null measurements from the crack measurements to obtain the actual net crack displacement, the null sensor response is often ignored because it is negligible. This approach would be acceptable for the in-plane displacements seen in Figure 3.10 where the in-plane null sensor measurements of 330 micro-inches are only 8% of the crack displacements, which exceed 4,240 micro-inches. On the other hand, the similar out-of-plane null measurements of 370 micro-inches account for 37% of the displacement relative to the smaller out-of-plane crack displacements of 1,010 micro-inches. Because the null measurements are considered large relative to the out-of-plane crack displacements, it would be less appropriate to not subtract them from the crack changes to obtain a net crack response.



a)



b)

**Figure 3.10 Ten day comparison of long-term in-plane and out-of-plane crack behavior
a) crack and null behavior for both directions measured b) enlargement of null
behavior only for both directions measured**

For the same 10-day period shown in Figure 3.10, a net (crack –null) response, shown by red diamonds, is plotted for the out-of-plane measurements in Figure 3.11. The thin gray line in Figure 3.11 shows the displacements measured by the crack sensor, previously seen as black diamonds in Figure 3.10a. Though the trends are similar, there exists a noticeable difference in the two plots displayed in Figure 3.11.

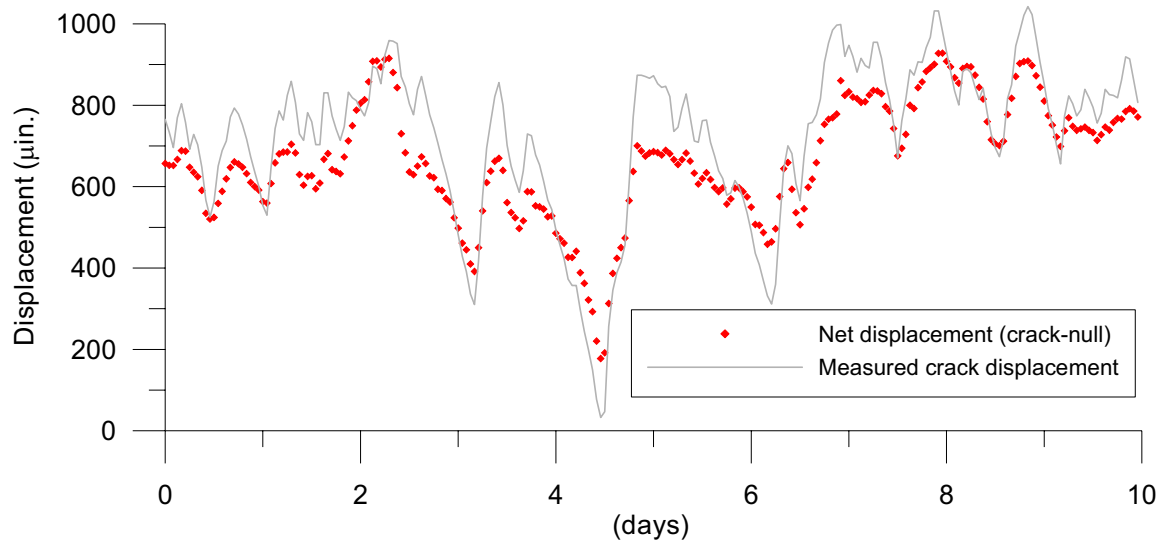


Figure 3.11 Comparison of net displacement and actual measured crack displacement in the field application of the out-of-plane measuring system

Dynamic Response

Dynamic field qualification of the out-of-plane crack measuring system involves more than twenty blasting events at the Wisconsin site beginning November 22nd 2005 as well as a variety of induced occupant events. During all events, the in-plane response was recorded to provide a comparison. All dynamic data, whether from a blast or induced occupant activity, was recorded at a high sampling rate of one-thousand cycles per second (1,000 Hz).

Figure 3.12 compares two-second time histories of in and out-of-plane response to a blast event. The top three time histories are those of orthogonal components of ground motion, shown at the same scale. The ground motions, which are considered typical for this site, ranged from 0.03 ips to 0.09 ips for PPV's in the vertical and transverse directions

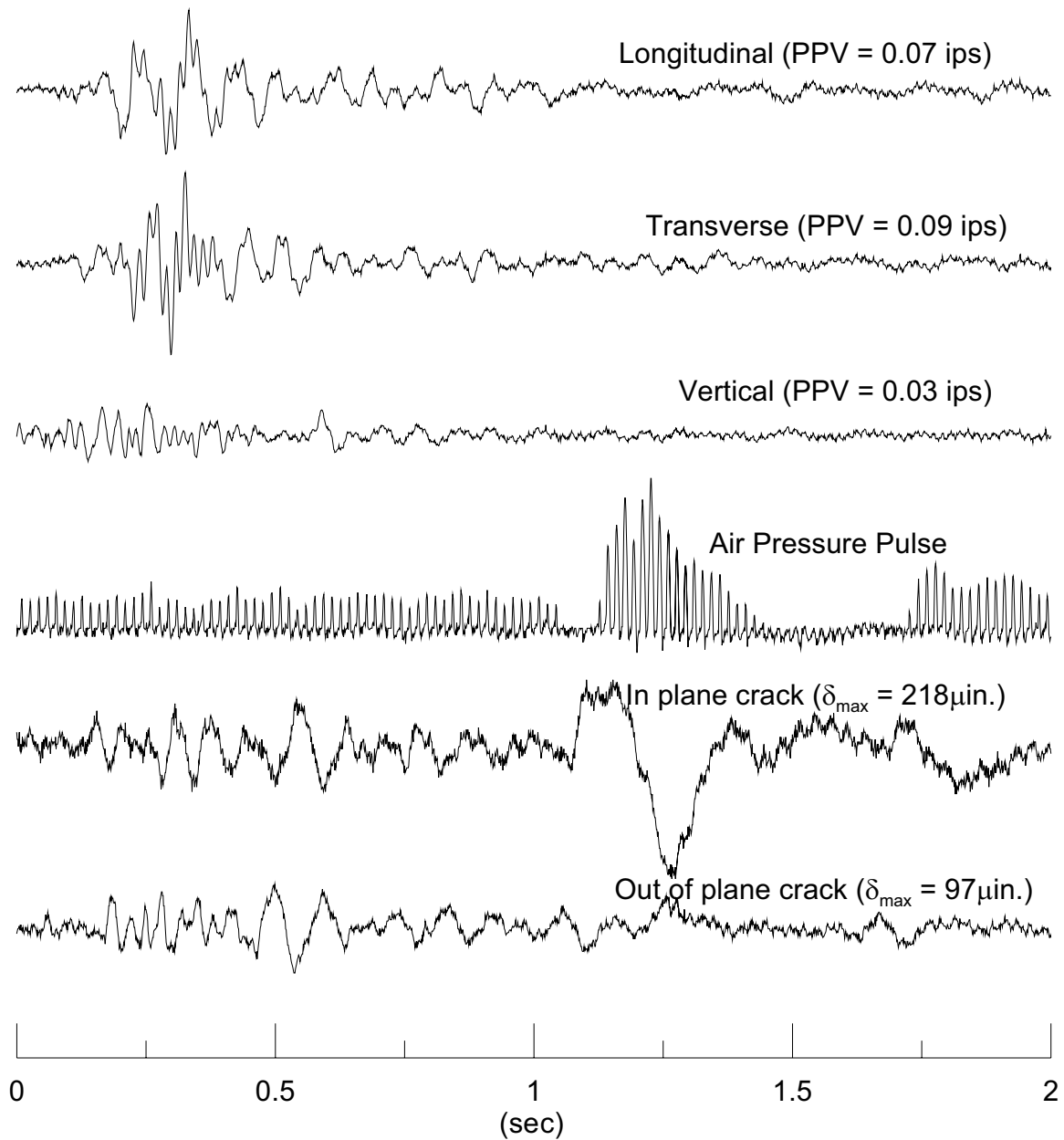


Figure 3.12 Ground motions and associated crack displacements for December 15th blast

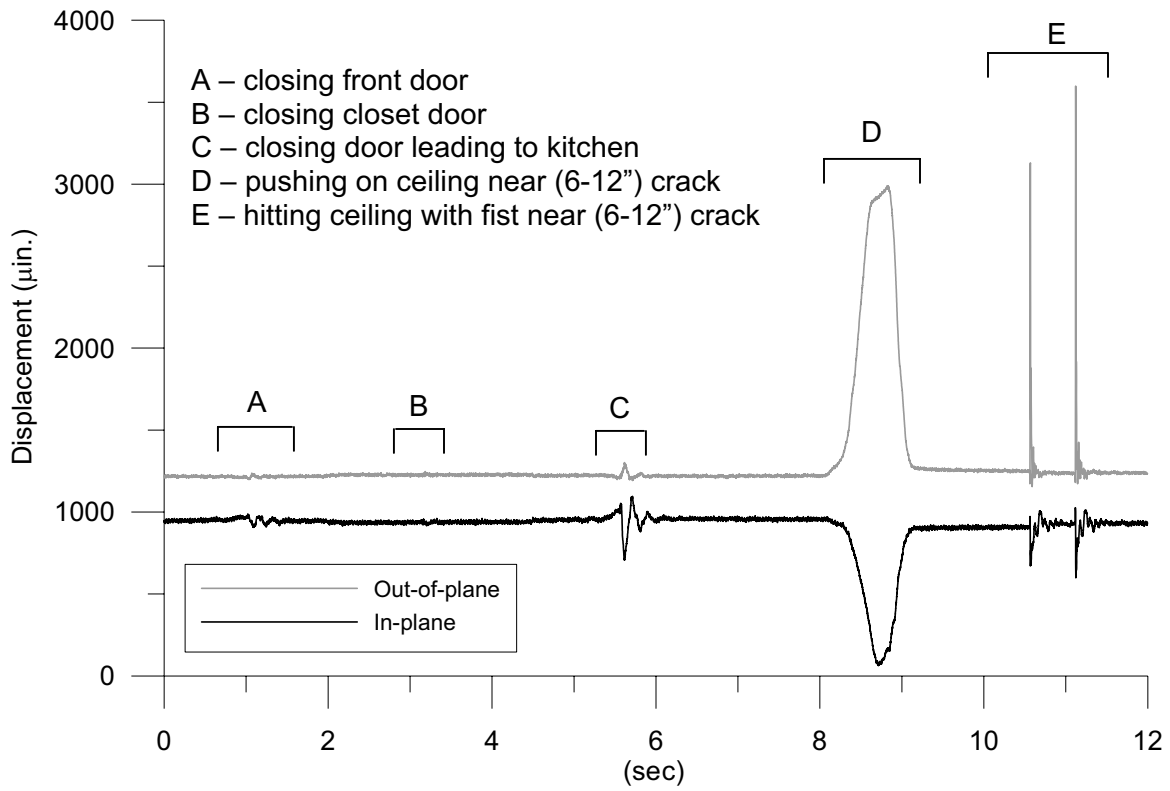
respectively. The bottom two time histories are those of the crack response, shown at the same scale; 218 micro-inches peak-to-peak in-plane and 97 micro-inches peak-to-peak out-of-plane. The unscaled middle plot is of the air pressure pulse included to show timing of the crack response to the air pressure pulse.

As illustrated in Figure 3.12, the out-of-plane crack response to the ground motions is very similar to the in-plane response considering both frequency content and amplitude. The in-plane crack movement is more sensitive to the air pressure pulse, whereas the out-of-plane direction exhibits minimal response if any at all. The large crack response to air over pressure pulse in the in-plane direction accounts for the large difference in peak-to-peak displacements for the two measured directions. For this particular blasting study, the air pressure pulse usually produced the maximum peak-to-peak response for the in-plane direction while the ground motions produced the maximum peak-to-peak out-of-plane crack response.

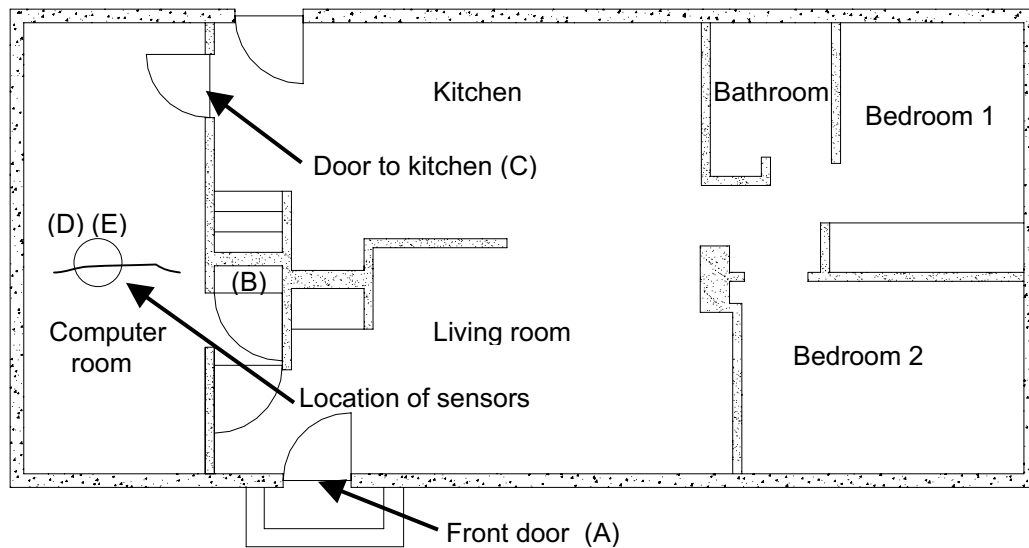
Occupant Activity

Similar to the occupant activity studies performed in Kentucky, the Wisconsin structure was perturbed to investigate how different activities affect in and out-of-plane crack response. Figure 3.13a compares crack response in the two directions to five activities including closing three doors, pushing the ceiling, and hitting the ceiling with a closed fist. The locations of these activities relative to the crack in the ceiling are represented on a floor plan of the structure in Figure 3.13b.

Surprisingly, closing the closet door, which is closest to the crack, had such a small effect on the crack displacement that it was not noticeable in the out-of-plane direction. Of



a)



b)

Figure 3.13 Crack response to occupant activity a) both directions of crack response to a variety of activities b) first level floor plan indicating where the occupant activity tests were performed

the door closings, the doorway to the kitchen induced the greatest crack response for both directions of measurement, even though it was much further away. Pushing and hitting the ceiling less than one foot from the crack had much larger impacts on crack displacement than the door closings and were in excess of 1500 and 2500 micro-inches respectively for the out-of-plane direction. However, it is unlikely a resident will push on or hit the ceiling, or wall for that matter, as often as a door would be opened and closed. Though it would be reasonable to assume these activities might occur while occupants reside in the structure. The door closings caused larger crack displacement in the in-plane direction while direct upward displacement of the ceiling caused larger displacements in the out-of-plane direction, as would be expected.

Since the crack responded more to the kitchen doorway closure than others, it was compared to a blast event produced by ground motions with a PPV of 0.07 ips in Figure 3.14. The in-plane crack response is shown by the black line for both the occupant activity and blast response while the out-of-plane direction is shown by the gray lines. Although not as large as closing the door, simply opening the door has a significant response in both directions as seen in the Figure 3.14. For these particular events, the in-plane kitchen door response of 230 micro-inches was greater than the in-plane blast response of 170 micro-inches. However, the out-of-plane direction received a larger response from the blast event of 100 micro-inches relative to the 90 micro-inch response to the door close. These simple daily activities can produce as much or more crack displacement than blast events.

A ceiling fan was located within a few feet of the sensors and was turned on and off while recording the crack response in both directions. Crack responses to this event are compared in Figure 3.15 to the same 0.07 ips blast event. The gray line represents the out-of-

plane crack response while the black line shows the in-plane response. In both directions measured, there exist three sharp spikes at the beginning of the fan response which correspond to tugging on the chain to initiate the proper rotation velocity. Similarly, the spike at approximately twenty-two seconds correlates to a chain pull to turn off the fan. The crack movements caused by the fan do not exceed blast displacements; however, the fan still produces noticeable response in both directions.

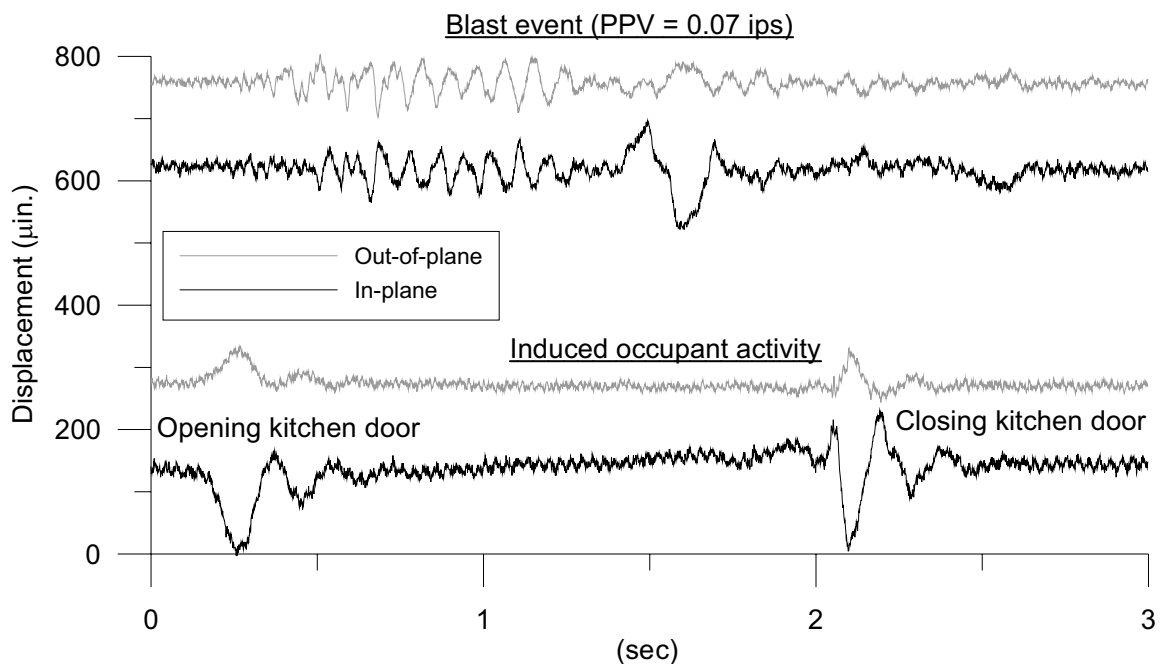


Figure 3.14 Crack response comparison of induced occupant activity (opening and closing of a door) and a blast event (Dec. 28th PPV = .07 ips) for both directions of displacement measured

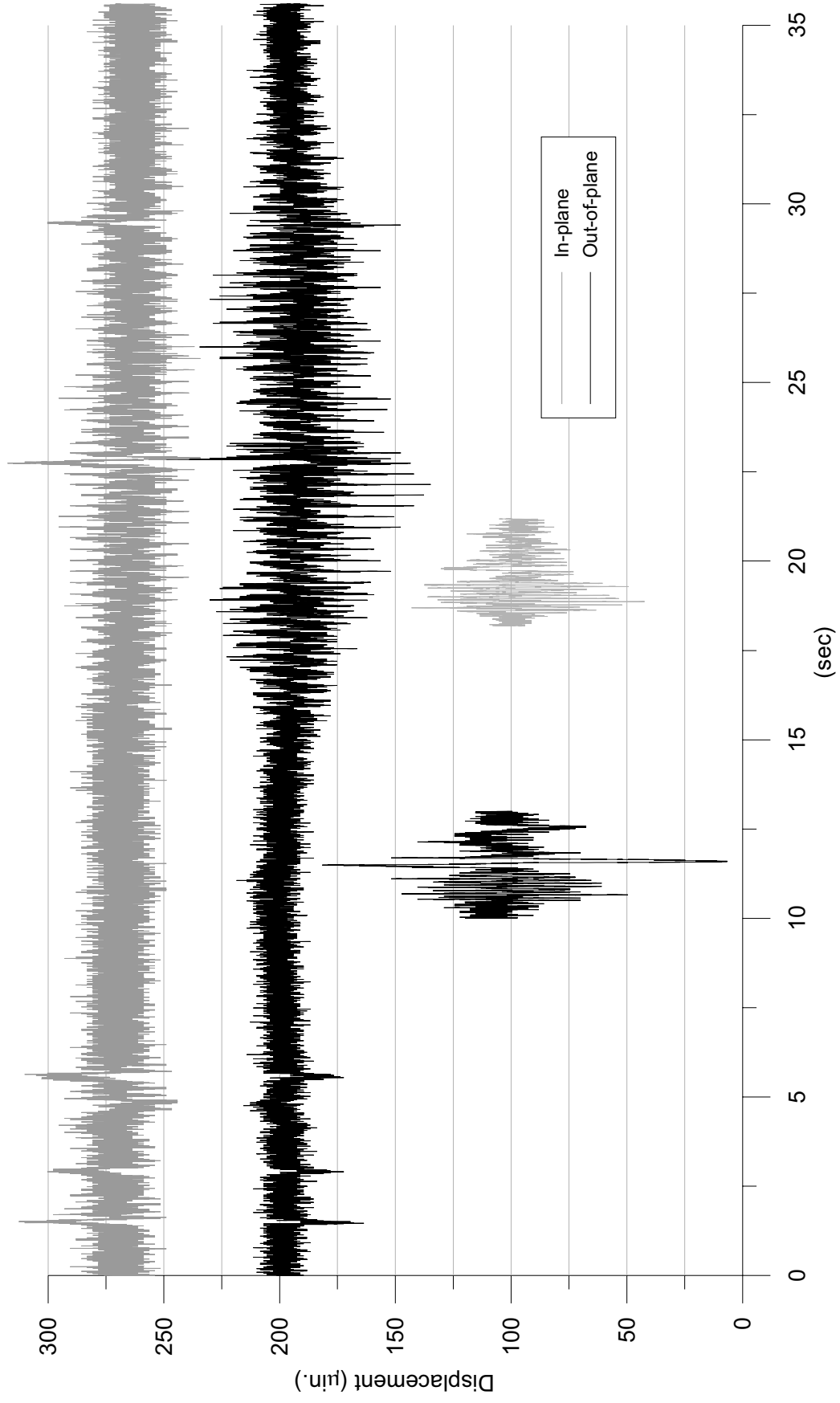


Figure 3.15 Comparison of crack response to ceiling fan and blast event (Dec. 28th PPV = .07 ips)

Wind Effects

Just as blast vibrations and human occupant activity cause crack displacements, so do wind induced distortions of a structure. In an effort to investigate the effect of wind on both in-plane and out-of-plane directions, responses at the Milwaukee test structure were recorded at a rate of ten samples per second (10 Hz) for some 20 hours during a particularly windy day. Testing began at 9:55am on January 24th and terminated approximately 6:30 am January 25th as seen in Figure 3.16. Shown as Figure 3.16a are the National Climatic Data Center (NCDC) wind conditions at Milwaukee Mitchell International Airport reported for the corresponding times (NCDC, 2005). The airport is located approximately five miles from the instrumented test site. Time “0” on Figure 3.16 corresponds to 9:55am January 24th, 2006. The following paragraph explains the process by which wind data were obtained from the NCDC.

Data from the NCDC are most easily obtained at <http://cdo.ncdc.noaa.gov/ulcd/ULCD>. Once the web page is accessed, the desired state of interest should be selected. Next, select the airport nearest the site for which the wind data is wanted. For this study, Milwaukee Mitchell International Airport in Milwaukee, WI was selected. Next, select the month and year corresponding to the date(s) of data desired. From this screen, both hourly observations and daily summaries can be downloaded in either .html (web) or ACSII (text) formats. When accessing the NCDC website from a university education connection (.edu), the information is granted free of charge. However, if accessing the NCDC website from a non-university connected computer, a nominal fee is charged to download the data. A general sample of a download can be viewed for both the hourly observations and daily summaries before purchasing a data download.

Figure 3.16*a* compares two sets of data; hourly wind velocity averages and maximum five-second wind gusts. The data labeled as wind averages are typically provided hourly and are averaged in some fashion to provide one value for the hour. The data labeled as wind gusts correspond to five-second averages of wind speeds which are listed daily. However, they can be listed more frequently on gusty days as shown for January 24th in Figure 3.16*a*. The wind gusts reported by NCDC all exceeded twenty miles per hour (mph) with a maximum of thirty-seven mph. Wind averages for the study ranged from thirteen to twenty-eight mph. These wind speeds would easily denote a day as being considered “windy” relative to typical local wind conditions.

The data from the air pressure transducer in Figure 3.16*b* has not been calibrated or converted to an air pressure unit and therefore is listed as millivolts (mv), which is the transducer output. This format cannot give an absolute value of wind pressure, although it yields relative values to show periods of low, moderate, and high winds and can be compared to pressure pulses associated with blasting events, which are also listed in millivolts. Air pressure is omni-directional. The air pressure transducer was located on the west side of the house, which may have influenced its response. Differences in wind directions measured and frequencies of reported results between the two sources are responsible for differences in the wind speed and air pressures in the plots.

The in and out-of-plane crack responses are also compared in Figures 3.16*c,d* respectively. The gradual yet large changes in crack displacement are mostly a result of temperature changes. At the scale shown, it is difficult to effectively detect transient crack behavior from wind effects. Therefore a closer view of three periods of differing wind levels are shown in Figure 3.17. However, the data show that the temperature and humidity induced

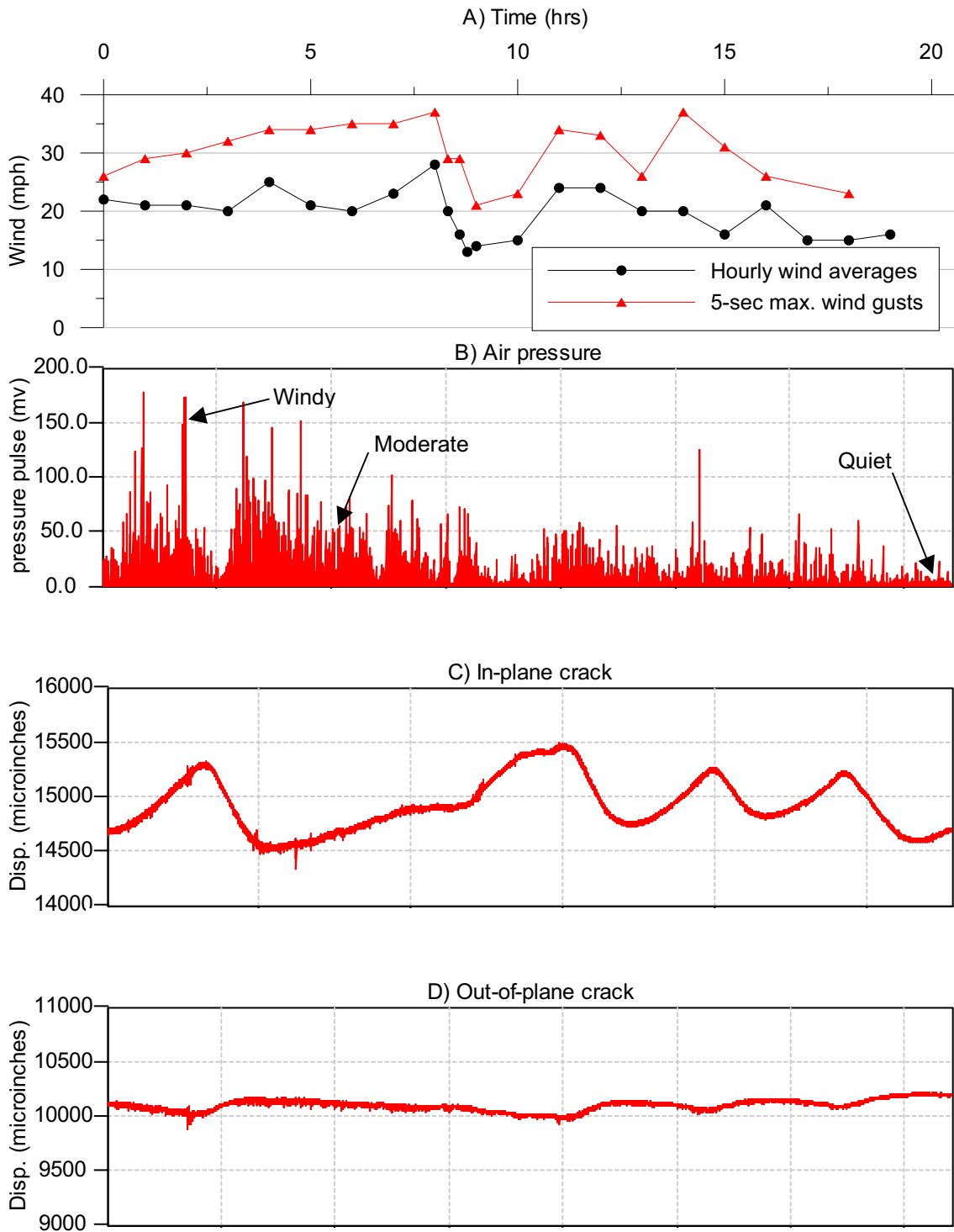


Figure 3.16 Comparison of 20 hours wind and air pressure data vs. crack displacement
a) Milwaukee airport wind data b) air pressure data obtained at site c) in-plane crack displacement d) out-of-plane crack displacement

effects remain more significant.

Thirty-second time histories from periods described as quiet, moderate, and windy on Figure 3.16a are shown in Figure 3.17 to display the detail of the wind conditions and corresponding crack behavior. On the left, part a) shows a period where the winds were relatively calm and as presumed, the associated crack behavior reflects a similar condition. In the middle, part b) shows a period of moderate winds with pressures slightly exceeding fifty millivolts. The out-of-plane crack movements are roughly 75 micro-inches peak-to-peak which are larger than the in-plane crack movements of approximately 50 micro-inches for the moderate wind period. The time period deemed as windy (part c) included pressures almost reaching 150 millivolts relating to 150 micro-inches crack displacement in the out-of-plane direction and 175 in the in-plane direction. Based upon the plots in Figure 3.17, a direct correlation can be made between the intensity of the wind and the amplitude of crack displacement for both in-plane and out-of-plane directions.

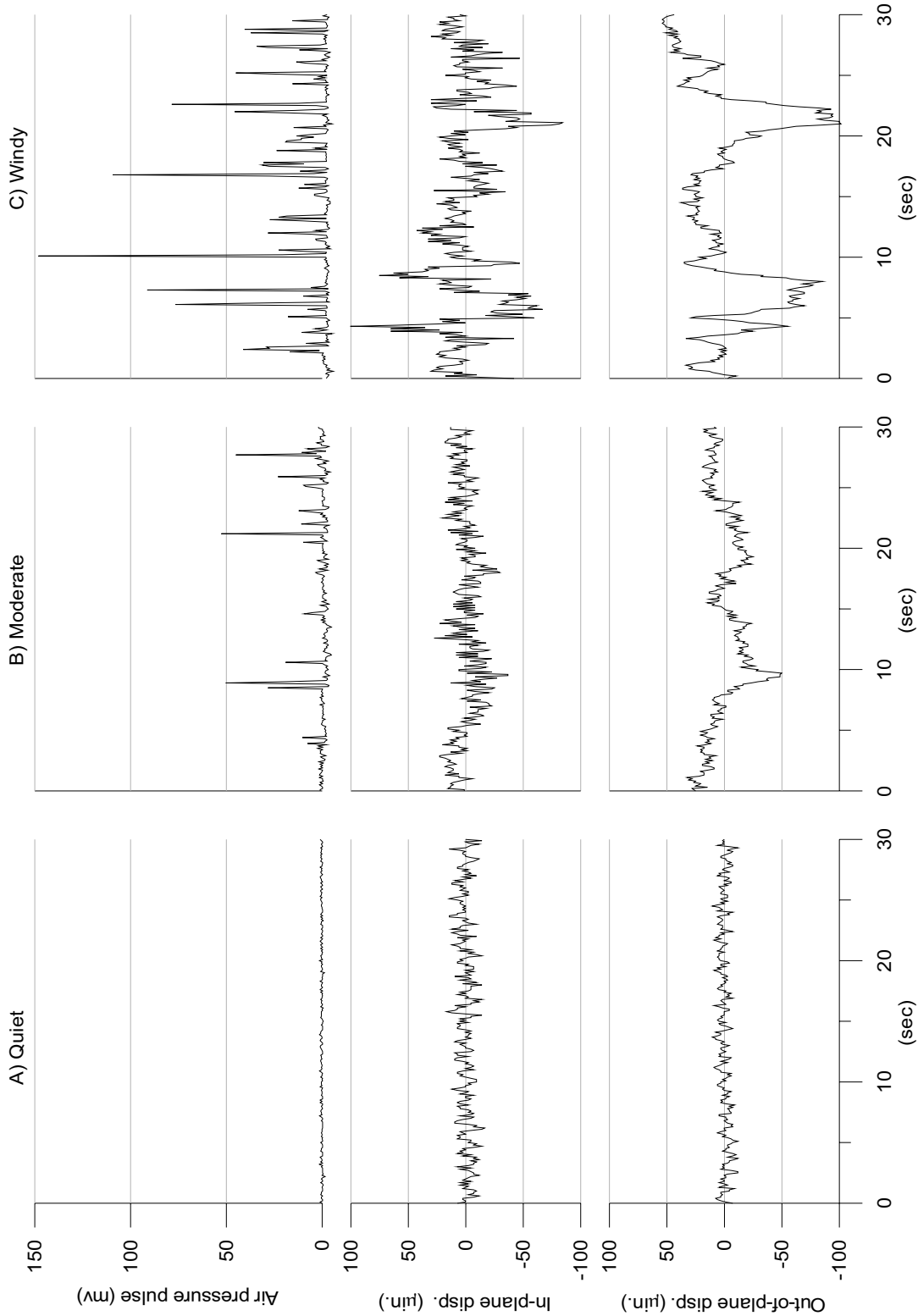


Figure 3.17 Crack behavior during varying degrees of windiness a) a period of low winds b) a period of moderate winds c) a period of high winds

Unexplained Responses

During the twenty hours of continuous recording at 10 samples per second, significant crack displacements occurred at times of calm or zero wind speeds. An example of this crack behavior is shown in Figure 3.18 and is portrayed at the same scales as Figure 3.17 for ease of comparison. In-plane crack response exceeds 200 micro-inches at a much lower frequency relative to blasting responses. The out-of-plane crack responded at the same time; however at a much lower amplitude. Since no blast event was recorded for January 24th

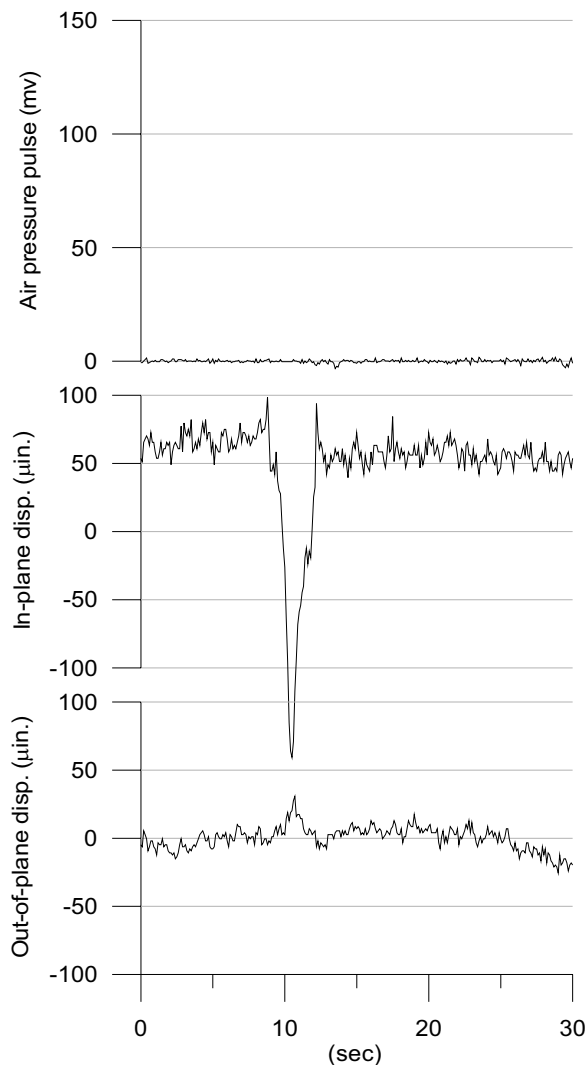


Figure 3.18 Crack behavior when no wind present

and the air pressure transducer displayed no response, the crack response must have been induced by some other phenomenon such as some form of occupant activity. Figure 3.18 provides information that significant crack activity can occur at unexpected times from unknown sources and can easily exceed displacements caused by blasting.

In effort to show the relative importance of wind effects on existing cracks in structures, Figure 3.19 compares two different wind events to a blast event. On the left, part a) of Figure 3.19 displays the first ten seconds of wind response captured during the period labeled as windy

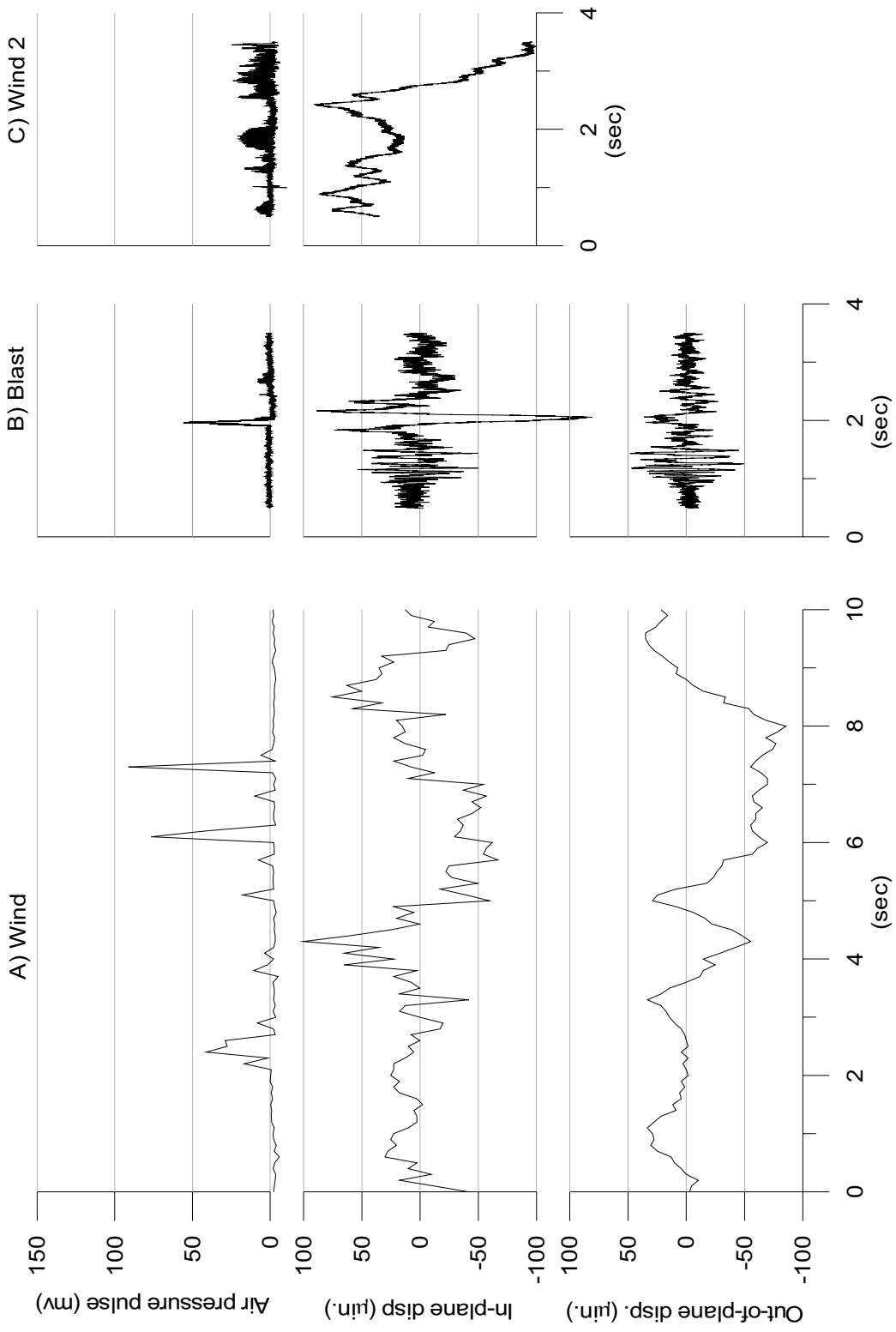


Figure 3.19 Comparison of crack behavior to outdoor winds and a blasting event a) period of high wind b) January 26th 2006 blast event of PPV = 0.09 ips c) wind induced crack movement obtained on October 30th 2004

in Figure 3.17*a*. In the middle, part b) of Figure 3.19 shows the air pressure and crack response due to a blast event that occurred on January 26th shortly after the twenty hour wind study. On the right, part c) is the response of a previous event which occurred in October 2004 that captured wind fluctuations and corresponding crack behavior following a trigger caused by an electrical noise spike. The data presented in part c) occurred prior to the installation of the out-of-plane crack sensors and therefore only provides insight to the in-plane crack movements.

For the data collected and presented, it appears that the wind induces crack movements equal to or larger than typical blasting in the in and out-of-plane directions for this particular ceiling crack. Data presented herein are for the one particular windy day; the crack movements would be expected to be larger for days when wind velocities are higher.

Chapter 4

Conclusions and Recommendations

This thesis summarizes two further increments of the development of the autonomous crack monitoring (ACM) system: 1) measurement of crack response in three materials in a structure subjected to blast vibrations from an underground aggregate mine 2) design and development of a mounting system to measure normal, or out-of-plane, crack response. The three cracks were located in exterior brick, drywall near an interior doorframe, and joint mortar between concrete masonry units of a basement wall. The mounting system involved a non-responsive block to which both the crack and null sensors were mounted, which was qualified by installation on a ceiling crack in a home adjacent to an operating quarry..

Conclusions regarding the differentiation of crack response in multiple materials will be subdivided into the following categories: long-term (environmental) response, dynamic (blast) response, and unusual dynamic behavior.

Analysis of the long-term, or environmental, response of the three cracks led to the following conclusions:

- Daily response of the exterior brick crack was the greatest of the three, and was probably the result of exposure to the largest fluctuations in temperature.

- Interior drywall crack response exhibited noticeable daily response while the basement crack responded mainly to long-term effects.
- Interior drywall crack response seemed to correlate most closely to indoor humidity changes, which were strongly influenced by the outdoor temperature.
- The 24-hour average seasonal response of all three cracks are at least an order of magnitude greater than the maximum blast induced crack displacements.

Examination of crack response to blast induced ground motions from underground mining resulted in the following conclusions:

- Responses of all three cracks increased with increasing measured peak particle velocity, measured peak ground displacement, and calculated peak relative displacement.
- On average the dynamic crack response correlated most closely with calculated peak relative displacements and correlated less well but similarly to both measured peak particle velocities and peak ground displacements calculated from particle velocity time histories.
- Crack response varied with location within the structure and/or type of material in which the crack exists with the basement crack being the most sensitive to blast events.
- Unlike surface quarries, this underground mine produced no air over pressure excitation and produced ground motions whose dominant frequencies were high.

Unusual crack behavior including response to occupant activity yielded the following conclusions:

- Common daily household activities such as walking through rooms and leaning on walls can cause as much or greater crack displacements than blasting events.
- Loosely attached surfaces containing a crack can amplify crack response to dynamic events as seen by the response of the crack in the exterior brick wall.
- Erratic, undefined, yet significant crack behavior often goes undetected with typical long-term recording methods.
- Crack response very similar to deliberately induced occupant activity response was detected during a special long-term, high sample rate study.
- Dynamic crack response (greater in magnitude than typical blast responses) was observed at times with no recorded ground motions.
- Environmentally induced crack response over a one-hour time period can exceed the crack displacement caused by a typical blast event.
- Electronic noise is present in this ACM system of approximately six to thirty percent of blast responses at peak-particle velocity equal to 0.1 ips.
- Wind can induce noticeable crack response; however, a more sophisticated system is required to more accurately and meaningfully analyze wind effects.

Conclusions regarding the qualification of the apparatus to measure crack response in the normal, or out-of-plane, direction will be subdivided into three sections: laboratory qualification, field qualification, and wind response.

Laboratory qualification provided the following conclusions:

- The new system can adequately record dynamic events similar in magnitude and frequency to those expected for blast induced crack responses.
- Temperature response of the glass block, aluminum mounting bracket, and sensor configuration was far greater than predicted for the glass block alone.
- The null sensor temperature response is large compared to the theoretical glass block response; however, it is small compared to crack displacements, which allows the system to function in a useful fashion.

Field qualification through recording normal crack response of a ceiling crack in the Milwaukee test house allowed the following conclusions:

- For the ceiling crack studied in the test structure, in-plane crack response to long-term environmental effects exceeds the out-of-plane, or normal, response.
- Null sensor responses for the in or out-of-plane configurations are the same regardless of the orientation of the sensor and the material on which it is affixed (glass or drywall).
- Because the long-term out-of-plane, or normal, response is smaller than typical in-plane responses, the sensor effects measured by the null sensor must be considered when assessing crack behavior in the out-of-plane direction.
- In and out-of-plane dynamic crack responses to ground vibrations are similar. However, the out-of-plane crack response to the air over pressure pulse is smaller than the in-plane response.

- Pushing or hitting the ceiling crack in the out-of-plane direction produces larger out-of-plane than in-plane response because of the greater vertical flexibility of the ceiling at the crack location.
- Opening and closing doors produces greater response in the in-plane than the out-of-plane direction.

Investigation of in-plane and out-of-plane crack response to wind effects results in the following conclusions:

- In-plane and out-of-plane crack displacements can be correlated to wind activity measured by an air pressure transducer.
- Wind produces significant in-plane and out-of-plane crack responses; however, blast induced air over pressure affects in-plane response more than out-of-plane.

This study has made significant progress in the development of the ACM system; yet recommendations for future work can be suggested. Noteworthy progress has been achieved in detecting dynamic crack behavior which occurs independently of blast vibrations. Long duration studies at high sample rates (fifty samples per second) similar to that undertaken with the multiple crack study should be performed at other test sites to further quantify and pinpoint these unusual crack motions. It is suggested that a multi-directional wind velocity sensor (anemometer) or an air over pressure transducer be installed with future ACM projects for real time triggering to better define and capture wind response. Finalizing a method to trigger the system off crack displacements as well

as ground motions would significantly increase the opportunity to capture wind and occupant activity events.

This thesis provides the first ACM instrumentation offering insight to crack behavior other than considering only the traditional in-plane perpendicular crack movements. The system designed to measure out-of-plane crack movements discussed herein has been qualified and performs sufficiently well in measuring dynamic and long-term crack motions in the respective direction. It should further be developed to measure crack displacement in-plane and parallel to the crack and the resulting improved system should be field qualified.

References

- Dowding, C.H. (1996). *Construction Vibrations*, Prentice Hall, Upper Saddle River, NJ.
- Dowding, C. and McKenna, L. (2003). *Addendum I. Direct Measurement of Crack Response of Four OSM Study Structures*, contained in “Comparative Study of Structure Response to Coal Mine Blasting”, U.S. Department of the Interior, Office of Surface Mining, Pittsburgh, PA.
- Louis, M. (2000). *Autonomous Crack Comparometer Phase II*, M.S. Thesis, Department of Civil and Environmental Engineering, Northwestern University, Evanston, IL.
- Marron, D. (2005). *private communication* Infrastructure Technology Institute, Northwestern University, Evanston, IL.
- McKenna, L.M. (2002). *Comparison of Measured Crack Response in Diverse Structures to Dynamic Events and Weather Phenomena*, M.S. Thesis, Department of Civil and Environmental Engineering, Northwestern University, Evanston, IL.
- Siebert, D.R. (2000). *Autonomous Crack Comparometer*, M.S. Thesis, Department of Civil and Environmental Engineering, Northwestern University, Evanston, IL.
- Snider, M.L. (2003). *Crack Response to Weather Effects, Blasting, and Construction Vibrations*, M.S. Thesis, Department of Civil and Environmental Engineering, Northwestern University, Evanston, IL.
- Petrina, M.B. (2004). *Standardization of Automated Crack Monitoring Apparatus for Long-Term Commercial Applications*, M.S. Thesis, Department of Civil and Environmental Engineering, Northwestern University, Evanston, IL.
- National Climatic Data Center (2005). <http://cdo.ncdc.noaa.gov/ulcd/ULCD>, U.S. Department of Commerce, Federal Building 151 Patton Avenue, Asheville, NC 28801
- Kaman Aerospace Corporation (2005). <http://www.kamansensors.com/html/core.htm>, Measuring and Memory Systems 217 Smith Street, Middleton, CT 06457
- Revey, G.F. (2005). *private communication* Revey Associates, Inc. PO Box 261219 Highlands Ranch, CO 80163
- Somat (2005). Infield version 1.5.1 Somat Corporation, Champaign, IL.
- SoMat (2004). TCE version 3.8.4c Somat Corporation, Champaign, IL.
- SoMat (2005). TCE version 3.8.5c Somat Corporation, Champaign, IL.